Identification of novel protein binding partners for the tumor suppressor DLC1

Von der Fakultät für Energie-, Verfahrens- und Biotechnik der Universität Stuttgart
zur Erlangung der Würde eines
Doktors der Naturwissenschaften (Dr. rer. nat.) genehmigte Abhandlung.

Vorgelegt von
Johanna Heering
aus Essen

Hauptberichter: Prof. Dr. Klaus Pfizenmaier
Mitberichter: Prof. Dr. Peter Scheurich
Tag der mündlichen Prüfung: 08.09.2009

Institut für Zellbiologie und Immunologie der Universität Stuttgart
2009

Abbreviations

% v/v	percent volume by volume
% w/v	percent weight by volume
℃	degree celsius
µg	microgram
bp	base pair
C (Cys)	cysteine
Cdc42	cell division cycle 42
cDNA	complementary DNA
cfu	colony forming unit
cm	centimeter
Dia	mammalian ortholog of Drosophila Diaphanous 1
DLC1	Deleted in Liver Cancer 1
DNA	deoxyribonucleic acid
E (Glu)	glutamic acid
EMT	epithelial-to-mesenchymal transition
FAK	focal adhesion kinase
FCS	fetal calf serum
fig	figure
g	force of gravity
GAP	GTPase activating protein
GDI	guanine nucleotide dissociation inhibitor
GDP	guanosine diphosphate
GEF	guanine nucleotide exchange factor
GFP	green fluorescent protein
GST	glutathione S-transferase
GTP	guanosine triphosphate
h	hour
HCC	hepatocellular carcinoma
HEK293T cells	human embryonic kidney cells
His	histidine
JNK	c-Jun N-terminal kinase
K (Lys)	lysine
kb	kilobase
LAR	leukocyte common antigen receptor
Leu	leucine
LH	liprin homology
LOH	loss of heterozygosity
min	minute

ml	milliliter
mRNA	messenger RNA
MTT	thiozolylblue tetrazolium bromide
nM	nanomolar
OD	optical density
ORF	open reading frame
p	phospho-
PAGE	polyacrylamide electrophoresis
PDGF	platelet-derived growth factor
PDK-1	3-phosphoinositide-dependant protein kinase-1
PI3K	phosphoinositide 3-kinase
PIP2	phosphatidylinositol (3,4)-bisphosphate
PIP3	phosphatidylinositol (3,4,5)-trisphosphate
PKB	protein kinase B
pmol	picomole
PTEN	phosphatase and tensin homolog deleted on chromosome ten
Rac1	Ras-related C3 botulinum toxin substrate 1
Rho	Ras homology
RNA	ribonucleic acid
rpm	rotations per minute
RT-PCR	reverse transcription-polymerase chain reaction
S (Ser)	serine
SAM	sterile alpha motif
SDS	sodium dodecyl sulfate
sec	seconds
SEM	standard error of the means
SH2	Src homology 2
siRNA	small interfering RNA
SRF	serum response factor
START	steroidogenic acute regulatory (StAR)-related lipid transfer
T (Thr)	threonine
Trp	tryptophan
WCE	whole cell extract
WHO	World Health Organization
Y (Tyr)	tyrosine
α	anti

Summary

Cancer, one of the major chronic health problems worldwide, is a genetic disease, which requires the cooperation of gain-of-function and/or loss-of-function mutations to either oncogenes or tumor suppressor genes, respectively. In the last decade, the Deleted in Liver Cancer (DLC) 1 gene has emerged as a novel tumor suppressor downregulated in a variety of cancer types including breast, liver, prostate and lung. DLC1 is a multidomain protein consisting of an N-terminal sterile alpha motif (SAM), a C-terminal START and an internal Rho GTPase activating (GAP) domain. Due to GAP-dependent and –independent mechanisms that are still poorly understood DLC1 is able to inhibit proliferation, migration and invasion of tumor cells. The goal of this thesis was the identification of novel DLC1 protein binding partners, in order to gain deeper insight into DLC1 regulation and molecular function. Therefore, a yeast-two-hybrid screen based on the Gal4-system was performed, using the DLC1 SAM domain as a bait and a cDNA library derived from human breast tissue as a prey.

One of the 16 putative binding candidates identified was the phosphatase and tensin homolog deleted on chromosome ten (PTEN), which is also a tumor suppressor frequently deleted or mutated in sporadic tumors of the breast, prostate, endometrium and brain. PTEN consists of an enlarged catalytic site that acts as a dual-specificity phosphatase for proteins and lipids. By dephosphorylation of its major lipid substrate phosphatidylinositol (3,4,5)-trisphosphate (PIP3) the PI3K signaling pathway is downregulated and cell proliferation and survival mediated by Akt/PKB activation are inhibited. Cell spreading and cell motility are also suppressed by PTEN activity. Pulldown assays and coimmunoprecipitation of DLC1 and PTEN confirmed association of the proteins in mammalian cells. The interaction of both proteins was stimulated upon PTEN activation by PDGF treatment, correlating with their colocalization at the plasma membrane. In overexpression experiments synergistic effects of the two proteins with regard to downstream signaling could not be observed. However, simultaneous loss of DLC1 and PTEN in the non-invasive MCF7 breast carcinoma cell line using RNA interference enhanced migration in an additive manner in wounding as well as in chemotactic transwell assays compared to singly depleted cells. These results suggest that the spatio-temporally restricted formation of a DLC1/PTEN complex, simultaneously inhibiting its individual downstream targets, guarantees the synchronization of cell migration processes. Thus, loss of both proteins is proposed to facilitate malignant transformation by increasing the metastatic potential of tumor cells.

Another putative DLC1 binding partner identified in the yeast-two-hybrid screen was liprin beta2 that belongs to a protein familiy comprising four alpha- and two beta-type family members, which all contain a C-terminal highly conserved liprin homology (LH) domain consisting of three SAM domains. Association of full-length DLC1 with liprin beta2 as well as with the additional family members liprin alpha1 and beta1 was confirmed biochemically by coimmunoprecipitation. Liprins are multivalent proteins that form complex structures due to homo- and heterodimerization. Additionally, alpha-type liprins interact with the LAR subfamily of receptor protein-tyrosine phosphatases, which are heterophilic receptors involved in cell adhesion and cell motility. Given the function of liprins as adaptor proteins at membrane proximal sites, it is conceivable that they contribute to DLC1 localization and/or scaffolding. It is thus of particular interest to investigate the biological impact of DLC1 binding to liprin proteins in future studies.

Zusammenfassung

Krebs, eines der größten chronischen Leiden weltweit, ist eine genetische Erkrankung, die die Kooperation von so genannten „Gain-of-Function“ und/oder „Loss-of-Function“ Mutationen in entweder Onkogenen oder Tumorsuppressorgenen bedingt. Das „Deleted in Liver Cancer (DLC) 1“ Gen, das in einer Vielzahl von Krebsarten wie Brust-, Leber- und Lungenkrebs herunterreguliert ist, wurde in den letzten zehn Jahren als neuer Tumorsuppressor entdeckt. DLC1 besitzt ein N-terminales steriles-alpha-Motiv (SAM), eine C-terminale START und eine interne Rho-GTPase-aktivierende (GAP) Domäne. Infolge GAP-abhängiger und –unabhängiger Mechanismen, die bisher noch kaum verstanden sind, ist DLC1 fähig, Proliferation, Migration und Invasion von Tumorzellen zu inhibieren. Das Ziel dieser Dissertation war die Identifizierung neuer DLC1 Proteinbindungspartner, um ein besseres Verständnis der DLC1 Regulation und molekularer Funktion zu gewinnen. Zu diesem Zweck wurde ein Hefe-zwei-Hybrid Screen basierend auf dem Gal4-System durchgeführt, in dem die DLC1 SAM-Domäne als Köder und eine cDNA Bibliothek aus humanem Brustgewebe als Beute benutzt wurden.

Einer der 16 identifizierten Bindungskandidaten war „Phosphatase and Tensin Homolog Deleted on Chromosome Ten“ (PTEN), ebenfalls ein Tumorsuppressor, der häufig in sporadischen Tumoren der Brust, Prostata, des Endometriums und Gehirns deletiert oder mutiert ist. PTEN besteht aus einer ausgedehnten katalytischen Region, die als dual-spezifische Phosphatase für Proteine und Lipide agiert. Durch Dephosphorylierung seines Haupt-Lipidsubstrates Phosphatidylinositol-(3,4,5)-trisphosphat (PIP3) wird der PI3K Signalweg herunterreguliert, wodurch Zellproliferation und Überleben vermittelt durch Akt/PKB Aktivierung inhibiert werden. Zellausbreitung und zelluläre Motilität werden ebenfalls durch PTEN-Aktivität supprimiert. „Pulldown“ Versuche und Koimmunopräzipitation von DLC1 und PTEN bestätigten die Assoziation der Proteine in Säugetierzellen. Die Interaktion beider Proteine konnte durch PDGF-vermittelte PTEN Aktivierung stimuliert werden, korrelierend mit ihrer Kolokalisation an der Plasmamembran. In Überexpressionsstudien konnten keine synergistischen Effekte der zwei Proteine hinsichtlich nachgeschalteter Signalwege beobachtet werden. Allerdings steigerte der durch RNA Interferenz hervorgerufene gleichzeitige Verlust von DLC1 und PTEN in der nicht-invasiven MCF7 Brustkrebszelllinie die Migration in „Wounding“ als auch in chemotaktischen „Transwell Assays“ additiv verglichen mit einfach-depletierten Zellen. Diese Ergebnisse lassen vermuten, dass die räumlich und zeitlich begrenzte Formierung eines DLC1/PTEN Komplexes, der in koordinierter Weise die individuellen nachgeschalteten Zielmoleküle inhibiert, die Synchronisation von Zellmigrationprozessen garantiert und dass somit der

Verlust beider Proteine die maligne Transformation durch die Erhöhung des metastatischen Potentials von Tumorzellen fördert.

Ein weiterer Bindungspartner von DLC1, der in dem Hefe-zwei-Hybrid Screen identifiziert wurde, war Liprin beta2, das zu einer Proteinfamilie gehört, die vier alpha- und zwei beta-Typ Familienmitglieder umfasst, von denen alle eine C-terminale, hoch konservierte Liprin-Homologie (LH) Domäne gebildet aus drei SAM-Domänen besitzen. Assoziation von „full-length“ DLC1 mit Liprin beta2 sowie mit den weiteren Familienmitgliedern Liprin alpha1 und beta1 wurde biochemisch durch Koimmunopräzipitation bestätigt. Liprine sind multivalente Proteine, die komplexe Strukturen aufgrund von Homo- und Heterodimerisierung bilden. Desweiteren interagieren die alpha-Typ Liprine mit der LAR Subfamilie der Rezeptor-Protein-Tyrosinphosphatasen, heterophile Rezeptoren, welche an Zelladhäsion und Zellmotilität beteiligt sind. Angesichts der Funktion von Liprinen als Adaptorproteine an membrannahen Stellen ist es denkbar, dass sie zur Lokalisation und/oder zum „Scaffolding“ von DLC1 beitragen. Es ist daher von besonderem Interesse, in zukünftigen Studien die biologische Wirkung der DLC1-Bindung an Liprine zu untersuchen.

1 Introduction

1.1 Cancer

Cancer belongs to the major chronic health problems worldwide. In economically developed countries it represents the second leading cause of death following cardiovascular diseases. In the year 2008 the incidence rate amounted to over 12 million and the number of people diagnosed with cancer is predicted to double till 2020 (World Cancer Report 2008, WHO). Among men, the most commonly diagnosed cancers include prostate, lung, stomach and liver, among women, breast cancer is one of the most prominent types and belongs to the most common causes of cancer-related deaths worldwide.

Carcinogenesis is a multistep process that requires the cooperation of multiple genetic alterations in critical genes – oncogenes, tumor suppressor and stability genes - leading to the malignant transformation of normal into tumor cells (Bishop, 1995). The initiation of tumorigenesis is entailed by the mutation of a single cell due to the influence of chemical carcinogens, physical processes like UV irradiation, tumor viruses, hereditary predisposition or spontaneous aberrations of the DNA. This results in chromosomal abnormalities of key regulatory genes involved in cell survival, proliferation, invasiveness, motility and drug resistance (Jackson & Loeb, 1998). A selective growth advantage driven by the influence of microenvironmental factors imparts the clonal expansion of this cell to a preneoplastic cell population. Accumulation of various other mutations during tumor progression finally leads to the conversion into the malignant cancer cells, which are characterized by six hallmarks: self-sufficiency in growth signals, insensitivity to growth-inhibitory signals, evasion of apoptosis, limitless replicative potential, sustained angiogenesis and tissue invasion and metastasis (Hanahan & Weinberg, 2000). A process known as epithelial-to-mesenchymal transition (EMT) is often activated during cancer invasion and metastasis. This transition results in loss of contacts with neighboring cells by repression of key adhesion molecules such as E-cadherin, remodelling of the actin cytoskeleton to acquire increased motility and proteolytic processing and secretion of extracellular matrix (Yang & Weinberg, 2008).

1.1.1 Oncogenes and tumor suppressors

Beside stability genes or so-called caretakers, which keep genetic alterations to a minimum due to their function in DNA repair but are not originally responsible for tumor development when mutated, two main types of genes play a crucial role in tumorigenesis: oncogenes and tumor suppressor genes.

The precursors of oncogenes, proto-oncogenes, are involved in cell growth and differentiation. Mutations render the genes constitutively active, which leads to an abnormal growth and increased survival. Point mutations or chromosomal rearrangement resulting in an aberrant protein with a different biological activity, gene amplification increasing the number of gene copies within a cell, and viral infection resulting in the control of a proto-oncogene under a more active viral promoter can be the reason for this activation (Croce, 2008).

Tumor suppressor genes are targeted in the opposite way: their gene products are rendered inactive by genetic alterations. Thus, repressive effects on cell growth and differentiation and promotion of apoptosis – the normal function of these proteins – are impaired (Sherr, 2004). In contrast to mutant oncogene alleles, which are typically dominant and some tumor suppressor genes, for which haploinsufficiency was described, mutant tumor suppressor alleles are usually recessive. This was firstly observed by A. G. Knudson in the retinoblastoma gene, whereupon he postulated the “two-hit hypothesis” (Knudson, 1971). Thus, a critical event for cancer development is the “loss of heterozygosity” (LOH) of tumor suppressor genes. Detection of a high LOH frequency is often used to determine chromosomal loci of putative tumor suppressors (Dutt & Beroukhim, 2007). Furthermore, in addition to mutational alterations, another mechanism for inactivating tumor suppressor genes is the methylation of their promoters. This epigenetic gene silencing is also frequently found in cancer cells (Esteller, 2002).

1.2 Rho signaling

Members of the Rho (Ras homology) family are small (20-30 kDa) GTPases, belonging to the Ras superfamily of monomeric GTP-binding proteins. So far, 20 members have been identified and can be divided into eight subfamilies: Rho (RhoA/B/C), Rac (Rac1/2/3 and RhoG), Cdc42 (Cdc42, TCL, TC10), Chp/Wrch, Rnd (Rnd1/2/3), RhoBTB (RhoBTB1/2), RhoD/RhoF and RhoH (Boureux, 2007). Rho GTPases have been implicated in many cellular processes, including actin and microtubule cytoskeleton organization, cell division, motility, cell adhesion, vesicular trafficking, phagocytosis and transcriptional regulation (Jaffe & Hall, 2005).

Most members of the Rho family – except Rnd1/2/3 and RhoH – act as molecular switches. Hence, they cycle between a GDP-bound, inactive and a GTP-bound, active state. Upon growth factor receptor activation or integrin signaling the exchange of GDP for GTP is induced, enabling the interaction with various effector molecules and, thus, triggering the

numerous downstream signaling pathways (Jaffe & Hall, 2005). The affinity of Rho proteins for GDP/GTP is very high with the consequence of a slow dissociation rate of the nucleotides. To ensure a precise spatial-temporal specific signal transduction upon stimulation, the exchange of GDP for GTP requires regulatory molecules, the guanine nucleotide exchange factors (GEFs). By decreasing the nucleotide affinity of Rho proteins GEFs promote the release of GDP, resulting in the subsequent replacement by GTP (Bos et al., 2007). On the contrary, GTPase activating proteins (GAPs) enhance the intrinsic catalytic activity of the small G proteins to hydrolyze the bound GTP, which is itself very weak (Bos et al., 2007). The activities of GAPs convert the Rho proteins back to the GDP-bound, inactive state. For some Rho GTPases a third class of regulators exists: the guanine nucleotide dissociation inhibitors (GDIs). They prevent nucleotide exchange and membrane association of the Rho proteins. The concert activities of GEFs, GAPs and GDIs guarantee the tight regulation of Rho GTPase signaling (Fig.1) (Grise et al., 2009).

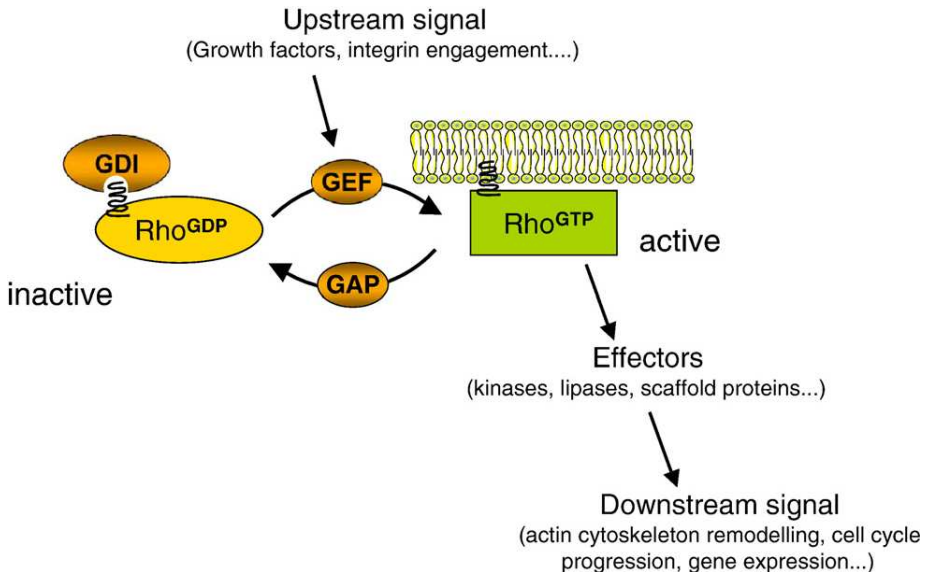

Fig.1: Regulation of Rho GTPases. Rho GTPases cycle between GTP- (active) and GDP- (inactive) bound states. GDIs sequester the GDP-bound GTPase in the cytoplasm. The exchange of GDP to GTP is promoted by GEFs and is associated with translocation of Rho proteins to cell membranes. GTP-bound GTPases interact with a range of effector proteins and modulate their ability to regulate cell behavior. Most Rho proteins show an intrinsic ability to hydrolyze GTP to GDP which can be catalyzed by GAPs. (taken from Grise et al., 2009)

The most prominent and extensively characterized Rho GTPase subfamilies are Rho, Rac and Cdc42, especially with regard to their effects on actin dynamics. Rho is known to induce actin stress fibers and focal adhesion complexes, whereas activation of Rac leads to the formation of lamellipodia and membrane ruffling, and Cdc42 causes the formation of filopodia (Jaffe & Hall, 2005). These processes are key steps in cell adhesion and cell migration and, hence, it is not surprising that deregulation of Rho proteins might contribute to EMT, invasion

and metastasis (Vega & Ridley, 2008). In addition, due to the various other biological functions deregulated signaling of Rho GTPases play also a role in tumor inititation (Jaffe & Hall, 2005). However, no gain- or loss-of-function mutations of Rho GTPases have been identified in human tumors, instead Rho proteins are rather found to be overexpressed (Gomez del Pulgar, 2005). Alternatively, alterations of their regulators might result in the disturbance of Rho GTPase signaling in cancer (Vega & Ridley, 2008).

1.2.1 The emerging family of RhoGAP proteins

As mentioned above, RhoGAPs – defined by a conserved RhoGAP domain of about 150 amino acids, sharing at least 20% homology between family members – play a crucial role in the regulation of Rho GTPases. Their importance is highlighted by the fact that the human genome is predicted to encode up to 80 proteins with a RhoGAP domain which can be divided into distinct subfamilies (Tcherkezian & Lamarche-Vane, 2007). Thus, the number of GAPs is nearly three-fold higher than that of their targets, the Rho proteins. Such overabundance might be explained by tissue-restricted expression, specificity for only a single GTPase and regulation of specific Rho signaling pathways, respectively. In addition, some GAP domains simply serve as a recognition module. Hence, the RhoGAPs act as effector or scaffold proteins, mediating cross-talk between Rho GTPases and other signaling pathways. The involvement in additional pathways is also assisted by their multidomain feature, what makes them not only signal terminators but pivotal players in many biological processes (Tcherkezian & Lamarche-Vane, 2007).

These important regulators are certainly regulated as well. To ensure a stringent regulatory control, numerous mechanisms including protein-protein interactions, lipid binding, phosphorylation and protein degradation affect their catalytic activity, substrate specificity, subcellular distribution and protein level (Bernards & Settleman, 2004).

1.3 The Deleted in Liver Cancer 1 (DLC1) gene

The Deleted in Liver Cancer 1 (DLC1) gene – also designated as ArhGAP7 or StarD12 – was originally identified in 1998 by representational difference analysis (a PCR-based subtractive hybridization technique) as a gene deleted in primary human hepatocellular carcinoma (HCC) and highly homologous to rat p122RhoGAP. Its gene locus was mapped to chromosome 8p22, a region that recurrently shows LOH or heterozygous deletions in

numerous solid tumors and haematological malignancies. Thus, it was proposed that DLC1 is a candidate tumor suppressor (Yuan et al., 1998).

In normal human tissues the protein is ubiquitously expressed (Durkin et al., 2002). Since identification of DLC1 as a protein deleted in liver cancer, its expression was determined in many other tumor types and, indeed, downregulation or even absence was detected in a number of human cancers including breast, colon, ovarian, lung and prostate (Plaumann et al., 2003; Ullmannova & Popescu, 2006; Yuan et al., 2004; Guan et al., 2006). This under-representation is caused by chromosomal deletions and aberrant promoter methylation. Somatic mutations in the coding region are rather uncommon, but have been recently reported (Durkin et al., 2007; Liao et al., 2008).

1.3.1 Structure

The DLC1 gene encodes a 1091 amino acid multidomain protein that consists of three functional domains. The N-terminus builds a sterile alpha motif (SAM) domain, which constitutes a very abundant protein-protein interaction motif. The carboxyterminal steroidogenic acute regulatory (StAR)-related lipid transfer (START) domain is found in 15 mammalian proteins and predicted to interact with and/or transfer lipids by forming a hydrophobic tunnel. However, the ligands for DLC1 START domain remain unknown and its function has to be further determined. The best characterized domain of DLC1 comprises the amino acid residues 639-847. This sequence constitutes a RhoGAP domain, making DLC1 a member of the large RhoGAP domain protein family (Fig. 2) (Durkin et al., 2007). *In vitro* studies revealed GAP activity of DLC1 for all three small GTPases of the Rho subfamily – RhoA, RhoB and RhoC – and to a lesser extent for Cdc42 (Healy et al., 2008). The region between the SAM and RhoGAP domains displays little overall sequence similarity with known protein modules, and large stretches of this middle region are predicted to adopt no globular conformation, conferring flexibility. This sequence is rich in serine residues and computer analysis revealed numerous potential phosphorylation sites. In addition, several proline-rich segments within this region could possibly act as docking sites for proline recognition domains such as Src homology 3 (SH3) modules (Durkin et al., 2007). Another important feature of this large unstructured sequence is a focal adhesion targeting (FAT) motif that mediates the association with the SH2 domain of tensins, a family of focal adhesion proteins (Liao et al., 2007).

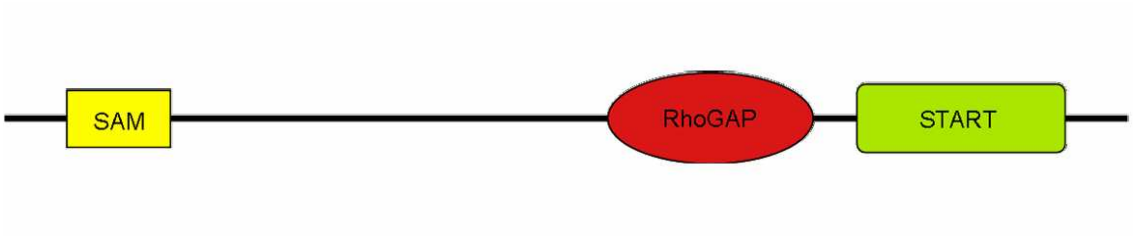

Figure 2: Schematic representation of the DLC1 domain structure. DLC1 is a multidomain protein that contains three globular domains: a C-terminal START domain, an internal RhoGAP domain and a N-terminal SAM domain. The region between SAM and RhoGAP domains is rich in serine residues and predicted to lack a secondary structure.

Since the discovery of DLC1, two closely related genes were identified, sharing the SAM-RhoGAP-START domain organization, namely DLC2 – also called StarD13 – and DLC3 – also known as StarD8. Together they constitute the DLC subfamily of RhoGAP proteins. The highest sequence conservation among these three proteins is found in their RhoGAP domain with 70% sequence identity (Durkin et al., 2007).

1.3.2 Biological function of DLC1 and its pivotal role in cancer

As a protein with GAP activity for small GTPases of the Rho family, a major function of DLC1 is certainly the regulation of cytoskeletal rearrangement and morphological changes. Thus, overexpression of DLC1 induced a rounded morphology and extensive membrane protrusions associated with the disassembly of actin stress fibers and disruption of focal adhesions – processes which are known to be reversely regulated by RhoA (Sekimata et al., 1999; Kim et al., 2007). The impact of such activity is pivotal for the cell fate. Hence, knockout mouse studies revealed an essential role of DLC1 for embryonic development. Homozygous mutant embryos died before 10.5 days post coitum with defects in the neural tube, brain, heart and placenta (Durkin et al., 2005).

Evidence for participation in tumor suppression firstly derived from experiments with ectopic expression of DLC1 in cancer cell lines lacking the endogenous protein. Restoration of DLC1 limited proliferation, colony formation and anchorage-independent growth in soft agar in hepatocellular, breast and lung cancer cell lines (Wong et al., 2005; Yuan et al., 2004; Yuan et al., 2003; Zhou et al., 2004). Furthermore, inhibition of cell proliferation in HCC and renal cell carcinoma cells was associated with the induction of apoptosis (Zhou et al., 2004; Zhang et al., 2009). In nude mice the *in vivo* tumorigenicity was abolished (Yuan et al., 2003). Moreover, DLC1 was defined as a metastasis suppressor in breast cancer cells (Goodison et al., 2005). This role is consistent with re-expression studies, demonstrating the inhibition of migration and invasion in HCC, breast, lung and ovarian cancer cell lines (Wong et al., 2005; Kim et al., 2007; Goodison et al., 2005; Qian et al., 2007; Syed et al., 2005). The

consequences of DLC1 ablation have only recently been investigated. siRNA mediated knockdown in breast cancer cell lines caused a dramatic increase in migration, which is in line with the opposite effects upon overexpression (Holeiter et al., 2008). With the use of a novel mouse model of liver cancer, Xue et al. provided evidence for the *in vivo* function as a bona fide tumor suppressor. They showed that shRNA-induced loss of DLC1 cooperated with c-Myc and p53 deficiency to promote the formation of liver tumors (Xue et al., 2008).

Many studies support the dependency of DLC1 tumor suppressive function on its GAP activity, because they reported that mutants lacking GAP activity were inactive with regard to cell growth inhibition (Wong et al., 2005). In addition, mutational analyis of cDNAs isolated from cancer patient samples detected two mutations within the linker region of DLC1 that resulted in a significant reduction of RhoGAP activity, impairing the suppression of tumor cell growth (Liao et al., 2008). The mechanism of cell motility regulation by DLC1 was further examined and also shown to be GAP dependent. Inactivation of RhoA by DLC1 was demonstrated to take place preferentially at the leading edge of cellular protrusions, inhibiting the activation of the downstream effector Dia1, which in turn results in inhibition of directed cell migration (Healy et al., 2008; Holeiter et al., 2008). Nonetheless, evidence for GAP independent tumor suppressor activities has recently emerged. Thus, the introduction of a GAP-inactive mutant of DLC1 in lung cancer cell lines was also able to reduce colony formation, anchorage-independent growth in soft agar, cell migration and invasion (Healy et al., 2008). Further investigations will be needed to figure out the underlying mechanism and discover possible involved protein interaction partners and signaling pathways.

1.3.3 Regulation

The current knowledge about regulation of DLC1 is very limited. As mentioned before, at the transcriptional level genetic and epigenetic mechanisms contribute to the control of its cellular concentrations. Thus, chromosomal deletion and hypermethylation of its promoter lead to loss of DLC1 expression (Wong et al., 2003; Yuan et al., 2003).

Little is known about the regulation at the protein level. Screening for DLC1 protein interaction partners by a yeast-two-hybrid approach revealed tensins, a focal adhesion protein family of four related members (tensin 1/2/3 and cten) that interact with the cytoplasmic tails of β integrins, as the first binding partners of DLC1 (Yam et al., 2006; Qian et al., 2007; Liao et al., 2007)). The association is mediated by the tensin Src homology 2 (SH2) domain and depends on tyrosine 442 in DLC1 but is phosphorylation independent. Through this interaction DLC1 is targeted to focal adhesions, which is essential for its biological activity (Qian et al., 2007). DLC1 was also reported to localize in caveolae (cholesterol-rich flask shape invaginations of the plasma membrane), where it interacts with

caveolin-1, but the function remains unclear (Yam et al., 2006). By contrast, the recently identified interaction with p120RasGAP, a protein, which promotes the inactivation of Ras, displays a negative regulation of DLC1 function by inhibiting its GAP and growth-suppressing activities (Yang et al., 2009).

Posttranslational modifications such as phosphorylation are a common theme in protein regulation. DLC1 was found to contain several phosphorylated sites by MS analysis (unpublished data of the own group). The role of these modifications has to be further determined. However, two serines within the middle region (Ser327 and Ser431) were shown to be phosphorylated by protein kinase D (PKD), stimulating the association with 14-3-3 proteins. This interaction resulted in the inhibition of DLC1 GAP activity. In addition, DLC1 was found to undergo rapid nucleocytoplasmic shuttling – its nuclear function remains to be determined – and through binding to 14-3-3 adaptors this shuttling was blocked, retaining the protein cytosolic. Thus, 14-3-3 protein interaction reveals an additional mechanism that contributes to regulation of DLC1 activity and compartmentalization (Scholz et al., 2009).

A recent study provides evidence for a novel mechanism of DLC1 regulation. A polybasic region adjacent to the RhoGAP domain was identified to mediate phosphatidylinositol (4,5)-bisphosphate (PIP2) binding, stimulating DLC1 GAP activity and, thus, downregulating Rho signaling (Erlmann, in revision). Hence, also the influence of lipid interaction contributes to the regulation of DLC1 tumor suppressive functions.

Certainly, several additional mechanisms might be involved in activity control, subcellular distribution and protein turn-over. The intrinsic SAM domain, for example, was shown to act as autoinhibitory domain of the RhoGAP activity (Kim et al., 2008). However, it is not known how this inhibition takes place. As SAM domains are conserved protein interaction motifs, one could imagine that association with other proteins might be involved.

1.3.4 The SAM domain of DLC1 – a protein module with high potential

Sterile alpha motif (SAM) domains are putative protein interaction modules that consist of approximately 70 amino acid residues and were initially identified as a conserved sequence found in 14 eukaryotic proteins. The designation derived from their predicted helical structure and the involvement of four of these proteins in yeast sexual differentiation (Ponting, 1995). Today, more than 1300 proteins containing SAM domains have been identified in all eukaryotes and some bacteria. This number is almost comparable with the number of proteins comprising the most common and well-known SH2 domain, highlighting the significance of SAM domains. In contrast to SH2 domains, generally binding to phosphorylated tyrosine residues, SAM domains have no common functional theme. Hence, they are very versatile in their binding properties. Several proteins with SAM domains exist in

a wide range of stoichiometries because of their feature to associate with themselves or other proteins with SAM domains. In addition to homo-SAM or hetero-SAM interactions also the heterotypic binding to non-SAM domain-containing proteins appears. Furthermore, even the interaction with RNA is described. Concordant with such binding diversity also the functional role of SAM domain-containing proteins is very pleiotropic from signal transduction to transcriptional and translational regulation (Qiao & Bowie, 2005).

Despite diverse interaction modes, the majority of the examined SAM domains adopt a uniform structure, consisting of five α-helices organized in a globular manner. Unlike this common feature, a recently published study revealed that the SAM domain of DLC1 – and DLC2, which was shown previously – adopt a unique fold with four nearly parallel α-helices. It was also shown that DLC1-SAM exists in a monomeric form and does not self-associate (Zhong et al., 2009). The role of this motif for DLC1 function is largely unknown. However, as mentioned above, the SAM domain was shown to be autoinhibitory (Kim et al., 2008). On the contrary, Zhong et al. have identified the eukaryotic elongation factor 1A1 (EEF1A1) as a novel binding partner for DLC1-SAM. The association was demonstrated to facilitate the recruitment of EEF1A1 to the membrane periphery and ruffles, thereby modulating cell migration (Zhong et al., 2009). The search for additional protein interaction partners will define the precise role of the SAM domain and, thus, also contribute to the understanding of DLC1 function in general.

1.4 Protein-protein interactions

The approximately 30,000 genes of the human genome are speculated to produce nearly $1x10^6$ proteins. The majority of these proteins do not act in an isolated manner but in concert with other proteins in complexes and networks. Such protein-protein interactions are key elements in all major biological processes, including the formation of macromolecular structures such as the cytoskeleton, cell signaling, gene expression, immune defence and metabolic pathways. Exploring these global protein interaction networks will be a requisite for the understanding of diseases and contributes to the discovery of drugs and new therapeutic strategies (Wells & McClendon, 2007).

Protein interactions are very diverse. They can occur between identical or non-identical polypeptides, forming homo- or heterodimers and, depending on their affinity, they can be transient or permanent (Nooren & Thornton, 2003). The forces that stabilize the association comprise hydrogen bonds, van der Waals forces, dipole, ionic and hydrophobic interactions (Reichmann et al., 2007). Often, conserved protein interaction motifs like SH2 or SAM

domains mediate the binding. A tight regulation of each interaction is given by modulation upon posttranslational modifications such as phosphorylation, acetylation or methylation. Also, the subcellular distribution influences the possibility of association. In addition, the interaction with a ligand may have impact on protein interactions. Thus, the GTP binding of Rho proteins provokes a conformational change, allowing the interaction with downstream signaling molecules (Vetter & Wittinghofer, 2001). The resulting effects from protein interconnections include alterations of kinetic enzyme properties, substrate channelling, creation of new binding sites, inactivation of proteins, change of substrate specificity or regulation of upstream or downstream action (Phizicky & Fields, 1995).

Because of the various aspects of protein-protein interactions, there are many approaches to investigate them. As a first step, the new binding partner for a protein of interest has to be identified. For that, several standard, biochemical methods such as coimmunoprecipitation or GST-pulldown assays, following 2D gel electrophoresis and mass spectrometry, are exerted. Another genetic technique, which is often used for screening of new protein interactions, is the yeast-two-hybrid system. In the second step, the association has to be further characterized. Beside the physical basis and determination of thermodynamic and energetic parameters, it is of particular interest to examine the function of the interaction.

1.4.1 The yeast-two-hybrid system

A milestone in proteomic research was the generation of a genetic system to study protein interactions in the yeast *Saccharomyces cerevisiae*; the yeast-two-hybrid approach. The basal concept of this technique takes advantage of the modularity of eukaryotic transcription factors. They consist of at least two domains, one, mediating the binding to a promoter DNA sequence, and a second, activating transcription (Hope & Struhl, 1986). The isolated domains are incapable of activating transcription unless physically, but not necessary covalently associated with the additional domain. So, in the yeast-two-hybrid technology a bait protein is fused to the DNA binding domain of a transcription factor – the most extensively used is the yeast GAL4 transcription activator - and a prey protein is fused to the appropriate activation domain. After expression of these two chimeras in yeast, the physical interaction with each other reconstitutes the functional transcription factor, leading to the activation of reporter genes, which is often measurable by growth under selective conditions or a color signal, resulting from the enzymatic activity of β-galactosidase (Fig. 3) (Fields & Song, 1989).

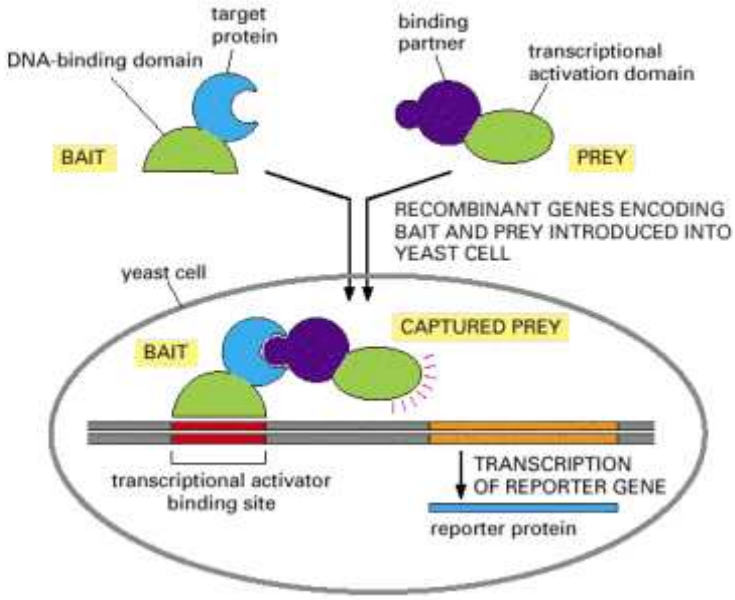

Figure 3: The yeast-two-hybrid approach. A target protein fused to the DNA binding domain of a yeast transcription factor is co-transfected with a prey consisting of the activation domain of the transcription factor and a putative binding partner of the target protein. Upon association of the target protein with its binding partner the transcription factor is reconstituted and activates the transcription of reporter genes. © 2002 by Bruce Alberts, Alexander Johnson, Julian Lewis, Martin Raff, Keith Roberts, and Peter Walter

A bait protein can be screened against genomic or cDNA prey libraries, expressing all encoded or expressed proteins in the organism or tissue of interest. The yeast-two-hybrid methodology is efficient and convenient to use. Actually, a majority of published protein-protein interactions are derived from yeast-two-hybrid screens (Suter et al., 2008).

Beside the many advantages of a fast and inexpensive screening for novel protein binding partners, the original yeast-two-hybrid system shows some limitations. For example, the two fusion proteins need to be targeted to the nucleus, which might be problematic for integral membrane or membrane-associated proteins due to their hydrophobic nature and non-nuclear localization. Furthermore, some interactions depend on posttranslational modifications that do not, or inappropriately, occur in yeast (Van Criekinge & Beyaert, 1999). To overcome these limitations, a multitude of variants have emerged. The split-ubiquitin system constitutes the basis for membrane yeast-two-hybrid systems. Prey and bait proteins are fused to either the C-terminal fragment of ubiquitin or the N-terminal fragment, respectively. Upon interaction in the cytosol, functional ubiquitin is reconstituted, which leads to the cleavage by endogenous ubiquitin-specific proteases and the release of a transcription factor (fused to the C-terminal ubiquitin fragment), activating reporter gene expression (Miller et al., 2005). The yeast tribrid system was firstly demonstrated for the detection of tyrosine phosphoprotein SH2 interactions involved in IgE receptor signaling. In this approach a third component, a specific cytosolic tyrosine kinase, was coexpressed with the prey and bait. Thus, tyrosine phosphorylation lacking in yeast could occur (Osborne et al., 1995). In principle, this system can be adapted to study protein-protein interactions, requiring any posttranslational modification. In this context, also the development of mammalian two-hybrid systems is helpful to overcome the failure of posttranslational modifications (Luo et al.,

1997). However, without the improvement of manipulating mammalian cell lines and parallel analysis of human cells in arrays mammalian two-hybrid methodologies are difficult to adapt for large-scale screenings (Suter et al., 2008).

1.5 The phosphatase and tensin homolog deleted on chromosome 10 (PTEN)

Mapping of homozygous deletions on human chromosome 10q23, a region with frequent occurrence of LOH, especially in late-stage tumors of the brain, breast and prostate, led to the identification of the phosphatase and tensin homolog (PTEN – at first also designated as MMAC1, mutated in multiple advanced cancers 1, or TEP1, TGF-β regulated and epithelial cell enriched phosphatase 1) as the relevant tumor suppressor gene (Li & Sun, 1997, Steck et al., 1997). Today, it is known that PTEN is the second most frequently mutated gene in human cancer after p53, emphasizing its crucial role in the prevention of cancerogenesis (Yin & Shen, 2008).

1.5.1 Structure

The PTEN gene encodes a 403 amino acid peptide with extensive homology to tensin and protein tyrosine phosphatases (Li & Sun, 1997). The protein comprises two major domains: an N-terminal domain with catalytic activity and a C-terminal domain (Lee et al., 1999). The catalytic activity of PTEN consists in the dephosphorylation of both lipid substrates as well as of serine/threonine and tyrosine residues of proteins. Thus, PTEN functions as a dual-specificity phosphatase. The carboxyterminus contains a C2 domain, interacting in a Ca^{2+}-independent manner with phospholipids, and a tail region including a consensus PDZ binding motif (Fig. 4) (Myers et al., 1997; Maehama & Dixon, 1998). In recent years, it turned out that this C-terminal domain is not only implicated in regulation and localization but also exhibits important functions for the tumor suppressive activity of PTEN (Raftopoulou et al., 2004; Shen et al., 2007).

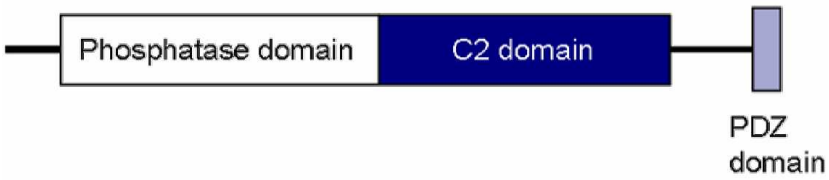

Figure 4: Modular architecture of PTEN. The N-terminus contains a catalytic domain with phosphatase activity for lipids and proteins. The following C2 domain interacts with phospholipids in a Ca^{2+}-independent manner. The C-terminal tail region harbors a PDZ binding motif which contributes to plasma membrane recruitment.

1.5.2 Cellular functions – more than the AKT pathway

The primary target for the lipid phosphatase activity of PTEN is the lipid second messenger phosphatidylinositol (3,4,5)-trisphosphate (PIP3), a key signaling component of the phosphoinositol 3-kinase (PI3K) pathway (Maehama & Dixon, 1998). Upon stimulation of receptor tyrosine kinases or G-protein coupled receptors, class I PI3K family members are activated to catalyze the conversion of PIP2 to PIP3, enabling the plasma membrane recruitment of PH-domain containing proteins such as Akt/PKB and PDK-1 and, thus, leading to the activation of other downstream signaling molecules. By removing the D3 phosphate from PIP3, generating PIP2, PTEN directly antagonizes the catalytic activity of PI3K, thereby inhibiting signals for growth, proliferation, metabolism and cell survival (Fig. 5) (Engelman et al., 2006).

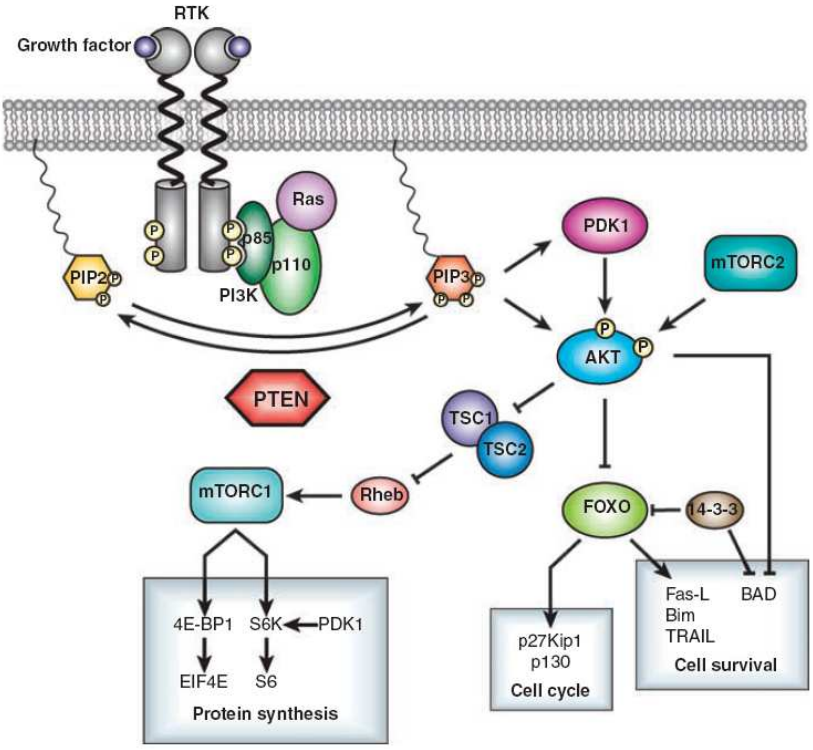

Figure 5: Simplified representation of the PI3K pathway. Upon growth factor stimulation PI3K is activated to catalyze the conversion of PIP2 to PIP3 following the recruitment of PDK-1 and Akt/PKB to the plasma membrane via their PH domains. Phosphorylation of Akt/PKB leads to phoshorylation of downstream effector molecules, resulting in cell growth, proliferation and cell survival. (Taken from Endersby & Baker, 2008)

Although Akt/PKB signaling is thought to be the predominant target, PTEN has been implicated in other pathways and lipid phosphatase-independent roles have been reported. Thus, a recent study revealed an association with the JNK signaling pathway (Vivanco et al., 2007).

PTEN phosphatase also targets different proteins. An inhibitory effect on integrin-mediated cell spreading and cell migration was shown to be the result of the direct association and dephosphorylation of focal adhesion kinase (FAK) and $p130^{Cas}$, a downstream effector of FAK (Tamura et al., 1998). Raftopoulou et al. demonstrated that the lipid phosphatase activity is dispensable for the inhibition of cell motility but the C2 domain plays an important role (Raftopoulou et al., 2004). However, in $PTEN^{-/-}$ cells the phosphorylation status of FAK and $p130^{Cas}$ remain unaffected, suggesting that PTEN is not a sole regulator of FAK/$p130^{Cas}$ (Liliental et al., 2000). Interestingly, PTEN null cells indeed exhibit enhanced cell motility but due to an upregulation of the two small GTPases Rac1 and Cdc42, and in this case the lipid phosphatase activity seems to be involved (Liliental et al., 2000). Furthermore, PTEN also interacts with receptor tyrosine kinases such as the platelet-derived growth factor receptor (PDGFR) and directly dephosphorylates the receptor (Mahimainathan & Choudhury, 2004).
In addition to a cytoplasmic localization and a mainly membrane associated activity, a pool of PTEN is also found in the nucleus, depending on cell cycle stage and differentiation status (Ginn-Pease & Eng, 2003). Here, a role in the maintenance of chromosomal integrity is proposed. PTEN was found to associate with the centromere by interaction with CENP-C which is required for proper kinetochore assembly and for the metaphase to anaphase transition during mitosis. Additionally, PTEN is able to regulate the transcription of Rad51, a key protein involved in double-strand breaks (Shen et al., 2007). Also, the modulation of activity and stability of p53 contributes to its important nuclear functions (Li et al., 2006).

1.5.3 Regulation of PTEN

PTEN is subject to various regulatory mechanisms, governing protein levels, activity, localization, binding partners and function.
Several studies revealed numerous transcription factors to upregulate PTEN transcription, including the peroxisome proliferation-activated receptor γ (PPARγ), the early growth-regulated transcription factor 1 (EGR1) and p53 (Patel et al., 2001; Virolle et al., 2001; Stambolic et al., 2001). However, although the induction of PTEN expression might be an important mechanism, a robust constitutive expression level is essential at all times (Salmena et al., 2008).
PTEN is modulated by multiple posttranslational modifications. Thus, acetylation as well as oxidation lead to the reduction of its activity (Okumara et al., 2006; Ross et al., 2007). In addition, a very important mechanism of regulation is the phosphorylation of a cluster of serine and threonine residues in the carboxyterminus of the protein. Casein kinase 2 (CK2), glycogen synthase kinase 3β (GSK3β) and probably additional kinases are implicated in this phosphorylation which renders the protein in a “closed” state (Torres & Pulido, 2001; Al-

Khouri et al., 2005). The phosphorylated C-terminus is proposed to interact with the internal C2 and phosphatase domain, serving as a pseudosubstrate and therefore causing auto-inhibition and keeping PTEN in the cytoplasm. After dephosphorylation, in which PTEN itself is thought to be involved (Raftopoulou et al., 2004), the C2 domain is more exposed, allowing translocation to the membrane and increasing catalytic activity (Fig. 6) (Odriozola, 2007).
In contrast to phosphorylation of the C-terminal residue cluster, leading to a more stable but inactive protein, PTEN is also phosphorylated at additional sites, promoting its degradation (Maccario et al., 2007).

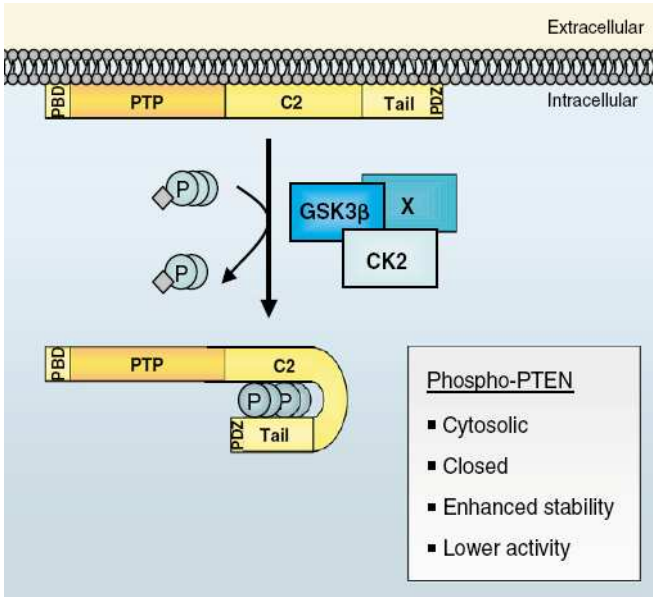

Figure 6: Regulation of PTEN by phosphorylation. Phosphorylation of PTEN in the C-terminus by GSK3β, CK2 and possibly other kinases causes the intramolecular interaction of the C-terminal tail with the C2 domain inducing a closed conformation and a predominantly cytosolic localization that inhibit PTEN activity but increase protein stability. (Taken from Tamguney & Stokoe, 2007

The interaction with other proteins also affects subcellular distribution and stability of PTEN. Hence, the association with members of the membrane-associated guanylate kinase inverted family (MAGI) via the PDZ binding motif results in stabilization (Wu et al., 2000) but also promotes membrane recruitment (Takahashi et al., 2006). Lipid binding plays an additional role in targeting PTEN to the membrane (Das et al., 2003; Vazquez et al., 2006).
A recent study revealed neural precursor expressed, developmentally downregulated 4-1 (NEDD4-1) as the first E3 ubiquitin ligase, promoting the proteasomal degradation of PTEN (Wang et al., 2007). Intriguingly, ubiquitination of PTEN means more than protein degradation. Beside polyubiquitination of PTEN followed by its degradation, NEDD4-1 also catalyzes monoubiquitination, promoting nuclear import (Trotman et al., 2007).

1.5.4 Perturbations of PTEN signaling

Due to the feature of PTEN to influence multiple crucial cellular processes, aberrant expression plays a critical role in the pathogenesis of numerous diseases such as diabetes, autism and cancer (Keniry & Parsons, 2008).

Germline mutations of PTEN cause various autosomal dominant disorders, including Cowden disease, Bannayan-Riley-Ruvalcaba syndrome and Lhermitte-Duclos disease, which are characterized by developmental disorders, neurological deficits, benign hamartomas and an increased risk of breast, thyroid and endometrial cancers (Salmena et al., 2008). As mentioned above, PTEN belongs to one of the most frequently mutated tumor suppressor genes. Genetic alteration of both PTEN alleles occurs in nearly all types of human cancers examined, with inactivation usually due to mutation accompanied by LOH (Kim & Mak, 2006). These genetic alterations range from point mutations – encoding mostly unstable and/or catalytically inactive proteins – to large chromosomal deletions (Steck et al., 1997; Georgescu et al., 2000). In addition, structural rearrangements within the PTEN gene – intragenic inversions, insertions, deletions and duplications known as gross PTEN mutations – are also among the observed mutations and occur in basal-like breast cancer (Saal et al., 2008). Aside from the genetic modification of PTEN, mechanisms such as DNA methylation, transcriptional repression and micro-RNA-directed mRNA degradation and translational disruption diminish PTEN expression in numerous tumors (Wiencke et al., 2007; Yang et al., 2008). Mouse models further illustrate the importance of PTEN in cancer. Homozygous deletion causes early embryonic lethality due to developmental defects in the mesoderm, endoderm and ectoderm (Di Cristofano et al., 1998; Podsypanina et al., 1999). Mice heterozygous for PTEN loss develop a broad range of tumors, including mammary, thyroid, endometrial and prostate cancers (Di Cristofano et al., 1998; Podsypanina et al., 1999; Stambolic et al., 2000). Conditional deletion of the PTEN gene in the mammary gland caused excessive ductal branching, precocious lobuloalveolar development and delayed involution. By 10 months of age, 50% of these mice (n=37) developed breast tumors (Li et al., 2002). These results suggest that PTEN is a haploinsufficient tumor suppressor gene, at least in specific mouse tissues. In addition, this assumption is corroborated by a hypomorphic mouse mutant series, in which PTEN dose is progressively decreased below heterozygous levels. The occurrence of invasive prostate cancer inversely correlated with cellular levels of PTEN protein, demonstrating a dose-dependent role in tumor suppression (Di Cristofano et al., 2001). Whether PTEN is also a haploinsufficient tumor suppressor gene in humans remains elusive. The inconsistent occurrence of monoallelic mutation of PTEN (30-40%) and biallelic loss (5%) in breast cancer provides support for such a notion. For other tumor types such as prostate cancer similar observations have been made (Salmena et al., 2008). However, the long latency observed in different mouse models suggests that PTEN is not sufficient for tumor initiation and requires additional mutations. Hence, a recently published study reported that combination of PTEN loss with expression of an activated ErbB2 resulted in the accelerated formation of breast cancer (Dourdin et al., 2008).

1.6 Liprin beta2

1.6.1 The liprin protein family

Liprin beta2 belongs to the family of leukocyte common-antigen-related (LAR) transmembrane tyrosine phosphatase-interacting proteins. This family consists of six mammalian members that can be subdivided into four alpha- and two-beta type isoforms. Liprin alpha1 as well as both beta subfamily members are broadly expressed in human tissue, whereas liprin alpha2 and liprin alpha3 expression is predominantly found in the brain. Liprin alpha4 shows the highest expression in muscle (Serra-Pages et al., 1998, Zürner & Schoch, 2009).

A notable feature of liprins is the high degree of sequence conservation within the C-terminal region which is designated as liprin homology (LH) domain and composed of three SAM domains. The N-termini of these proteins are predicted to form coiled-coil regions (Serra-Pages et al., 1998). Furthermore, they also contain a PDZ binding motif at their very C-terminus (Fig. 7).

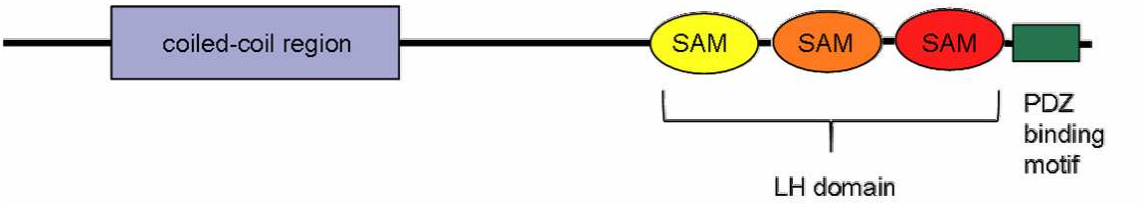

Figure 7: The overall structure of liprin proteins. The highly conserved C-terminus of liprins consists of three SAM domains forming the LH domain and a PDZ binding motif. The N-terminus is predicted to form coiled-coil regions mediating homodimerization of the proteins.

Via the coiled-coil regions liprins are able to homodimerize or heterodimerize only with the members of the same subfamily. In contrast, the LH domains mediate heterodimerization between alpha and beta isoforms. Thus, liprins are multivalent proteins that form complex structures. Additionally, alpha-type liprins interact with the LAR subfamily of receptor protein-tyrosine phosphatases (RPTPs) via their LH domain. This interaction was firstly discovered by searching for candidate proteins binding the cytoplasmic region of LAR (Serra-Pages et al., 1995). Liprin alpha1 was found as an interacting partner and colocalization was observed at the discrete ends of focal adhesions. Afterwards, the association of LAR with the other alpha–type but not with both beta-type liprins was demonstrated (Serra-Pages et al., 1998). It was shown that liprin alpha2 altered the cellular distribution of LAR in COS cells, suggesting that liprin expression modifies LAR localization. The influence of the two beta isoforms on LAR function is not well understood, but the capability of heterodimerization with their alpha-

type family members proposes an indirect regulation. Yet, it is unknown, whether alpha liprins can simultaneously bind LAR subfamily RPTPs and beta liprins, or whether the RPTPs and beta liprins compete for alpha liprin binding. Thus, a positive, activating as well as a negative, inhibitory influence could be assumed.

1.6.2 The LAR subfamily of RPTPs

The LAR subfamily of RPTPs is classified as receptor type IIa protein-tyrosine phosphatases (Andersen et al., 2001) and composed of three vertebrate homologs: LAR, PTP-σ and PTP-δ. PTP-σ and -δ are predominantly expressed in the nervous system, whereas LAR is also expressed in basal lamina-associated epithelial tissues (Schaapveld et al., 1998). The structures of all highly resemble that of the other two members. The large extracellular domains of LAR-RPTPs generally consist of three immunoglobulin-like (Ig-like) domains and four to eight fibronectin type III (FNIII) domains, depending on alternative splicing which is spatially and temporally regulated (Pulido et al., 1995). A hydrophobic transmembrane region is followed by two cytosolic protein-tyrosine phosphatase domains, a membrane proximal (D1) and a membrane distal (D2). It was shown that only D1 is catalytic active while D2 seems to have a more regulatory function (Streuli et al., 1990).

As the resemblance of their extracellular regions to cell adhesion molecules (CAMs) suggests, they are involved in adhesion signaling by transducing extracellular signals into intracellular signaling pathways. Except PTP-δ which mediates only homophilic cell-cell adhesion, the other two family members are also able to act as heterophilic receptors. Thus, for LAR, the laminin-nidogen complex was found as one ligand (O´Grady et al., 1998). The signal transduction pathways downstream of the LAR-RPTPs are mainly unknown but involve cytoskeleton remodeling. For LAR, Trio, a large multidomain protein with guanine nucleotide exchange factor domains for Rac1 and RhoA, was found as a binding partner (Debant et al., 1996). By regulation of this protein actin polymerization and focal adhesion assembly are affected upon LAR activation.

LAR plays an important role in E-cadherin-dependent cell-cell communication. By association and direct dephosphorylation of beta-catenin the pool of free cytoplasmic beta-catenin is kept low which prevents the disruption of the cadherin-catenin complex. In the human breast cancer cell line MCF7 the expression of LAR increased with cell density confirming its function in the maintenance of contact inhibition (Symons et al., 2002). Furthermore, suppression of cell migration due to reduced levels of free phosphorylated beta-catenin was shown (Müller et al., 1999). In addition, another substrate of LAR is the death-associated protein kinase (DAPK). Stimulation of this kinase by LAR-mediated dephosphorylation leads to the inhibition of cell adhesion/migration and promotes apoptosis (Wang et al., 2007).

Beside the predominant function of LAR-RPTPs in the nervous system, promoting axonal guidance and neuronal growth, $LAR^{-/-}$ mice revealed the importance of these receptors for mammary gland development and function. Females of these mice were incapable of delivering milk due to an impaired terminal differentiation of alveoli at late pregnancy when LAR expression normally elevates (Schaapveld et al., 1997). Interestingly, LAR expression is significantly increased in breast cancer (Yang et al., 1999) and might correlate with breast cancer metastatic prognosis (Levea et al., 2000), providing a role in malignant transformation.

1.6.3 Cellular role of liprin proteins

Since their characterization in 1995, the main research on liprins was focused on their activity in the nervous system where they are essential for axonal guidance, trafficking of synaptic vesicles and the formation of a functional presypnaptic active zone in cooperation with LAR by recruiting and stabilizing a vast array of proteins (Fig. 8) (Stryker & Johnson, 2007).

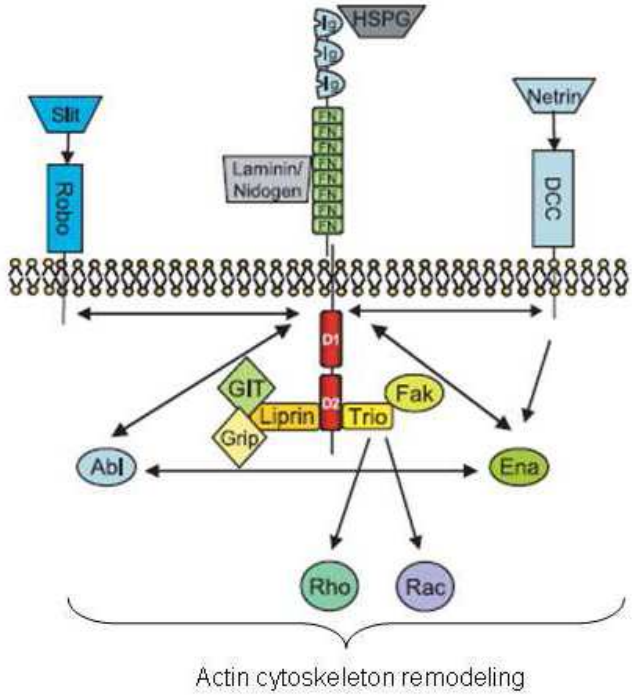

Figure 8: The LAR-liprin network. Possible interactions between LAR, liprins and effectors of actin cytoskeleton remodeling in the growth cone are presented. (Taken from Chagnon et al., 2004)

In recent years, additional functions of the liprin proteins have emerged. For example, the metastasis-associated protein S100A4 (Mts1) was shown to interact with liprin beta1 (Kriajevska et al., 2002). This protein is involved in the modulation of cell motility, invasiveness, angiogenesis and p53-dependent apoptosis and is highly expressed in metastatic tumors. However, the mechanism of the interplay with liprin beta1 remains

elusive. For liprin alpha1 an association with the candidate tumor suppressor Inhibitor of growth 4 (ING4) was described. Both proteins colocalize and interact in lamellipodia, inhibiting cell motility and, thus, preventing invasion and metastasis (Shen et al., 2007).

1.7 Goals

The aim of this work was to identify novel protein interaction partners of the tumor suppressor DLC1 to get further insights into mechanisms of its regulation, activity and/or crosstalk with other signaling pathways. Therefore, a yeast-two-hybrid screen was performed, using the SAM domain of DLC1 as bait and a human mammary gland cDNA library as a prey. After isolation and sequencing of positive yeast clones, the interaction between DLC1 and PTEN – one of the putative candidates – was characterized biochemically and their functional relationship was investigated. Finally, the work focused on the association of DLC1 with a second putative binding partner; liprin beta2.

2 Material and Methods

2.1 Materials

2.1.1 Chemicals and Consumables

Acrylamide (Rotiphorese Gel 30)	Carl Roth GmBH & Co., Karlsruhe, Germany
L-Adenine hemisulfate salt	Sigma-Aldrich, Taufkirchen, Germany
Agar	Carl Roth GmBH & Co., Karlsruhe, Germany
Agarose	Carl Roth GmBH & Co., Karlsruhe,Germany
Ammonium persulfate (APS)	Carl Roth GmBH & Co., Karlsruhe, Germany
Ampicillin	Sigma-Aldrich, Taufkirchen, Germany
L-Arginine HCL	Sigma-Aldrich, Taufkirchen, Germany
3-AT (3-amino-1,2,4-triazole)	Sigma-Aldrich, Taufkirchen, Germany
β-glycerophosphate	Sigma-Aldrich, Taufkirchen, Germany
β-Mercaptoethanol (βME)	Sigma-Aldrich, Taufkirchen, Germany
Blocking reagent	Roche Diagnostics, Basel, Switzerland
Blotting Paper, 3MM	Whatmann, Schleicher Schuell, Dassel, Germany
Bovine Serum Albumin (BSA)	Sigma-Aldrich, Taufkirchen, Germany
5-Brom-4-chlor-3-indolyl-β-D-galactopyranoside (X-Gal)	Carl Roth GmbH & Co., Karlsruhe, Germany
Bromphenol blue	Serva, Heidelberg, Germany
Biodyne® Nylon Transfer Membrane	PALL, Ann Arbor, MI, USA
Cell culture flasks and dishes	Greiner, Frickenhausen, Germany
Crystol violet	Merck, Darmstadt, Germany
Difco peptone	Carl Roth GmbH & Co., Karlsruhe, Germany
Dimethyl sulfoxide (DMSO)	Carl-Roth GmBH & Co., Karlsruhe, Germany
Dithiothreitol (DTT)	Carl-Roth GmBH & Co., Karlsruhe, Germany
DNAorange	Sigma-Aldrich, Taufkirchen, Germany
Dropout (DO) Supplements	Carl Roth GmbH & Co., Karlsruhe, Germany
Ethanol	VWR, Darmstadt, Germany
Ethidium bromide	Roche Diagnostics, Basel, Switzerland
Ethylene di-amine tetra-acetic acid (EDTA)	Sigma-Aldrich, Taufkirchen, Germany
Fluoromount-G	Southern Biotechnology, Birmingham, UK
Gene Ruler 1 kb Ladder	MBI Fermentas, St. Leon-Rot, Germany

D-Glucose	Carl Roth GmbH & Co., Karlsruhe, Germany
Glass beads, acid-washed	Sigma-Aldrich, Taufkirchen, Germany
Glutathione Sepharose beads	GE Healthcare, Munich, Germany
Glycerol	Carl-Roth GmbH & Co., Karlsruhe, Germany
Glycine	Carl-Roth GmbH & Co., Karlsruhe, Germany
Goat Serum	Invitrogen/ Gibco, Auckland, New Zealand
HEPES (4-(2-hydroxyethyl)-1-piperazineethanesulfonic acid)	Carl-Roth GmbH & Co., Karlsruhe, Germany
HRP SuperSignal®West substrate pico	Pierce Biotechnology, Rockford, USA
HRP SuperSignal®West substrate dura	Pierce Biotechnology, Rockford, USA
L-Histidine HCL monohydrate	Sigma-Aldrich, Taufkirchen, Germany
Imidazole	Merck Biosciences, Darmstadt , Germany
L-Isoleucine	Sigma-Aldrich, Taufkirchen, Germany
Isopropanol	Carl Roth GmbH & Co., Karlsruhe, Germany
Isopropyl-β-D-thiogalactopyranoside (IPTG)	Carl Roth GmbH & Co., Karlsuhe, Germany
Kanamycin	Carl Roth GmbH & Co., Karlsruhe, Germany
KCl	Carl-Roth GmbH & Co., Karlsruhe, Germany
L-Leucine	Sigma-Aldrich, Taufkirchen, Germany
Lithium acetate (LiAc)	Carl Roth GmbH & Co., Karlsruhe, Germany
L-Lysine	Sigma-Aldrich, Taufkirchen, Germany
Methanol	Carl-Roth GmbH & Co., Karlsruhe, Germany
L-Methionine	Sigma-Aldrich, Taufkirchen, Germany
Magnesium chloride ($MgCl_2$)	Carl-Roth GmbH & Co., Karlsruhe, Germany
Medical X-ray film	CEA, Strangnas, Sweden
NP-40 (Nonidet P40)	Sigma-Aldrich, Taufkirchen, Germany
“PageRuler” prestained protein ladder	MBI Fermentas, St. Leon-Rot, Germany
Paraformaldehyde (PFA)	Electron Microscopy Science, Hatfield, USA
Passive lysis buffer for luciferase reporter assay	Promega, Mannheim, Germany
L-Phenylalanine	Sigma-Aldrich, Taufkirchen, Germany
Phenylmethylsulphonyl fluoride (PMSF)	Sigma-Aldrich, Taufkirchen, Germany
Polyethylene glycol 4000	Merck, Darmstadt, Germany
Polyvinylidene difluoride membrane (PVDF)	Carl Roth GmbH & Co., Karlsruhe, Germany
Protein G Sepharose	GE Healthcare, Munich, Germany

Puromycin	Calbiochem, San Francisco, USA
RIA vials	Sarstedt AG, Nürnbrecht, Germany
RNAse A	Applichem, Darmstadt, Germany
Salmon Sperm carrier DNA	Sigma-Aldrich, Taufkirchen, Germany
Sodium azide	Sigma-Aldrich, Taufkirchen, Germany
Sodium chloride	Carl Roth GmbH, Karlsruhe, Germany
Sodium dodecyl sulfate (SDS)	Carl Roth GmbH & Co., Karlsruhe, Germany
Sodium fluoride	Carl Roth GmbH & Co., Karlsruhe, Germany
Sodium orthovanadate	Sigma-Aldrich, Taufkirchen, Germany
Tetramethyldiethyldiamine (TEMED)	Sigma-Aldrich, Taufkirchen, Germany
Thiozolylblue tetrazolium bromide (MTT)	Sigma-Aldrich , Taufkirchen, Germany
L-Threonine	Sigma-Aldrich, Taufkirchen, Germany
Tris-(hydroxymethyl)-aminomethane (Tris)	Carl Roth GmbH & Co., Karlsruhe, Germany
Triton X-100	Carl Roth GmbH & Co., Karlsruhe, Germany
L-Tryptophan	Sigma-Aldrich, Taufkirchen, Germany
Tween-20	Carl Roth GmbH & Co., Karlsruhe, Germany
L-Tyrosine	Sigma-Aldrich, Taufkirchen, Germany
L-Uracil	Sigma-Aldrich, Taufkirchen, Germany
L-Valine	Sigma-Aldrich, Taufkirchen, Germany
Yeast extract	Carl Roth GmbH & Co., Karlsruhe, Germany
Yeast nitrogen base without amino acids	Difco™ (Becton and Dickinson), Lawrence, Kansas, USA

2.1.2 Kits

DC Protein Assay Kit	Biorad, Munich, Germany
First Strand cDNA Synthesis Kit	MBI Fermentas, La Jolla, CA, USA
PureLink™HiPure Plasmid DNA Purification Kit for Midi preparation of plasmid DNA	Invitrogen, Karlsruhe, Germany
PureLink™ HiPure Plasmid Gigaprep Kit	Invitrogen, Karlsruhe, Germany
PureLink™ PCR Purification Kit	Invitrogen, Karlsruhe, Germany
PureLink™ Quick Gel Extraction Kit	Invitrogen, Karlsruhe, Germany
PureLink™ RNA Micro Kit	Invitrogen, Karlsruhe, Germany
QIAprep Spin Miniprep Kit	QIAGEN, Hilden, Germany
REDTaq® ReadyMix™ PCR Reaction Mix	Sigma-Aldrich, Taufkirchen, Germany

2.1.3 Enzymes

Calf Intestine Alkaline Phosphatase (CIAP)	MBI Fermentas, St. Leon-Rot, Germany
PfuUltra^{TM} High-Fidelity DNA Polymerase AD	Stratagene, La Jolla, CA, USA
Restriction enzymes	MBI Fermentas, St. Leon-Rot, Germany
T4 DNA Ligase	MBI Fermentas, St. Leon-Rot, Germany

2.1.4 Oligonucleotides

All primers and siRNAs were obtained from MWG Biotech AG, Ebersberg, Germany.

Primers

ADInsert Screen-F	5´-CTA TTC GAT GAT GAA GAT ACC CCA CCA AAC C-3´
ADInsert Screen-R	5´-GTG AAC TTG CGG GGT TTT TCA TGA TCT ACG AT-3´
BamHI-DLC1-F	5'-CGC GGA TCC TGC AGA AAG AAG CCG GAC CC-3'
BamHI-DLC1-ΔSAM-F	5'-CGC GGA TCC ATT AGT CCT CAT CGG AAA CGA AG-3'
BamHI-LB1-F	5´-CGC GGA TCC ATG ATG AGT GAT GCA AGT GAC AT-3`
BamHI-LB2-F	5´-CGC GGA TCC GCT TCT GAT GCT AGT CAT GCG C-3´
BamHI-PTEN-F	5´-CGC GGA TCC ACA GCC ATC ATC AAA GAG ATC-3´
BamHI-PTEN-ΔCat-F	5´-CGC GGA TCC GTG TAT TAT TAT AGC TAC CTG TTA AAG-3´
DLC1-BamHI-R	5'- CGC GGA TCC TCA CCT AGA TTT GGT GTC TTT GG-3'
DLC1-K714E-F	5´-CGT GGC AGA CAT GCT GGA GCA GTA TTT TCG AG-3´
DLC1-K714E-R	5´- CTC GAA AAT ACT GCT CCA GCA TGT CTG CCA CG-5´
DLC1-rtpcr-F	5´-AGC CCC TGC CTC AAA GTA TT-3´
DLC1-rtpcr-R	5´-ATG GGC GTC ATC TGA TTC TC-3`
DLC1-SAM-BamHI-R	5´-CGC GGA TCC TCA ACT TCG TTT CCG ATG AGG AC-3´
DLC1-SAM-XhoI-R	5´-CGC CTC GAG TCA ACT TCG TTT CCG ATG AGG ACT-3´
EcoRI-DLC1-F	5´-CCG GAA TTC TGC AGA AAG AAG CCG GAC AC-3´
EcoRI-LA1-F	5´-CCG GAA TTC TAT GAT TGT CGA GGT GAT GCC-3´
GAPDH-rtpcr-F	5´-CCC CTT CAT TGA CCT CAA CTA-3`
GAPDH-rtpcr-R	5´-CGC TCC TGG AAG ATG GTG AT-3`
LA1-EcoRI-R	5´-CCG GAA TTC TTA GCA GGA GTA AGT CCT GAC TG-3´
LB1-BamHI-R	5´-CGC GGA TCC TCA AAC GTT TGA GTC TTC ATC TG-3´
LB2-BamHI-R	5´-CGC GGA TCC TCA GCT AAT CTG TCC CAC CTG G3´

LB2-rtpcr-F	5´-TTG AGA CCC AGA AGC TCG AT-3´
LB2-rtpcr-R	5´-TGG TTT AAC AGC CCC GTA AG-3´
PTEN-BamHI-R	5´-CGC GGA TCC TCA GAC TTT TGT AAT TTG TGT ATG CTG-3´
PTEN-C124S-F	5´-GTT GCA GCA ATT CAC AGT AAA GCT GGA AAG GGA CG-3´
PTEN-C124S-R	5´-CGT CCC TTT CCA GCT TTA CTG TGA ATT GCT GCA AC-3´
PTEN-S385A-F	5´-CTG ACA CCA CTG ACG CTG ATC CAG AGA ATG-3´
PTEN-S385A-R	5´-CAT TCT CTG GAT CAG CGT CAG TGG TGT CAG-3´
PTEN-ΔC-BamHI-R	5´-CGC GGA TCC TCA CTC CTC TAC TGT TTT TGT GAA G-3´
PTEN-ΔPDZ-BamHI-R	5´-CGC GGA TCC TCA ATC TTC ATC AAA AGG TTC ATT TCT-3

siRNAs

siDLC1 #1	5'-GGA CAC GGU GUU CUA CAU C dTdT-3'
siDLC1 #2	5´-UUA AGA ACC UGG AGG ACU A dTdT-3´
siLacZ	5'-GCG GCU GCC GGA AUU UAC C dTdT-3'
siPTEN #1	5´-AAC AGU AGA GGA GCC GUC AAA dTdT-3´
siPTEN #2	5´-CGU UAG CAG AAA CAA AAG GAG dTdT-3´

2.1.5 cDNA library

Pre-made human mammary gland cDNA library cloned into the pACT2 vector containing Gal4 AD, and carrying the yeast *Leu2* transformation marker for selection in Leu^- yeast (Clontech Laboratories, Mountain View, USA).

2.1.6 Yeast and bacterial strains

strain	**genotype**	**Source**
AH109	MATa, trp1-901, leu2-3, 112, ura3-52, his3-200, gal4Δ, gal80Δ, LYS2::$GAL1_{UAS}$-$GAL1_{TATA}$-HIS3, $GAL2_{UAS}$-$GAL2_{TATA}$-ADE2, URA3:: $MEL1_{UAS}$-$MEL1_{TATA}$-lacZ	Clontech Laboratories, Mountain View, USA
E. coli DH5α	fhuA2 Δ(argF-lacZ)U169 phoA glnV44 Φ80 Δ(lacZ)M15 gyrA96 recA1 relA1 endA1 thi-1 hsdR17	Invitrogen, Karlsruhe, Germany

E. coli XL-1 blue	RecA1 endA1 gyrA96 thi-1 hsdR17 supE44 RecA1 lac (F´proAB lacqZDM15 Tn10 (Tet1)	Stratagene, La Jolla, CA, USA

2.1.7 Mammalian cell lines

HEK293T	human embryonic kidney cells	American Type Culture Collection (ATCC), Manassas, VA, USA
HEK293T FlipIn-DLC1	FlpIn T-Rex 293 stably cotransfected with pcDNA5/FRT/TO-GFP-DLC1 and Flp recombinase expression plasmid pOG44	G. Holeiter, IZI, University of Stuttgart, Germany
MCF7	human breast carcinoma cell line	Institute of Clinical Pharmacology, Robert Bosch hospital, Stuttgart, Germany
MDAMB231	human breast carcinoma cell line	The Walter and Eliza Hall Institute of Medical Research and Bone Marrow Research Laboratories, Royal Melbourne Hospital, Parkville, Victoria, Australia

2.1.8 Cell culture reagents

10 x Trypsin EDTA	Invitrogen, Karlsruhe, Germany
Blasticidin S	Invitrogen, Karlsruhe, Germany
Collagen R solution	Serva, Heidelberg, Germany
DMEM, RPMI 1640, OptiMEM	Invitrogen, Karlsruhe, Germany
Doxycycline, HCl	Merck Biosciences, Darmstadt, Germany
FCS	PAA, Laboratories, Pasching, Austria
G418	Invitrogen, Karlsruhe, Germany
Heregulin	Tebu-Bio, Offenbach, Germany
Hygromycin-B	Invitrogen, Karlsruhe, Germany
Lipofectamine™ 2000	Invitrogen, Karlsruhe, Germany
Oligofectamine	Invitrogen, Karlsruhe, Germany

Platelet-Derived Growth Factor (PDGF-BB)	R&D, Wiesbaden, Germany
TransIT-293 Transfection reagent	Mirus Bio, Madison, USA

2.1.9 Antibodies

Primary antibodies

Antibody	Species	Dilution	Source
Anti-Akt	rabbit	1:1000 (WB)	Cell Signaling Technology, Danvers, MA, USA
Anti-Akt (pT308), phospho-specific (polyclonal)	rabbit	1:1000 (WB)	Cell Signaling Technology, Danvers, MA, USA
Anti-Dia1 (monoclonal)	mouse	1:500 (IF)	BD Biosciences, Franclin Lakes, USA
Anti-DLC1 (monoclonal)	mouse	1:500 (WB)	BD Biosciences, Franclin Lakes, USA
Anti-FAK	mouse	1:1000 (WB),	BD Biosciences, Franclin Lakes, USA
Anti-FAK (pY397), phospho-specific (monoclonal)	mouse	1:1000 (WB), 1:500 (IF)	BD Biosciences, Franclin Lakes, USA
Anti-Flag M2	mouse	1:5000 (WB), 1:2500 (IP), 1:5000 (IF)	Sigma-Aldrich, Taufkirchen, Germany
Anti-GFP (monoclonal)	mouse	1:2000 (WB)	Roche Diagnostics, Basel, Switzerland
Anti-GST (polyclonal)	goat	1:5000 (WB)	GE Healthcare, Munich, Germany
Anti-HA Ab 9E10 (monoclonal)	mouse	1:5000 (WB)	H. Böttinger, IZI, University Stuttgart
Anti-PTEN (monoclonal)	rabbit	1:2000 (WB), 1:100 (IF)	Cell Signaling Technology, Danvers, MA, USA
Anti-tubulin (monoclonal)	mouse	1:2000 (WB)	Sigma-Aldrich, Taufkirchen, Germany

Secondary antibodies

Antibody	Species	Dilution	Source
Alexa Fluor® 488 anti-mouse	goat	1:500 (IF)	Invitrogen, Karlsruhe, Germany
Alexa Fluor® 488 anti-rabbit	goat	1:500 (IF)	Invitrogen, Karlsruhe, Germany
Alexa Fluor® 546 anti-mouse	goat	1:500 (IF)	Invitrogen, Karlsruhe, Germany
Alexa Fluor® 546 anti-rabbit	goat	1:500 (IF)	Invitrogen, Karlsruhe, Germany
AP-anti-goat IgG	rabbit	1:10000 (WB)	Sigma-Aldrich, Taufkirchen, Germany
HRP-anti-mouse IgG	sheep	1:10000 (WB)	GE Healthcare, Munich, Germany
HRP-anti-rabbit IgG	donkey	1:10000 (WB)	GE Healthcare, Munich, Germany

2.1.10 Buffers and Solutions

Alkaline phosphatase (AP) buffer	100 mM Tris/HCl, pH 9,5, 100 mM NaCl, 5 mM MgCl2
Blocking solution (microscopy)	5% (v/v) goat serum, 0.1% (v/v) Tween20 in PBS
Blocking solution (Western blot)	0.5% (v/v) blocking solution, 0.05% (v/v) Tween20, 0.01% (v/v) thimerosal in PBS
Blotting buffer	200 mM glycine, 25 mM Tris base, 20% (v/v) methanol
Coomassie blue solution	0.1% Comassie blue R-250 in 40% Methanol, 10% acetic acid
Dropout (DO) Solution (-Leu/ -Trp/ -His) (10x)	200 g/l L-adenine hemisulfate salt 200 mg/l L-arginine HCl 300 mg/l L-isoleucine 300 mg/l L-lysine HCl

	200 mg/l L-methionine 500 mg/l L-phenylalanine 2000 mg/l L-threonine 300 mg/l L-tyrosine 200 mg/l L-uracil 1500 mg/l L-valine dissolved in 1 l H_2O
Firefly substrate	470 µM D-luciferin, 530 µM ATP, 270 µM coenzyme A, 33 mM DTT, 20 mM Tricine, 2,67 mM $MgSO_4$, 01 mM EDTA, pH 7,8
His-solution (50x)	1 g/l L-histidine HCl monohydrate dissolved in 1 l H_2O
Laemmli protein sample buffer (5x)	400 mM Tris, pH 6.8, 500 mM dithiothreitol, 50% (v/v) glycerol, 10% (w/v) SDS, 0.2% (w/v) bromophenol blue
Leu-solution (50x)	5 g/l L-leucine dissolved in 1 l H_2O
Luria-Bertani (LB) medium	10 g peptone, 5 g yeast extract, 5 g sodium chloride, ad 1 l H_2O
Lysis buffer (NEB)	50 mM Tris pH 7.5, 150 mM NaCl, 10 mM NaF, 20 mM ß-glycerolphosphate, 1 mM EDTA, 0,5% (v/v) NP-40, 1mM Na_3VO_4, 0.5 mM PMSF, Complete
Lysis buffer (RIPA)	50 mM Tris pH 7.5, 150 mM NaCl, 10 mM NaF, 20 mM ß-glycerolphosphate, 1 mM EDTA, 1% (v/v) Triton X-100, 0,1% (v/v) SDS, 0,25% (v/v) NaDOC, 1mM Na_3VO_4, 0.5 mM PMSF, Complete
Phosphate Buffered Saline (PBS)	140 mM NaCl, 2.7 mM KCl, 8 mM Na_2HPO_4, 1.5 mM KH_2PO_4

PBS-Tween	0.05 % (v/v) Tween20 in PBS
PEG/LiAc solution	40 % (v/v) PEG, 1 % (v/v) LiAc , 1% (v/v) TE
Renilla substrate	0,7 µM coelenterazine, 2,2 mM Na_2EDTA, 0,44 mg/ml bovine serum albumin, 1,1 M NaCl, 1,3 mM NaN_3, 0.22 M potassium phosphate buffer, pH 5,0
S1 resuspension buffer	50 mM Tris pH 8.0, 10 mM EDTA, 0.1 mg/ml RnaseA
S2 lysis buffer	200 mM NaCl, 1% SDS in ddH_2O
S3 neutralization buffer	2.8 M potassium acetate in ddH_2O, pH 5.1
SD medium	6.7 g yeast nitrogen base without amino acids, 2% (w/v) Glucose, 100 ml 10x Dropout Solution, 25 ml 50x Trp-, Leu- or His-solution if required, 20 g Agar (for plates), ad 1 l H_2O
SDS-PAGE running buffer	25 mM Tris pH 8.8, 192 mM glycine, 0.1% SDS
Solubilization solution	10% SDS, 50% N,N-dimethylformamide
Tris-Acetat-EDTA (TAE), pH 8,0	40 mM Tris-acetate, 1 mM EDTA, pH 8.3
TE buffer (10x)	M Tris-HCl, 10 mM EDTA, pH7.5
Trp-solution (50x)	1 g/ l L-tryptophan dissolved in 1 l H_2O
YPD medium	20 g/l Difco peptone, 10 g/l yeast extract, 20 g/l agar (for plates), 2% (w/v) glucose, ad 1 l H_2O
Z buffer	16.1 g/l $Na_2HPO_4 * 7\ H_2O$, 5.5 g/l $NaH_2PO_4 * H_2O$, 0.75 g/l KCl, 0.246 g/l $MgSO_4 * 7\ H_2O$, adjust to pH 7.0
Z buffer/X-gal solution	100 ml Z buffer, 0.27 ml β-mercaptoethanol, 1.67 ml X-gal stock solution (20 mg/ml in DMF)

2.2 Methods

2.2.1 Yeast-two-hybrid system

For the performance of the yeast–two-hybrid screen the MATCHMAKER GAL4 Two-Hybrid System 3 from Clontech was used.

Amplification of the cDNA library

The titer of the cDNA library was determined according to the manufacturer´s instructions. Afterwards the library was plated onto LB/amp plates at a density high enough to yield almost confluent colonies (20 000 – 40 000 cfu per 15 x 15 cm plate). The amount of plated cfu was chosen to obtain at least 2-3 times the number of independent clones in the library. The plates were incubated at 37℃ for 18-20 h. Colonies were pooled by scraping into LB/glycerol and subsequently, plasmid DNA was prepared using the PureLink™ HiPure Plasmid Gigaprep Kit from Invitrogen.

Yeast storage

For preparing a yeast glycerol stock, single colonies were scraped from the agar plate and resuspended in 200-500 µl of YPD medium (or the appropriate SD medium for transformed yeast strains). After dispersing the cells by vortexing, sterile 50% glycerol was added to a final concentration of 25%. The vials were frozen at -70℃.

To recover frozen yeast, a small portion of the frozen glycerol stock was streaked onto a YPD (or appropriate SD) agar plate. The plate was incubated at 30℃ until yeast colonies reached nearly 2 mm in diameter (approximately 3-5 days). These colonies were used as a working stock. The plates were sealed with parafilm and stored at 4℃ for up to two months.

Yeast culturing

One large (2-3 mm diameter) fresh (<2-months old) colony from the working plate was inoculated in 5 ml of YPD (or appropriate SD) medium, and vigorously vortexed for ~1 min to disperse the cells. This suspension was incubated at 30℃ for 16-18 h with shaking at 230-270 rpm, yielding a stationary phase culture (OD_{600}>1.5). To obtain a mid-log phase culture, the overnight culture was transferred into fresh medium and incubated at 30℃ for 3-5 h with shaking at 230-250 rpm to produce a culture with an OD_{600}~0.4-0.6.

Salmon sperm carrier DNA

100 mg salmon sperm carrier DNA (sodium salt) were dissolved in 50 ml TE buffer (2mg/ml) and allowed to dissolve for several hours. Every hour the molecular weight was checked on a 0.75% agarose gel to get an optimal size between 7-10 kb. Finally, after 4 h, the DNA was sheared by passing 10 times through a 10 ml pipette. Afterwards, the DNA was boiled and stored in small aliquots at -20℃. Just before use, the solution was heated for 10 min at 95℃ and quickly chilled on ice for 1-2 min.

Preparation of competent yeast cells

1 ml of YPD or appropriate SD medium was inoculated with several colonies (2-3 mm in diameter), vigorously vortexed to disperse any clumps and transferred into a flask with 50 ml YPD or SD medium. This culture was incubated at 30°C for 16-18 h with shaking at 250 rpm to yield a stationary phase culture (OD_{600}>1.5). Afterwards, 300 ml YPD were inoculated with overnight culture to yield an OD_{600}=0.2-0.3 and then incubated at 30℃ for at least 3 h with shaking (230 rpm) until an OD_{600}=0.4-0.6. Cells were centrifuged at 1000 x *g* for 5 min at room temperature (Jouan G4i centrifuge, Thermo Scientific, Waltham, MA, USA). Cell pellets were pooled and washed with 50 ml H_2O. After a second centrifugation, the pellet was resuspended in 1.5 ml freshly prepared 1x TE/1x LiAc.

Yeast transformation

For small-scale transformation, 0.1 µg of the bait plasmid DNA (pGBKT7-SAM) was mixed with 100 µg salmon sperm carrier DNA in a fresh 1.5 ml tube. 100 µl of competent yeast cells were added and mixed well by vortexing. Then, 600 µl sterile PEG/LiAc solution were added and the tube was vortexed vigorously followed by an incubation at 30℃ for 30 min. After addition of 70 µl DMSO and gentle inversion of the tube, a heat shock was performed for 15 min at 42℃. Then, cells were chilled on ice for 1- 2 min, centrifuged for 5 sec at maximum speed at room temperature (Eppendorf Centrifuge 5415 R, NeoLab, Heidelberg, Germany), washed with 1 ml TE buffer and resuspended in 500 µl TE buffer. 100 µl of the suspension were plated on 10 x 10 cm SD/-Trp agar plates and incubated up-side-down at 30℃ until yeast colonies appeared.

For large-scale transformation of the library, 40 µg of plasmid DNA were distributed to five 2 ml tubes and mixed with 400 µg salmon sperm carrier DNA and 200 µl of competent yeast cells (pre-transformed with the bait) per tube. The amount of PEG/LiAc constituted 1.2 ml, and 140 µl DMSO were added to each tube before the heat shock. The procedure and incubation times were the same as for small-scale transformation. The yeast suspension

weas spread on 15 x 15 cm SD/-His/-Trp/-Leu agar plates (200 µl per plate). Additionally, 100 µl of a 1:100 and 1:10 dilution were plated on 10 x 10 cm SD/-Trp/-Leu agar plates to determine the transformation efficiency. For calculation of the transformation efficiency, colonies (cfu) grown on the dilution plates were counted and then, the amount of cfu/µg DNA could be defined via the following formula:

$$\frac{\text{cfu x total suspension vol. (µl)}}{\text{Vol. plated (µl) x dilution factor x amount DNA used (µg)}} = \text{cfu/µg DNA}$$

Colony-Lift Filter Assay

This assay was performed with fresh colonies from the library transformation. A sterile nylon transfer membrane was placed onto the surface of the plate and gently rubbed to improve attachment of the colonies to the membrane. Three holes were poked through the membrane in an asymmetric way to mark the orientation of the membrane on the agar plate. Then, the membrane was carefully lifted off the agar plate with forceps and transferred to a pool of liquid nitrogen (colonies facing up) for 10 sec, until the filter was frozen completely. Afterwards, the membrane was removed from the liquid nitrogen and thawed at room temperature. For each plate of transformants to be assayed, a fresh sterile Whatman filter was pre-soaked in 5 ml of Z buffer/X-gal solution in a clean 15 x 15 cm plate. After the freeze/thaw cycle, the membranes were placed onto the pre-soaked filters (colonies side up) to allow the X-gal solution to get into contact with the colonies and incubated at 30℃. The appearance of blue colonies was checked periodically. The β-galactosidase-producing colonies were identified by aligning the filter with the agar plate using the orientation marks. Corresponding positive colonies were picked from the original plates and plated on a fresh SD/-Trp/-Leu/-His agar plate as working plate.

Plasmid isolation from yeast

4 ml of SD/-Trp/-Leu/-His were inoculated with a large (2-4 mm) fresh yeast colony from the working plate and vortexed vigorously to disperse any cell clumps. The culture was incubated at 30℃ overnight with shaking at 230-250 rpm. Subsequently, cells were spun down for 5 min at 5000 x *g* (Eppendorf Centrifuge 5415 R, NeoLab, Heidelberg, Germany) and resuspended in 250 µl P1 buffer of the QIAprep Spin Miniprep Kit from QIAGEN. After addition of 50-100 µl glass beads, each sample was vortexed for 5 min at high speed. When the beads were settled, the supernatant could be transferred to a fresh 1.5 ml tube and the DNA was prepared according to the kit´s protocol.

2.2.2 Molecular biology

Enzymes for DNA digestions and dephosphorylation were utilized as recommended by the supplier (MBI Fermentas, St. Leon-Rot, Germany).

DNA digestion

For DNA digestions of PCR products, purified samples were incubated with the appropriate enzyme for 3 h at 37°C. Digestions for checking insert orientation after ligations were performed with 3 µl of DNA and incubated for 1 h at 37°C. The generated fragments were checked on agarose gels.

Polymerase Chain Reaction (PCR)

For PCR, 10 ng of template DNA were amplified using 1 µl DNA polymerase with proof reading function, 10 pmol of oligonucleotides, 1 µl dNTPs (10 mM) and 5 µl of enzyme buffer (10x) using the RoboCycler 96 Gradient Cycler (Stratagene, La Jolla, CA, USA). The final volume of the reaction was 50 µl. Annealing temperatures and amplification times were adjusted to melting points of the appropriate primers and the size of the amplified DNA product.

Ligation of DNA fragments

For the ligation of DNA fragments with the appropriate cloning vector, 1 µl of T4 DNA ligase was used. The final volume of each sample was 10 µl. Vector and insert were added in a ratio between 1:4 - 1:8. Samples were incubated at room temperature for 2 h.

Transformation of E.*coli*

For plasmid transformation, 50 µl of chemically competent E.*coli* DH5α were thawed on ice for 5 min, gently mixed with 5 µl of each ligation sample and incubated for 30 min on ice. After a heat shock at 42°C for 90 sec, the bacteria were chilled on ice for 1 min before 1 ml of LB medium was added followed by incubation for 1 h at 37°C. Finally, the bacteria were plated onto LB agar plates containing 25 µg/ml kanamycin or 100 µg/ml ampicillin according to the utilized cloning vector and incubated at 37°C overnight.

Plasmid isolation from E.*coli*

To check insertion and orientation of ligated DNA fragments, plasmid DNA was isolated in a small scale. Therefore, 6 colonies of each approach were inoculated in 6 x 3 ml LB medium with appropriate antibiotics according to the cloning vector and grown overnight at 37℃ with shaking at 180 rpm. 1.5 ml of each bacterial culture was centrifuged for 5 min at 13 000 rpm (Eppendorf Centrifuge 5415 R, NeoLab, Heidelberg, Germany) and pellets were resuspended in 150 µl S1 lysis buffer. 150 µl S2 lysis buffer were added following addition of 150 µl S3 neutralization buffer after a 5 min incubation. The precipitate was seperated by centrifugation for 5 min at 13 000 rpm. The DNA was precipitated by adding 100% ethanol to the supernatant and incubating for 10 min on ice. Afterwards, the samples were centrifuged for 10 min at 13 000 rpm and washed with 70% ethanol. After removing the ethanol by another centrifugation, the DNA was dried at 50℃ a nd resolved in 30 µl ddH_2O.

For large-scale preparations of plasmid DNA, 100 µl of the bacterial suspensions used for the small-scale isolations were inoculated in 100 ml LB medium with appropriate antibiotics and incubated overnight at 37℃ with shaking (180 r pm). Plasmids were isolated using the PureLink^{TM}HiPure Plasmid DNA Purification Kit from Invitrogen according to the manufacturer´s instructions. Precipitated DNA was resuspended in 200 µl ddH_2O. Purity and concentration were determined by UV-absorption measured photometrically in the nanodrop device (ND-1000, Thermo Fisher Scientific, Waltham, USA).

Cloning strategies

The cloning of pEGFPC1-DLC1 WT, K714E and ΔSAM were not part of this thesis and have been described elsewhere (Holeiter et al, 2008; Scholz et al., 2009). Subcloning into the pEFrPuro-FlagA vector was performed by digesting insert and vector plasmids with *BamHI* and subsequent ligation. Primers used for PCR reactions are listed in section 2.1.4. Insert integrity was verified by sequencing by GATC Biotech, Konstanz, Germany.

DLC1-SAM constructs

To generate the bait plasmid for the yeast-two-hybrid screen – pGBKT7-DLC1-SAM – the SAM domain of DLC1 was amplified by PCR using EcoRI-DLC1-F and DLC1-SAM-BamHI-R as primers and pEGFPC1-DLC1 as a template followed by subcloning as a EcoRI/BamHI fragment into the pGBKT7 vector. For cloning of a fusion construct consisting of the SAM domain and GST, the primers BamHI-DLC1-F and DLC1-XhoI-R and pEGFPC1-DLC1 as template were used in a PCR to amplify the SAM domain. Afterwards, the cDNA was subcloned into the pGEX6P3 vector as a BamHI/XhoI fragment.

PTEN constructs

A plasmid encoding myc-tagged PTEN was kindly provided by B. Lüscher (University Aachen). The PTEN cDNA was amplified by PCR using the primers BamHI-PTEN-F and PTEN-BamHI-R as listed in the table and subcloned into the pEGFPC1 vector (Clontech) as a BamHI fragment. PTEN deletion mutants were generated by PCR using the following primers: pEGFPC1-PTEN-ΔCat (BamHI-PTEN-ΔCat-F and PTEN-BamHI-R), pEGFPC1-PTEN-ΔPDZ (BamHI-PTEN-F and PTEN-ΔPDZ-BamHI-R) and pEGFPC1-PTEN-ΔC (BamHI-PTEN-F and PTEN-ΔC-BamHI-R). cDNAs digested with BamHI were subsequently cloned into pEGFPC1. The point mutants of PTEN (C124S and S385A) were generated by site-directed mutagenesis. Therefore, a PCR with reverse complementary primers containing the mutation was performed. These primers (PTEN-C124S-F/PTEN-C124S-R and PTEN-S385A-F/PTEN-S385A-R, respectively) were designed according to the QuickChange Site-directed Mutagenesis protocol from Stratagene. Also, cycling parameters for the PCR were chosen as written by the manufacturer´s instructions. The remaining wildtype methylated template DNA was subsequently digested by the methylation sensitive restriction enzyme *Dpn*I. Afterwards, digested BamHI fragments were subcloned into the pEGFPC1 (pEGFPC1-PTEN-S385A) and the pEFrPuro-HA vectors (pEFrPuro-HA-PTEN-C124S), respectively.

Liprin constructs

Full ORF clones containing the coding sequences for liprin alpha1, beta1 and beta2, respectively, were sustained from the RZPD (Heidelberg). cDNAs were amplified by PCR using the following primers: liprin alpha1 (EcoRI-LA1-F and LA1-EcoRI-R), liprin beta1 (BamHI-LB1-F and LB1-BamHI-R) and liprin beta2 (BamHI-LB2-F and LB2-BamHI-R). Liprin alpha1 was subcloned into the pEGFPC1 vector as a EcoRI fragment and liprin beta1 and beta2 were subcloned as BamHI fragments.

Bacterial expression of GST proteins

E. *coli* were transformed with pGEX6P3-SAM or GST alone. One colony of each was cultured in 5 ml ampicillin containing LB medium over night at 37℃ with shaking. The next day, 500 ml LB medium with ampicillin were inoculated with the overnight cultures. Protein expression was induced with 0.1 mM IPTG for 3 h at 30℃ after reaching an OD_{600}=0.5. The bacterial cultures were harvested by centrifugation for 15 min at 4000 rpm (Avanti J-30I, Beckmann Coulter GmbH, Krefeld, Germany) and pellets were resuspended in 15 ml PBS containing Complete protease inhibitors. After adding lysozyme (100 µg/ml), the suspensions were incubated for 10 min and then sonicated 3x for 10 sec on ice (Sonopuls HD 2200, Bandelin electronic, Berlin, Germany), Triton X-100 was added to a final concentration of 1%

and the lysate centrifuged for 10 min at 8,000 x *g*. Purification of GST-tagged proteins was performed with glutathione resin. The resin was washed with PBS and the purity and amount of bound GST proteins was then determined by SDS-PAGE and Coomassie staining.

Semi-quantitative RT-PCR

Total RNA was extracted using the PureLink™ Micro-to-Midi™ Total RNA Purification System from Invitrogen following the manufacturer's instructions. RNA was reverse transcribed into cDNA using a First Strand cDNA Synthesis Kit with random hexamer primers. The cDNA was then used as a template for PCR analysis with REDTaq PCR Master Mix using primers specific for DLC1 or liprin beta2. The housekeeping gene glyceraldehyde-3-phosphate dehydrogenase (GAPDH) was amplified as an internal control.

2.2.3 Protein biochemistry

Protein extraction, GST pulldown and immunoprecipitation

Whole cell extracts (WCE) were obtained by solubilizing cells in RIPA buffer for direct protein analysis or in NEB for pulldowns and coimmunoprecipitations, respectively. Lysates were clarified by centrifugation at 16,000 x *g* for 10 min (Eppendorf Centrifuge 5415 R, NeoLab, Heidelberg, Germany). Pulldowns were performed by incubating WCE with GST-SAM beads for 2 h. Beads were washed 3x with NEB. For immunoprecipitations, equal amounts of protein were incubated with specific antibodies for 4 h on ice. Immune complexes were collected with protein G-Sepharose and washed 3x with NEB. Precipitated proteins were released by boiling in sample buffer for 5 min.

For determination of protein concentrations, the DC Protein Assay from Biorad was utilized according to the manufacturer´s instructions. The principle of this reaction is based on the Lowry Assay.

SDS polyacrylamide gel electrophoresis (SDS PAGE)

For protein analysis after extraction and denaturation in 1x Laemmli SDS sample buffer at 95°C for 5 min, separation of proteins was performed by discontinuing Tris/glycine SDS-PAGE, using a vertical gel electrophoresis chamber (Phase, Luebeck, Germany). Depending on the proteins loaded, seperating gels contained 8 to 12% of acrylamide. Stacking gels contained 5% acrylamide. The gels were run for 1 h 30 min at 50 mA.

Composition of SDS gels

	Seperating gel		Stacking gel
	8%	12%	5%
H_2O	6.9 ml	4.9 ml	3.4 ml
acrylamide	4 ml	6 ml	0.83 ml
1,5 M Tris pH 8,8	3.8 ml	3.8 ml	-
1 M Tris pH 6,8	-	-	0.63 ml
SDS (10% w/v)	0.15 ml	0.15 ml	0.05 ml
APS (10% w/v)	0.15 ml	0.15 ml	0.05 ml
TEMED	0.009 ml	0.006 ml	0.005 ml

Western Blotting

For Western blot analysis, the proteins separated by SDS PAGE were transferred onto polyvinylidine difluoride membranes (Roti® PVDF, Roth) for 2 h at 1.5 – 1.6 mA/cm^2 by using a semi-dry blotting chamber (Phase, Luebeck, Germany). After blocking with 0.5% blocking reagent in PBS for 30 min at room temperature, incubation with specific primary antibodies diluted in blotting buffer containing 0.05% azide was carried out at 4℃ overnight. The next day, the membrane was washed 3x with PBS-Tween for 5 min and the appropriate secondary antibody was added for 1 h followed by three washing steps with PBS-Tween for 10 min. In case of horseradish peroxidase-coupled secondary antibodies, proteins were visualized using the ECL detection system (Pierce Biotechnology, Rockford, USA) according to the manufacturer's specifications and exposure to an X-ray film. Films were developed with an X-OMAT 1000 processor (Kodak). For visualization of proteins detected by alkaline phosphatase-coupled secondary antibodies, NBT/BCIP as a substrate in AP buffer was added and the color reaction was stopped by washing in water.

2.2.4 Cell biology

Cell culture and transfection

Cells were cultured in RPMI media (RPMI 1640 + L-glutamine) supplemented with 10% heat inactivated FCS in a humidified atmosphere of 5% CO_2 at 37℃. To keep selection pressure on the stably transfected HEK293T DLC1 FlpIn cells, 15 µg/ml blasticidin S and 100 µg/ml hygromycin B were added to the medium. Expression of DLC1 was induced by addition of 10

ng/ml doxycycline and incubation for 6-24 h at 37°C. HEK293T cells were transfected with TransIT and MCF7 cells with Lipofectamine 2000 according to the manufacturers' instructions. For RNAi, cells were transfected with siRNAs (100 pmol siRNA per one 6-well plated with 1 x 10^5 MCF7 the day before) using Oligofectamine reagent according to the manufacturer's instructions.

Immunofluorescence microscopy

Cells grown on glass coverslips coated with 25 µg/ml collagen were washed once with PBS + $CaCl_2$/$MgCl_2$, fixed with 4% PFA in PBS for 15 min, washed with PBS, incubated with 150 mM glycine, washed again with PBS, permeabilized with 0.2% Triton X-100 in PBS and after washing with PBS-T (PBS with 0.1% Tween-20) blocked with blocking buffer (PBS-T supplemented with 5% goat serum) for 30 min at RT. Cells were then incubated with primary antibody in blocking buffer for 2 h, washed four times for 5 min with PBS-T, and then incubated with secondary antibody in blocking buffer for 1 h at RT. Cells were again washed four times with PBS-T before mounting in Fluoromount G. Confocal analysis was performed with a Leica TCS SL microscope using 488, 543 and 561 nm excitation and a 40X / 1.25 HCX PL APO oil objective lens. Images were processed with Adobe Photoshop.

Cell migration assays

Transwells (8.0-µm membrane pores; Costar, Baar, Swiss) were coated with 2.5 µg/ml collagen over night at 4°C. Cells were harvested, washed twice with 5 ml medium supplemented with 0.5% FCS, and after counting, 1 x 10^5 cells in 100 µl medium (with 0.5% FCS) were added to the top chamber and allowed to migrate for 8 h in the case of serum and over night in the case of PDGF as a chemoattractant. The bottom chamber was supplemented with 10% FCS or 30 ng/ml PDGF in medium containing 0.5% FCS. Cells on the top surface of the membranes were removed using a cotton swab and cells on the underside were fixed in 4% PFA and stained with 0.1% crystal violet. Quantification was done by counting the number of cells in 5 independent microscopic fields at a 20-fold magnification. Experiments were performed in duplicate.

Wound healing assays

MCF7 cells (6 x 10^5) were seeded into 12-well dishes. The next day, confluent cell monolayers were wounded with a sterile white micropipette tip and plates were returned to the tissue culture incubator. Images of at least three defined positions were captured at the beginning and 24 h later (AxioCam MRc, Carl Zeiss AG, Oberkochen, Germany).

Cell proliferation assays

MCF7 cells were plated at a density of 5 x 10^4 cells/ well in 100 µl medium into 96 well plates (n = 3), and cell proliferation was determined by a colorimetric MTT assay for 5 days. Cells were incubated with 10 µl of 3-(4,5-dimethylthiazol-2yl-)2,5-diphenyl tetrazolium bromide solution (5mg/ml) for 3 h. Cells were lysed by incubation with 100 µl solubilization solution over night at 37℃ and the absorbance at 595 nm was determined after background subtraction at 655 nm using a Tecan Infinite 200M plate reader.

Luciferase reporter assays

HEK293T FlpIn-DLC1 cells were grown on collagen-coated (25 µg/ml) 24-well dishes and transfected with 50 ng each of the 3DA.Luc firefly luciferase reporter containing 3 SRF binding elements, pRL-TK, a Renilla luciferase plasmid under the control of the thymidine kinase promoter, and pEGFPC1-PTEN or empty vector, respectively. After serum starvation over night, DLC1 expression was switched on by addition of 10 ng/ml doxycycline and, 4 h later, cells were stimulated with 15% FCS for 4 h. Cells were lysed with 300 µl passive lysis buffer and luciferase activities in 10 µl lysate were measured by addition of 50 µl firefly substrate, followed by addition of 100 µl Renilla substrate. Luminescence was measured with a Tecan Infinite 200M plate reader.

3 Results

3.1 Searching for novel protein binding partners of DLC1 via a yeast-two-hybrid screen

To identify new protein interactors of DLC1 in order to further understand the molecular mechanism of its tumor suppressive activity and its regulation, a yeast-two-hybrid screen constituted a powerful tool. Because of our particular interest in the role of DLC1 in breast carcinogenesis, a library of proteins expressed in human breast tissue (Human Mammary Gland MATCHMAKER cDNA Library, Clontech) was screened for binding to the tumor suppressor. This library was generated by an oligo-dT primed RT-PCR from mRNA of normal, whole breast tissue, pooled from six Caucasians. The produced cDNA was cloned into the pACT2 expression vector (Trp resistance), fusing it to the activation domain of Gal4, which is encoded by the vector. After obtaining this premade cDNA library, the titer was determined and library plasmids were amplified to obtain sufficient amounts of DNA for screening. The SAM domain of DLC1 was chosen as a bait because of its feature as a highly conserved protein interaction motif. Therefore, the first N-terminal 86 amino acids of DLC1 forming this domain were cloned into the pGBKT7 vector containing a leucine selection marker and encoding the DNA binding domain of Gal4. An interaction of the bait with a library protein would lead to the recombination of Gal4 to a functional transcription factor and as a result to the activation of reporter genes (lacZ and HIS3).

Before performing the screen, auto-activation of the bait construct was examined - approximately 5% of all proteins have some latent activating activity (Van Criekinge & Beyaert, 1999) - by transforming it into the yeast strain AH109 (Trp, Leu and His auxotroph) and testing the growth on His-deficient medium, a feature of yeast clones expressing HIS3 and, thus, having an active Gal4. A weak activation of HIS3 was present, leading to moderate background growth. This growth was inhibited by adding 20 mM 3-AT (3-amino-triazole), a competitive inhibitor of the HIS3 gene product. The amount of 3-AT necessary to inhibit the background growth was optimized by testing concentrations between 1 mM up to 40 mM. The lowest concentration that allowed only small colonies to grow after one week was 20 mM 3-AT and therefore used for the screening. In fact, too high 3-AT concentrations can also inhibit the growth of weak DLC1 interactors.
Next, in a sequential transformation of bait plasmid and library the screen was started. The bait was introduced into AH109 by a small-scale transformation and selected transformants were then cultured and transformed with the AD fusion library through a large-scale

transformation. Finally, the yeast suspension was plated onto 15 x 15 cm large SD/-Trp/-Leu/-His agar plates and incubated at 30℃. Through determination of the transformation efficacy, the number of screened clones was calculated to correspond to 3 x 10^6. Since the library consisted of approximately 3.5 x 10^6 independent clones, the possibility that the bait was tested for interaction with the majority of these clones was high. After 5-15 days, yeast colonies appeared. To enforce the stringency of the screen, these colonies were further examined for β-galactosidase activity by performing X-gal colony-lift filter assays on every plate. In the end, a total number of 215 yeast colonies turned blue and therefore represented putative interaction partners of the SAM domain of DLC1 because of the expression of both reporter genes that are under control of the Gal4 transcription factor. The experimental approach is summarized in Figure 9.

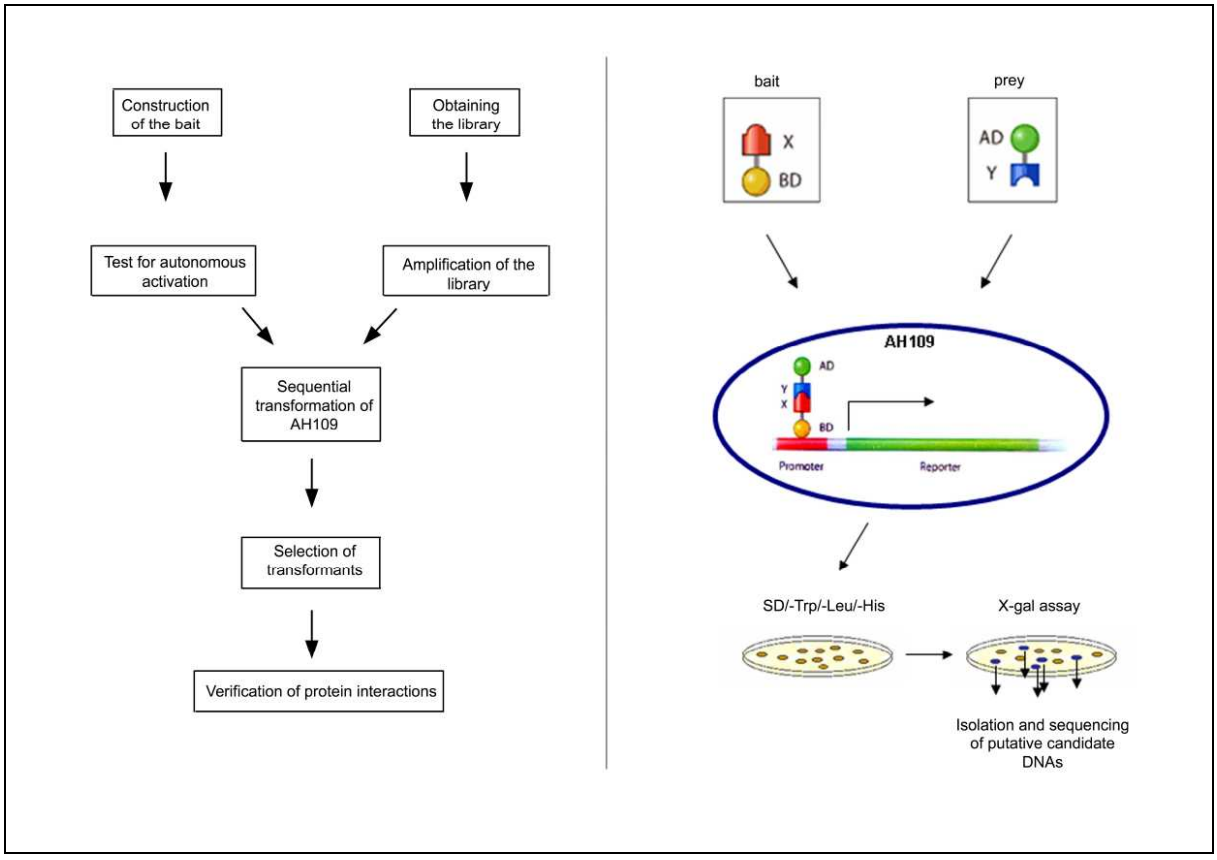

Figure 9: Flowchart of the yeast-two-hybrid approach performed in this thesis.

Inserts of positive clones were amplified via PCR to analyze if they had taken up more than one library plasmid. cDNA library plasmids of the remaining clones were isolated from yeast, transformed into E.*coli* and sequenced. Exclusion of colonies containing more than one cDNA plasmid resulted in the selection of 143 clones appropriate for sequencing analysis. These were analyzed using NCBI Data Base http://www.ncbi.nlm.nih.gov/BLAST/ in order to

determine the identity of the genes. Genes encoding potential interacting partners of the DLC1 SAM domain are listed in Table 1. Since proteins like collagen-related proteins, ribosomal, mitochondrial and heat shock proteins, immunoglobulins, MHC and Zn-finger proteins are found as common false positives in many screenings, the interesting interaction partners are marked in bold letters. In addition, 3 yeast open reading frames, 11 unknown genes, 14 genes that were out of frame and 73 sequences which showed no similarity to any protein in the data base were identified. Within this thesis, the focus was on the characterization of the potential interaction between DLC1 and two of the 16 putative candidates: PTEN and liprin beta 2.

Table 1: List of genes encoding putative interacting partners of the DLC1 SAM domain

pACT2-clone	Human Homologue	Accession. Nr.
2	**Actin, alpha**	NM_001613
7, 22, 24, 49, 80, 141	**Eukarytiotic elongation translation factor 1 alpha 1 (EEF1A1)**	NM_001402
8	Ubiquitin C	NM_021009
12	Replication initiator 1	NM_001099695
14, 121	**Thioredoxin interacting protein**	NM_006472
35	**Dynein heavy chain**	NM_001376
36, 113	**Actin, beta**	NM_001101
39	Tata-box-associated factor	NM_005640
54	Gamma-butyrobetaine hydroxylase 1	NM_003986
60	**Fatty acid binding protein**	NM_001442
65	NADH Dehydrogenase	NM_004544
72	Small nuclear ribonucleoprotein polypeptide G	NM_003096
76	**Actin, gamma**	NM_001614
81	Suppressor of Ty5 homolog	NM_003169
109	**Liprin beta 2**	NM_003621
126, 165	**Apolipoprotein D**	NM_001647
127	**Phosphatase and tensin homolog deleted on chromosome ten (PTEN)**	NM_000314
128	**Coatomer protein complex, subunit beta 2**	NM_004766
138	AT rich interactive domain 4B (RBP1-like)	NM_031371
140	Activator of heat shock 90kDa protein ATPase	NM_152392

	homolog 2	
143	**Protocadherin 1**	NM_032420
146	Major histocompatability complex, class I, A (HLA-A)	NM_002116
151, 153	**Peroxiredoxin 6**	NM_004905
163	Heterogenous nuclear ribonucleoprotein F	NM_001098204
174	Immunoglobulin J polypeptide (IgJ)	NM_144646
187	Poly (ADP-ribose) polymerase family, member 1 (PARP1)	NM_001618
190	**Unc-84 homolog B/ Sun2**	NM_015374
194	**Coiled-coil domain containing 14**	NM_022757
195	Collagen, type 1, alpha 1	NM_000088
199	**Protein tyrosine phosphatase, non-receptor type 11 (PTPN11)**	NM_002834
204	Ribosomal protein SA	NM_002295
211	Aldo-keto reductase family 1, member C3	NM_003739
213	Lysyl-tRNA synthetase (KARS)	NM_005548

3.2 Characterization of the DLC1 – PTEN interaction

3.2.1 The DLC1 SAM domain associates with full-length PTEN

The yeast-two-hybrid system is used to screen a high number of potential protein interaction partners in a relatively short period. Nevertheless, like in every screening approach false positives might be detected. These may occur due to a variety of reasons, e.g. direct interaction between the prey component of the transcription activation domain fusion and the upstream activating sequences in the reporter construct, an irrelevant interaction between a prey peptide fragment and the bait – so-called time/space constraints – or an indirect binding through a third, “bridging” protein. Furthermore, in the screen only fragments of the library proteins were cloned which could result in conformational alterations, thereby influencing binding ability. Thus, it is imperative that interactions identified in a yeast two-hybrid screen are confirmed by at least one alternative, non-yeast-based assay.

For this purpose, a pulldown assay seemed to be a first adequate experiment to confirm the interaction between DLC1 and PTEN. Therefore, the isolated SAM domain of DLC1 was coupled to GST and incubated with MCF7 cell lysates. GST-SAM but not GST alone was found to precipitate endogenous PTEN (Fig. 10A). Further evidence for the interaction of the two proteins is provided by coimmunoprecipitation experiments. Here, HEK293T cells were transiently transfected with plasmids encoding full-length Flag-DLC1 and GFP-PTEN, and DLC1 was immunoprecipitated with Flag-specific antibody from cell lysates. By immunoblotting with a GFP-specific antibody, PTEN was readily detected in the immunoprecipitate (Fig. 10B). A DLC1 mutant protein lacking the aminoterminal SAM domain failed to precipitate PTEN, indicating that the interaction was specific and mediated by the SAM domain of DLC1 (Fig. 10B).

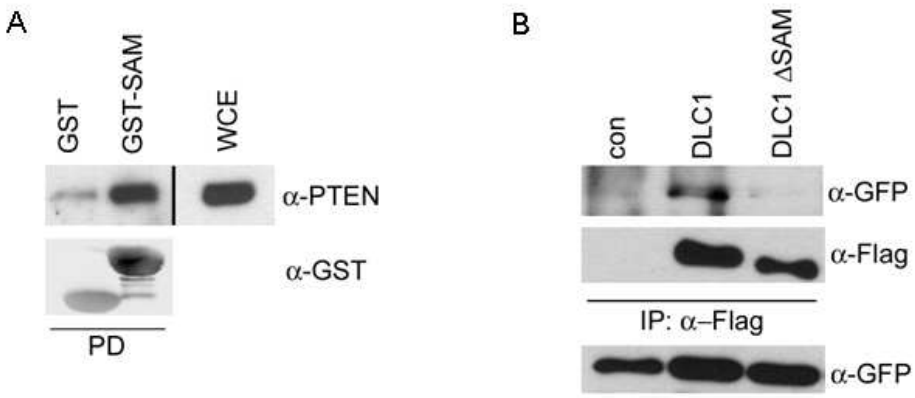

Figure 10: DLC1 and PTEN physically interact via the DLC1 SAM domain. (A) WCE of MCF7 cells were incubated with glutathione beads coupled to GST-SAM, or GST alone, and bound proteins were separated by SDS-PAGE. Endogenous PTEN was detected by Western blotting with a PTEN-specific antibody (top panel). The integrity of the GST proteins was verified by probing the membrane with GST-specific antibody (bottom panel). (B) HEK293T cells were transiently transfected with GFP-tagged PTEN and empty vector (con), Flag-tagged full-length DLC1 or DLC1-ΔSAM expression vectors, respectively. Full-length DLC1 and DLC1-ΔSAM were immunoprecipitated from WCE with Flag-specific antibody and immune complexes were separated by SDS-PAGE. Coprecipitated PTEN was detected by Western blotting with GFP-specific antibody (top panel). Immunoprecipitation of full length DLC1 and DLC1-ΔSAM was verified by probing the membrane with Flag-specific antibody (middle panel), and expression of PTEN was verified by immunoblotting of WCE with GFP-specific antibody (bottom panel).

3.2.2 DLC1 preferentially interacts with activated PTEN

Next, it was interesting to identify the region in PTEN mediating association with DLC1. The fragment isolated in the yeast-two-hybrid screen was composed of amino acids 288 to 403. This sequence includes part of the C2 domain and the C-terminal PDZ binding motif. Various PTEN deletion constructs were generated that lacked the aminoterminal catalytic domain (PTEN-ΔCAT), the carboxyterminal PDZ binding motif (PTEN-ΔPDZ) or the entire carboxy-terminus (PTEN-ΔC). These were transiently transfected into HEK293T cells and cell lysates were tested for binding to GST-SAM or GST alone in pulldown assays. All deletion mutants were still able to interact with DLC1 (Fig. 11A), suggesting that the C2 domain is involved in mediating interaction with DLC1.

Interestingly, the PTEN mutant lacking the carboxyterminal tail interacted particularly well with DLC1 (Fig. 11A). Similarly to PTEN-ΔC, the point mutant PTEN-S385A also demonstrated increased association with DLC1 (Fig. 11A). The carboxyterminal tail contains several phosphorylation sites, which are known to keep the protein in an inactive state (Vazquez & Devreotes, 2006). Upon activation, PTEN is dephosphorylated, leading to its recruitment to the plasma membrane where it is turned over rapidly. Serine 385 has been characterized as a priming phosphorylation site and a PTEN-S385A mutant possesses increased activity and membrane binding properties (Odriozola et al., 2007). The strong interaction of this mutant with DLC1 suggests that DLC1 preferentially interacts with active, dephosphorylated PTEN.

To further validate this assumption, the potential regulation of DLC1-PTEN complex formation was investigated in response to PDGF treatment of cells. PDGF is known to potently activate the PI3K signaling pathway, concomitant with its negative regulator PTEN. HEK293T cells were transiently transfected with expression vectors encoding Flag-DLC1 and GFP-PTEN, serum-starved over night and then stimulated with PDGF for different periods of

time (Fig. 11B). Notably, the amount of PTEN detected in DLC1 immunoprecipitates underwent a transient increase, peaking after 15 min of PDGF stimulation (Fig. 11B). To confirm that the endogenous proteins also interact in response to PDGF stimulation, PTEN was immunoprecipitated from lysates of the breast carcinoma cell line MDAMB231, which expresses relatively high levels of DLC1. Indeed, endogenous DLC1 was detected in PTEN immunoprecipitates of PDGF-stimulated MDAMB231 cells (Fig. 11C).

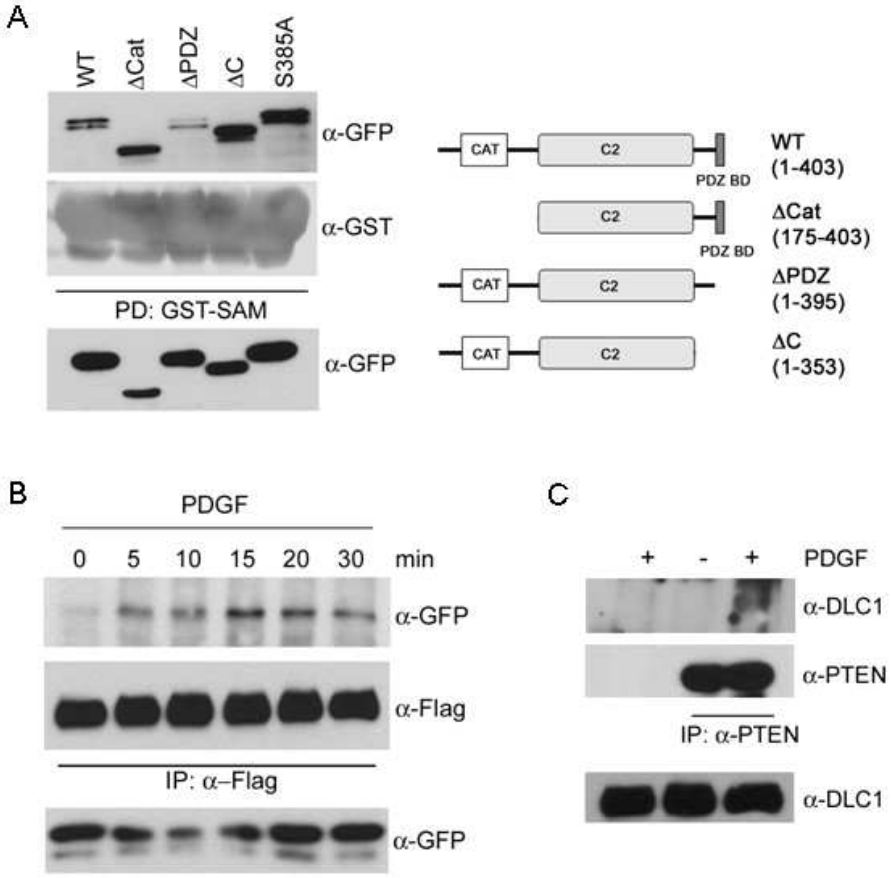

Figure 11: PTEN activation promotes the association with DLC1. (A) HEK293T cells were transiently transfected with vectors encoding full-length and the different schematically represented GFP-tagged PTEN deletion mutants. WCE were subjected to a pulldown with GST-SAM beads, bound proteins were separated by SDS-PAGE and detected by immunoblotting with GFP-specific antibody. The integrity of GST-SAM was verified by probing the membrane with GST-specific antibody (middle panel) and the expression of the different PTEN variants was verified by immunoblotting of WCE with GFP-specific antibody (bottom panel). (B) HEK293T cells were transiently transfected with expression vectors encoding Flag-DLC1 and GFP-PTEN. The next day, cells were starved over night and then treated with 30 ng/ml PDGF for the indicated times prior to lysis. DLC1 was immunoprecipitated from WCE with Flag-specific antibody and immune complexes were separated by SDS-PAGE. Coprecipitated PTEN was detected by immunoblotting with GFP-specific antibody (top panel). Immunoprecipitation of DLC1 was verified by reprobing the membrane with Flag-specific antibody (middle panel), and expression of PTEN was verified by immunoblotting of WCE with GFP-specific antibody (bottom panel). (C) MDAMB231 cells were starved over night and left untreated (-) or treated with 30 ng/ml PDGF for 15 min (+) prior to lysis. PTEN was immunoprecipitated from WCE with a PTEN-specific antibody and immune complexes were separated by SDS-PAGE. Coprecipitated DLC1 was detected by immunoblotting with a DLC1-specific antibody (top panel); the left lane shows an IP control without antibody. Immunoprecipitation of PTEN was verified by reprobing the membrane with PTEN-specific antibody (middle panel), and DLC1 expression by immunoblotting of WCE with DLC1-specific antibody (bottom panel).

3.2.3 Colocalization of DLC1 and PTEN at the plasma membrane

To visualize where DLC1 and PTEN act in the cell, both proteins were transiently coexpressed in MCF7 cells and their subcellular localization was analyzed by confocal microscopy. Because both DLC1 and PTEN have been reported to lead to dissolution of focal adhesions and actin stress fibers when overexpressed (Sekimata et al., 1999; Tamura et al. 1998), the inactive variants (DLC1-K714E and PTEN-C124S) were used in this analysis to conserve cellular morphology. Localization of PTEN is known to be cell type dependent and was seen mainly in the cytosol and in the nucleus as previously described for MCF7 cells (Ginn-Pease & Eng, 2003). A small proportion of the protein also resided at the plasma membrane. Partial colocalization with DLC1 could be observed at the cell periphery (Fig. 12). This is in accordance with the observation that DLC1 preferentially associates with activated PTEN which is recruited to the membrane (Fig. 11). Furthermore, since the PDZ binding motif of PTEN has been reported to be involved in membrane recruitment by protein-protein interaction (Vazquez et al., 2001), the very low binding efficiency of the mutant PTEN-ΔPDZ to GST-SAM in the pulldown experiment may also be explained by the stronger interaction of DLC1 with membrane-bound PTEN (Fig. 11A).

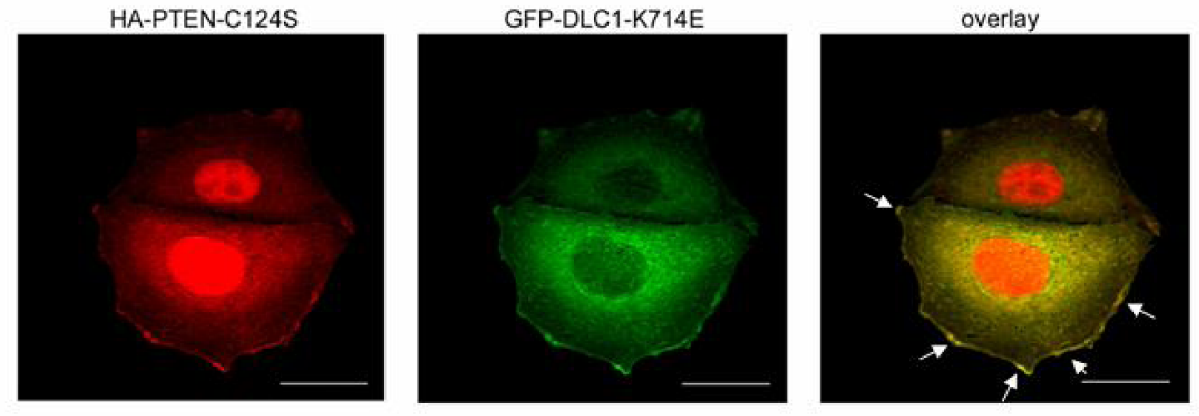

Figure 12: DLC1 and PTEN colocalize at the plasma membrane. MCF7 cells were transiently transfected with expression vectors encoding GFP-DLC1-K714E and HA-PTEN-C124S. The next day, cells were fixed and stained with HA-specific primary and Alexa Fluor 546-labeled secondary antibody (red). Colocalization areas of a representative cell are marked with arrows in the overlay. The images shown are stacks of several confocal sections. Scale bars = 20 µm.

3.2.4 PTEN does not alter DLC1 GAP activity and even PTEN function is not directly influenced by DLC1

The exciting question that arises upon finding novel protein-protein interactions is that of the biological impact. In the case of DLC1-PTEN interaction one could imagine that it either influences DLC1 GAP activity, and thus Rho signaling, or modulates PTEN phosphatase

function. To address the possible impact of PTEN on DLC1-mediated suppression of Rho signaling, a luciferase assay measuring endogenous Rho activity was performed. Therefore, HEK293T FlpIn-DLC1 cells were transfected with a serum response factor (SRF) responsive reporter along with an expression vector encoding GFP-PTEN or empty vector, and serum-starved over night. After induction of DLC1 expression by adding doxycycline, cells were stimulated with serum which activates SRF-mediated transcription in a Rho-dependent way. In accordance with published data (Holeiter et al., 2008; Scholz et al., 2009) DLC1 expression potently inhibited SRF activity which increased upon serum stimulation. When PTEN was coexpressed with DLC1, inhibition was slightly greater; however, expression of PTEN alone also inhibited SRF activity to some extent (Fig. 13). The greater inhibition seen when both proteins were coexpressed may thus simply be an additive effect and does not provide support for a stimulatory effect of PTEN on DLC1 GAP activity.

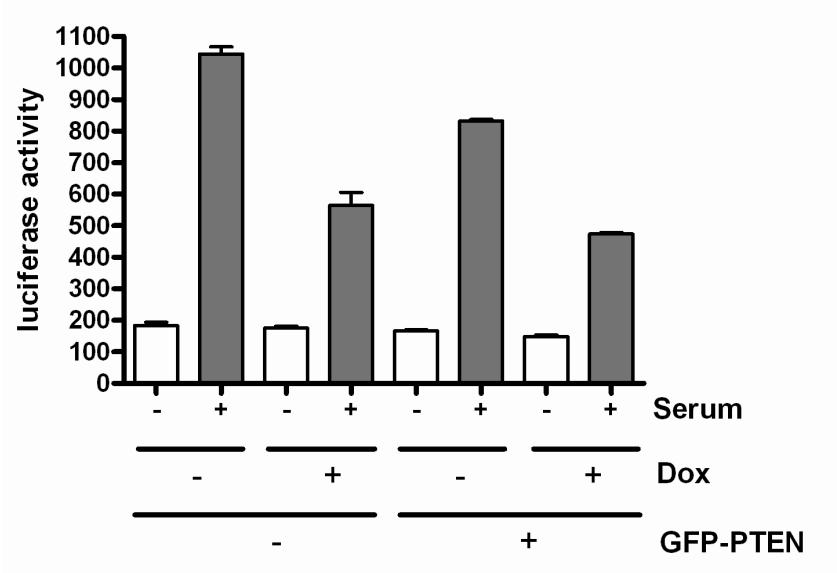

Figure 13: GAP activity of DLC1 is not influenced by PTEN. HEK293 FlpIn-DLC1 cells that express DLC1 in an inducible manner (Scholz et al., 2009) were transfected with the SRF-responsive 3DA.Luc firefly luciferase reporter along with plasmids encoding Renilla luciferase and GFP-PTEN (+) or empty vector (-). Cells were serum-starved over night either in the absence (-) or presence of doxycycline (DOX; +) to induce expression of DLC1. The next day, cells were left untreated (-) or stimulated with serum for 6 h (+) and lysed. Firefly luciferase activity in cell lysates of triplicate samples was determined and normalized by Renilla luciferase activity. Error bars represent SEM.

To examine the putative influence of DLC1 on PTEN function, firstly the effect of DLC1 coexpression on the lipid phosphatase activity of PTEN was investigated. Hence, MCF7 cells were transfected with expression vectors encoding DLC1, PTEN, DLC1 plus PTEN or empty vector, respectively, serum-starved over night and stimulated with heregulin – a strong stimulus of the PI3K pathway – for 15 and 30 minutes. The amount of activated Akt/PKB was analyzed by immunoblotting. As expected, overexpression of PTEN reduced pAkt levels in comparison with the control. Interestingly, DLC1 overexpression also led to a decreased amount of activated Akt. The coexpression of both proteins, however, did not promote a

further reduction (Fig. 14A). This result suggests that there is no cooperation between PTEN and DLC1 concerning the regulation of the PI3K pathway.

To further investigate the potential collaboration of DLC1 and PTEN in terms of signaling by focal adhesion kinase (FAK) which was shown to be a protein target of the phosphatase (Tamura et al., 1998), MCF7 cells were again transfected with expression vectors encoding DLC1, PTEN, DLC1 plus PTEN or empty vector, respectively, held in suspension for one hour and plated onto collagen-coated dishes for two and six hours to stimulate the formation of new adhesions. Overexpression of PTEN prevented upregulation of pFAK as did overexpression of DLC1, which was reported previously (Kim et al., 2007). Overexpression of both PTEN and DLC1 did not reduce pFAK levels further, which again points to a lack of synergism (Fig. 14B).

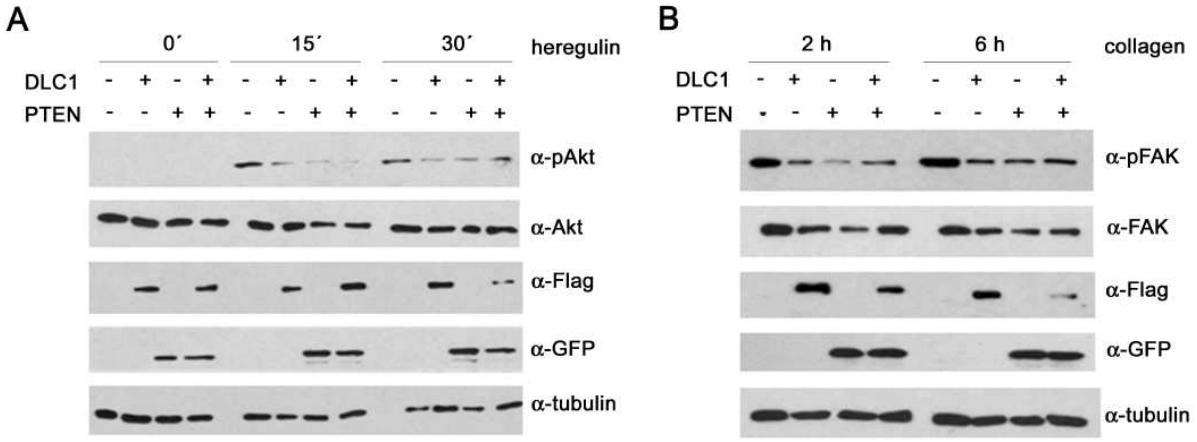

Figure 14: The impact of PTEN on Akt and FAK signaling are DLC1-independent. (A, B) MCF7 cells were transiently transfected with expression plasmids encoding Flag-DLC1 and GFP-PTEN, or empty vector (-). (A) After 48 hours, cells were serum-starved over night following stimulation with heregulin (25 ng/ml) for 15 min and 30 min, respectively. Cells were lysed in RIPA buffer and equal amounts of total protein were subjected to SDS-PAGE and transferred to membrane. The amount of phosphorylated Akt was analyzed by immunoblotting using a pAkt (T308)-specific antibody (top panel). Total amounts of Akt were analyzed with a Akt-specific antibody (panel 2). Expression of DLC1 and PTEN was analyzed with Flag and GFP-specific antibodies, respectively (panels 3, 4). Equal loading was verified by reprobing the membrane with a tubulin-specific antibody (bottom panel). (B) Two days post transfection, cells were harvested and replated onto collagen-coated dishes for 2 h and 6 h, respectively. Cells were lysed in RIPA buffer, proteins were separated by SDS-PAGE and analyzed by immunoblotting. Total and phosphorylated amounts of FAK were analyzed with FAK- and pFAK (Y397)-specific antibodies, respectively (panel 1, 2). DLC1 and PTEN expression were detected by using Flag- and GFP-specific antibodies, respectively (panels 3, 4). Equal loading was verified by probing with a tubulin-specific antibody (bottom panel).

Since there was no obvious dependency of DLC1 GAP activity on PTEN and no detectable influence of DLC1 on PTEN function concerning PI3K and FAK signaling, the interaction of the two proteins may possibly be required for the spatial and temporal coordination of the distinct signaling pathways during tumor suppression.

3.2.5 Simultaneous downregulation of PTEN and DLC1 in MCF7 cells does not confer a growth advantage

Transformation of a normal to a tumor cell requires a variety of different mutations to oncogenes and tumor suppressor genes, finally leading to a more proliferative, non contact-inhibited growing, aberrantly differentiated, immortalized phenotype with invasive potential. The frequent loss of PTEN protein expression (Depowski et al., 2001, Perren et al., 1999) and also loss of DLC1 expression in breast cancer (Plaumann et al, 2003; Ullmannova & Popescu, 2006) raised the question how simultaneous loss of these tumor suppressors contributes to oncogenic transformation of breast cancer cells. Therefore, both genes were silenced individually and in combination in MCF7 cells which express both wild type PTEN and DLC1. To first verify silencing efficiency and specificity, cells were transfected with PTEN- and DLC1-specific siRNAs, respectively, and a siRNA targeting β-galactosidase (siLacZ) as a control. Whole cell lysates were prepared three days post transfection and analyzed by immunoblotting. As shown in Figure 15A, PTEN and DLC1 proteins were almost completely downregulated by the respective siRNAs. Consistent with its role as negative regulator of the PI3K signaling pathway, downregulation of PTEN led to increased levels of phosphorylated Akt (Fig. 15A). Interestingly, downregulation of DLC1 also slightly enhanced phosphorylated Akt levels (Fig. 15A). No changes in the total level of phosphorylated FAK were observed (Fig. 15A).

To analyze the impact of PTEN and DLC1 loss on cell proliferation, MCF7 cells lacking DLC1 or PTEN, or both, were subjected to an MTT assay. While silencing of PTEN led to an increased growth rate of cells compared to the siLacZ control, knockdown of DLC1 did not favor cell proliferation (Fig. 15B). Accordingly, the combined knockdown of both genes did not confer a proliferation advantage to cells over those lacking only PTEN.

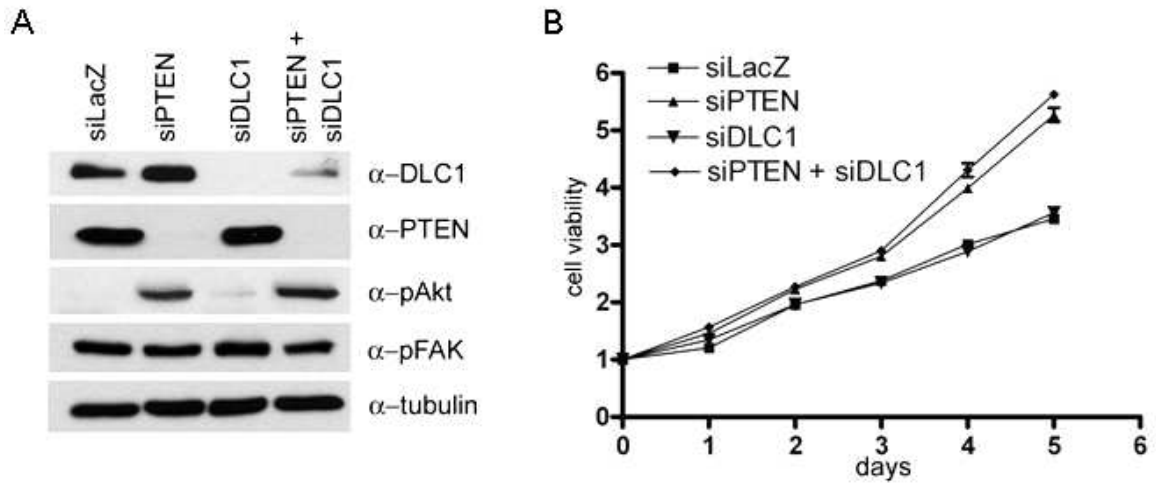

Figure 15: Simultaneous downregulation of PTEN and DLC1 in MCF7 cells does not enhance cell proliferation. (A & B) MCF7 cells were transiently transfected with siRNAs specific for PTEN, DLC1 or PTEN plus DLC1. A LacZ-specific siRNA was used as a negative control and to adjust the siRNA amount in each transfection mix. (A) Three days post transfection, cells were lysed, and equal amounts of total protein were subjected to SDS-PAGE and transferred to membrane. PTEN and DLC1 expression was analyzed by immunoblotting using PTEN- and DLC1-specific antibodies (top panels). The amount of phosphorylated Akt and FAK were analyzed with pAkt(T308)- and pFAK(Y397)-specific antibodies, respectively (panels 3 & 4). Equal loading was verified by reprobing the membrane with tubulin-specific antibody (bottom panel). (B) For analysis of cell proliferation, cells were harvested three days post transfection and replated into 96 well plates in triplicates. Cell proliferation was determined on five consecutive days by performing a colorimetric MTT assay as described in the Material and Methods section.

3.2.6 Joint depletion of DLC1 and PTEN enhances cell migration

PTEN plays a key role in regulating migration of different mammalian cell types (Kölsch et al., 2008; Leslie et al., 2005) and it was shown that silencing of DLC1 enhances breast cancer cell migration (Holeiter et al., 2008). It was therefore investigated how the simultaneous loss of PTEN and DLC1 influences the migratory behavior of MCF7 cells by performing wound healing assays. Confluent cell monolayers were wounded with a pipette tip and wound closure was monitored after 24 hours. Consistent with their role as negative regulators of cell migration, cells lacking PTEN closed the wound faster than the siLacZ control, as did cells lacking DLC1 (Fig. 16A). Interestingly, joint depletion of PTEN and DLC1 enabled cells to completely close the wound by 24 hours (Fig. 16A). The same results were obtained with cells treated with mitomycin C, ruling out a proliferative effect in this assay (data not shown). To further analyze cell motility, transwell filter assays were employed, in which cells were seeded in medium containing 0.5% serum into the top chambers and allowed to migrate across the filter towards a 10% serum gradient in the bottom chambers. Again, cells lacking PTEN and DLC1, respectively, demonstrated increased cell migration (Fig. 16B, top panel). In the absence of both proteins, cell migration was significantly enhanced even further (Fig. 16B, top panel), which was confirmed with independent siRNAs for both PTEN and DLC1 (Fig. 16C). These results are in accordance with those obtained in wound healing assays and suggest that the simultaneous loss of PTEN and DLC1 has an additive effect on cell migration.

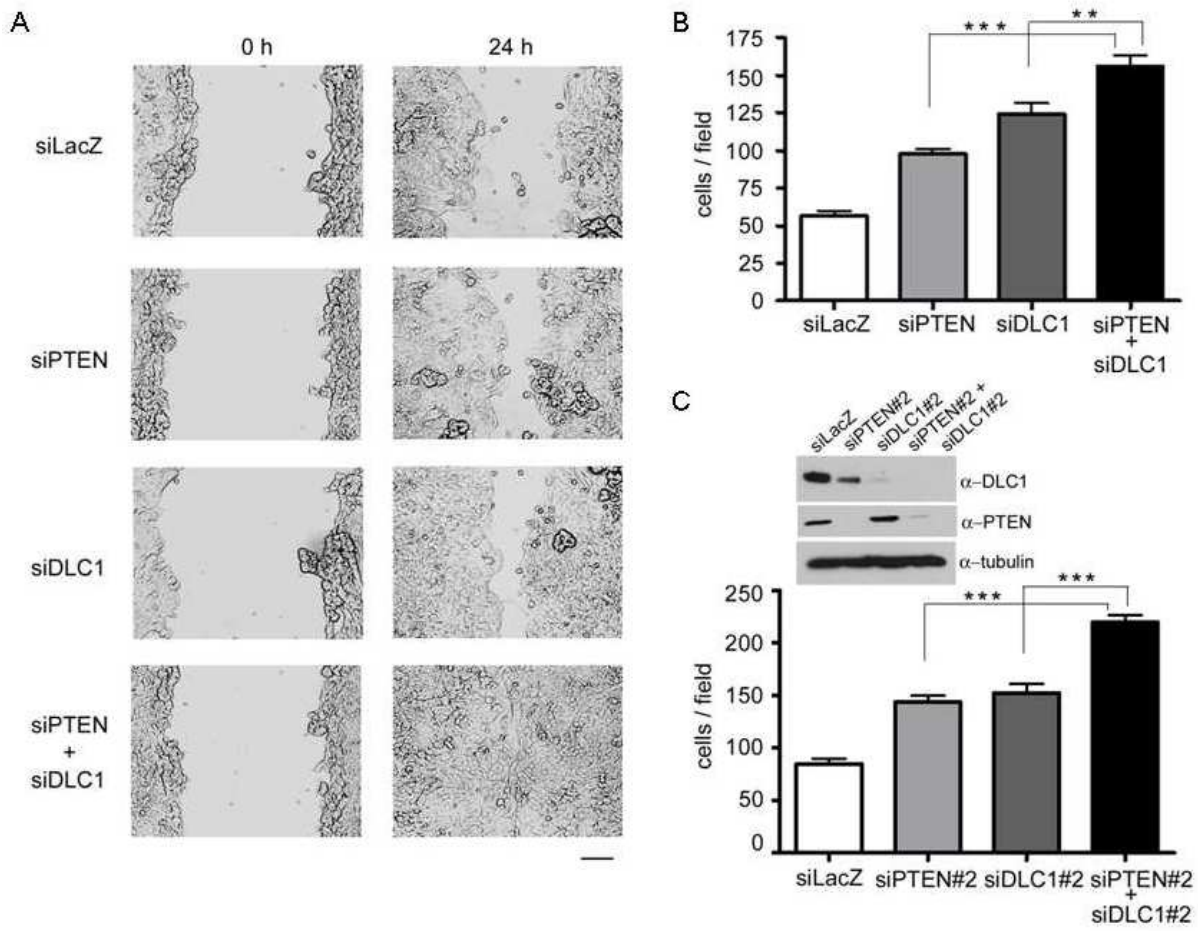

Figure 16: Simultaneous knockdown of DLC1 and PTEN enhances cell migration. (A-C) MCF7 cells were transiently transfected with the indicated siRNAs and harvested three days post transfection. (A) Cells were replated at high density and, the next day, confluent monolayers were scratched with a white pipette tip. Pictures were taken at a 10-fold magnification to document the scratch at time point zero and after incubation for 24 h. This experiment was performed 3 times and for each condition 3 independent images were captured. Scale bar = 200 µm. (B, C) 10^5 cells were seeded in medium containing 0.5% FCS into the upper chamber of a transwell; the lower well contained medium supplemented with 10% FCS. Cells that had migrated across the filter after 8 h were fixed and stained. The number of migrated cells was determined by counting five independent microscopic fields (20-fold magnification). Data shown are the mean of duplicate wells and error bars represent SEM. A representative experiment out of four is shown. Results for single- versus double-transfected cells were statistically significant (two-tailed unpaired t-test, $p < 0.001$ (***), $p < 0.01$ (**)). (C) Efficient silencing of DLC1 and PTEN using independent siRNAs was verified by immunoblotting as described in Figure 15A.

Since PDGF was demonstrated to stimulate the association between DLC1 and PTEN (Fig.11), it was interesting to investigate whether cell migration of cells lacking PTEN and DLC1 was also enhanced in response to growth factor treatment using PDGF as a chemoattractant in the transwell assays. Again, cells in which both DLC1 and PTEN were depleted displayed enhanced migration compared to cells lacking only one of the proteins (Fig. 17).

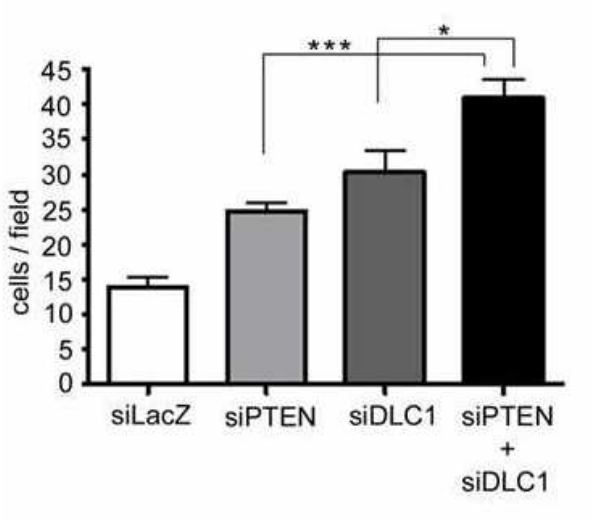

Figure 17: PDGF-induced chemotaxis is enhanced in DLC1/PTEN depleted cells. MCF7 cells were transiently transfected with the indicated siRNAs. Three days post transfection, 10^5 cells were seeded in medium containing 0.5% FCS into the upper chamber of a transwell. The lower well contained medium supplemented with 0.5% FCS plus 30 ng/ml PDGF. Cells that had migrated across the filter after overnight incubation were fixed and stained. The number of migrated cells was determined by counting five independent microscopic fields (20-fold magnification). Data shown are the mean of duplicate wells and error bars represent SEM. One representative experiment out of three is shown. Results for single- versus double-transfected cells were statistically significant (two-tailed unpaired t-test, $p < 0.001$ (***), $p < 0.05$ (*)).

3.2.7 Activation of FAK and Akt in DLC1/PTEN negative cells

It was demonstrated by Holeiter et al. that the Rho effector protein Dia1 is required for enhanced migration of MCF7 cells lacking DLC1 (Holeiter et al., 2008). The regulation of cell migration by PTEN is suggested to be independent of its lipid phosphatase activity, potentially mediated by direct dephosphorylation of FAK (Tamura et al., 1998). To investigate how these molecular targets are influenced in PTEN/DLC1 negative cells, cells transfected with the respective siRNAs and subjected to a wounding assay were immunostained with antibodies specific for phosphorylated, active FAK (Y397) and Dia1, respectively. In accordance with reported observations, Dia1 was enriched in membrane protrusions of DLC1-depleted cells at the wound edge compared to the siLacZ control, whereas PTEN loss did not affect Dia1 localization (Fig. 18). In cells lacking PTEN, enhanced pFAK staining in cells migrating to close the wound was observed, which was not the case in siLacZ control and DLC1-negative cells (Fig. 18). When cells were cotransfected with siRNAs specific for PTEN and DLC1, staining for both pFAK and Dia1 in migrating cells at the wound edge was increased (Fig. 18).

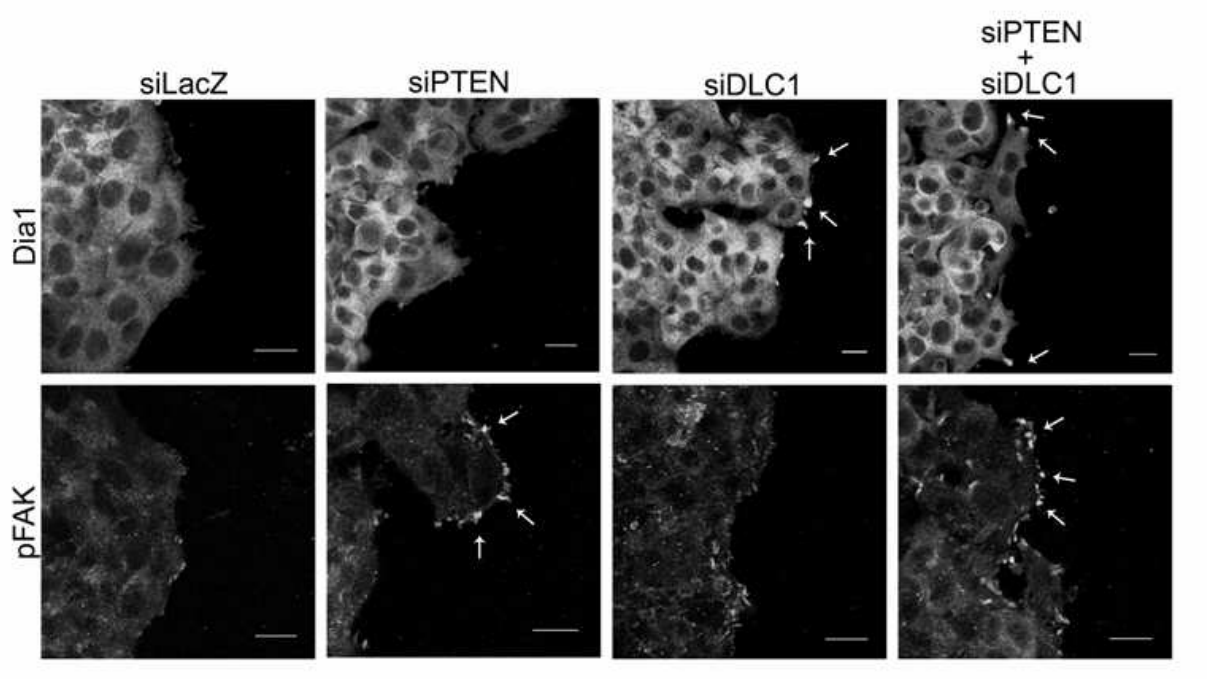

Figure 18: Dia1 and pFAK localization in PTEN/DLC1 negative cells. MCF7 cells were transfected with the indicated siRNAs and plated onto collagen-coated coverslips two days post transfection. Confluent cell monolayers were wounded with a pipette tip, fixed 6 h later and stained with Dia1- and pFAK-specific monoclonal antibodies, followed by Alexa Fluor 488-conjugated secondary antibody. Representative cells with elevated pFAK- and Dia1 staining are marked with arrows. Images are stacks of several confocal sections. Scale bar = 20 µm.

In summary, the interaction between DLC1 and PTEN found in the yeast-two-hybrid screen could be confirmed with the full-length proteins in mammalian cell lines. The DLC1 SAM domain was sufficient for the interaction and within PTEN the C2 domain was mapped to mediate the interaction. The physical association was dynamically regulated in response to PDGF stimulation. No reciprocal influence on the individual enzymatic activities was detected, but it could be shown that the combined loss of PTEN and DLC1 in breast cancer cells led to a more migratory phenotype. The results suggest that the two proteins act in concert to locally inactivate their respective signaling pathways, ensuring the tight control of cell migration processes.

3.3 The association of DLC1 and liprin beta2

3.3.1 DLC1 interacts with liprin beta2 in mammalian cells

After identification of liprin beta2 as a potential binding partner of DLC1 in the yeast-two-hybrid screen, again, the first step was to verify this interaction by further assays. The fragment that was fished as the interacting part was composed of amino acids 732 to 836, comprising parts of the very C-terminal SAM domain and the PDZ binding motif. To clarify if full-length liprin beta2 was also able to bind the SAM domain of DLC1, a pulldown experiment was performed. Therefore, cell lysates of MCF7 cells were incubated with GST-SAM and GST alone, respectively. Indeed, GST-SAM precipitated endogenous liprin beta2, but not GST alone (Fig. 19A).

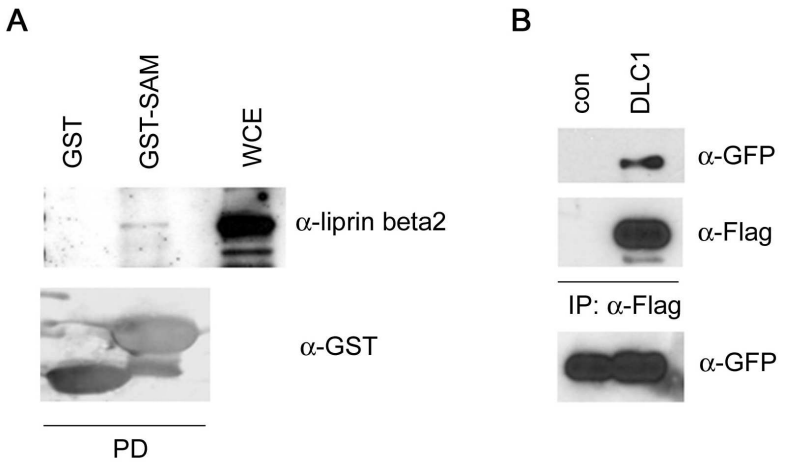

Figure 19: Liprin beta2 associates with DLC1. (A) WCE from MCF7 cells were incubated with glutathione beads coupled to GST-SAM, or GST alone, and bound proteins were separated by SDS-PAGE. Endogenous liprin beta2 was detected by Western blotting with a liprin beta2-specific antibody (top panel). The integrity of the GST proteins was verified by probing the membrane with GST-specific antibody (bottom panel). (B) HEK293T cells were transiently transfected with an expression vector encoding GFP-tagged liprin beta2 and empty vector (con) or Flag-tagged DLC1 expression vector. DLC1 was immunoprecipitated from WCE with Flag-specific antibody, and immune complexes were separated by SDS-PAGE. Coprecipitated liprin beta2 was detected by Western blotting with GFP-specific antibody (top panel). Immunoprecipitation of DLC1 was verified by probing the membrane with Flag-specific antibody (middle panel), and expression of liprin beta2 was verified by immunoblotting of WCE with GFP-specific antibody (bottom panel).

To provide further evidence for an association of DLC1 with liprin beta2, HEK293T cells were transiently transfected with plasmids encoding Flag-DLC1 or empty vector, respectively, and GFP-liprin beta2. DLC1 was immunoprecipitated with a Flag-specific antibody from cell lysates. Coimmunoprecipitated liprin beta2 was detected by immunoblotting using a GFP-specific antibody. Indeed, liprin beta2 was detectable in the DLC1 immunoprecipitate but not in the control, confirming the specificity of the binding (Fig. 19B).

3.3.2 DLC1 and liprin beta2 are coexpressed in a subset of breast cancer cell lines

As mentioned before, the interactions that occur in the yeast-two-hybrid system are not always of biological relevance. Proteins can bind to each other although being expressed in different tissues or at different stages of development under normal physiological conditions. To address whether DLC1 and liprin beta2 are present in the same cells, the expression of both was examined by semi-quantitative RT-PCR of different breast cancer cell lines. In most cases DLC1 mRNA was accompanied by liprin beta2 mRNA (Fig. 20A). In addition, protein levels were analyzed in some of these cell lines and, again, cell lines positive for both DLC1 as well as liprin beta2 were identified (Fig. 20B). Thus, an interaction of DLC1 with liprin beta2 could be of potential relevance in the context of breast cancer.

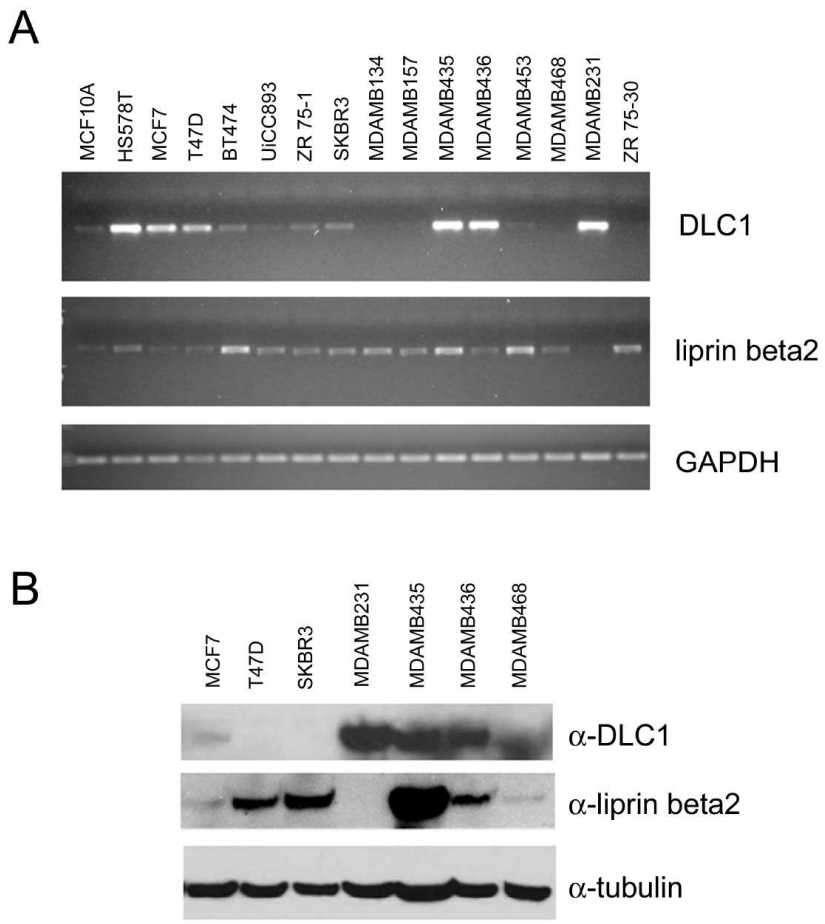

Figure 20: DLC1 and liprin beta2 are coexpressed in breast cancer cell lines. (A) Semi-quantitative RT-PCR analysis of DLC1 and liprin beta2 genes. cDNA from the breast epithelial cell lines indicated was amplified using specific primers that span introns in the genomic sequence. GAPDH was amplified as a loading control. (B) Cells of the indicated breast cancer cell lines were harvested, lysed in RIPA buffer, equal amounts of protein were subjected to a SDS-PAGE and transferred to membrane. DLC1 and liprin beta2 expression were analyzed by using DLC1- and liprin beta2-specific antibodies, respectively (top panels). Equal loading was verified by reprobing with a tubulin-specific antibody (bottom panel).

3.3.3 The interaction with DLC1 is a common feature of liprin family members

Since the interacting fragment of liprin beta2 fished in the screen consisted of carboxyterminal amino acids forming parts of the third, most C-terminal SAM domain belonging to the LH domain, which is highly conserved among all liprin family members, it is conceivable that not only the beta2 isoform represents a binding partner of DLC1. To prove this hypothesis, liprin alpha1 as the prototype of liprins and liprin beta1 as an additional member of the beta-type subfamily were tested for their ability to associate with DLC1. Flag-tagged DLC1 was coexpressed with either GFP-tagged liprin alpha1, beta1 or beta2, respectively, in HEK293T cells. DLC1 was immunoprecipitated from whole cell extracts using a Flag-specific antibody. By immunoblotting with a GFP-specific antibody all three isoforms could be detected in the immunoprecipitate (Fig. 21). The signal for liprin beta1 was very weak and was the lowest compared to that for liprin alpha1 and beta2, but nevertheless all three members associated with DLC1. As a next step, it will be of interest to address how binding of the different liprin family members affects DLC1 activity and impacts on cell fate.

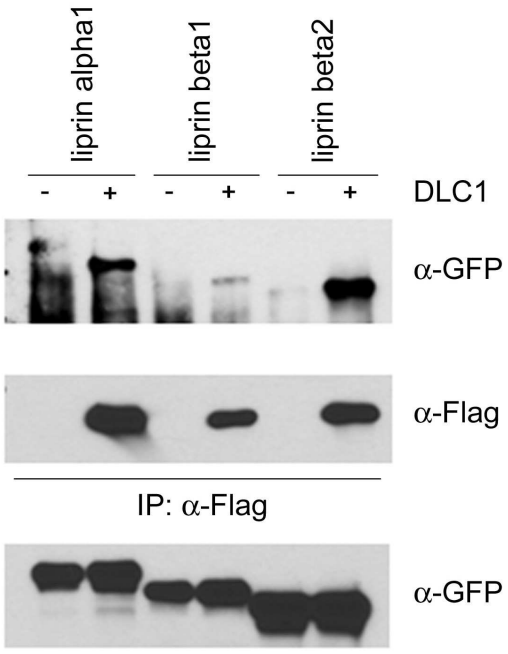

Figure 21: Liprin alpha1 and beta1 are coimmunoprecipitated by DLC1. HEK293T cells were transiently transfected with GFP-tagged liprin alpha1, beta1 or beta2 expression vectors and Flag-tagged DLC1 (+) or empty vector (-), respectively. DLC1 was immunoprecipitated from WCE with Flag-specific antibody and immune complexes were separated by SDS-PAGE. Coprecipitated liprins were detected by Western blotting with GFP-specific antibody (top panel). Immunoprecipitation of DLC1 was verified by probing the membrane with Flag-specific antibody (middle panel), and expression of liprin isoforms was verified by immunoblotting of WCE with GFP-specific antibody (bottom panel).

4 Discussion

4.1 The yeast-two-hybrid screen

Since the identification of DLC1 as a candidate tumor suppressor protein in liver cancer (Yuan et al., 1998) many studies reported its downregulation in numerous other solid tumors, including breast and lung cancer (Plaumann et al., 2003; Yuan et al., 2004), and haematological malignancies (Ullmannova-Benson et al., 2009). Oncogenic inhibition was shown to be dependent on its GAP activity, which is specific for RhoA, B and C and to a lesser degree for Cdc42. Thus, by the negative regulation of RhoGTPase signaling DLC1 plays a pivotal role in the control of cell proliferation and cell motility, which is a relevant feature of metastasis. Additionally, previous reports also demonstrated GAP-independent mechanisms, by which DLC1 functions as a tumor suppressor (Qian et al., 2007; Healy et al., 2008). However, it has to be further elucidated which pathways in addition to those downstream of Rho GTPases are targeted by DLC1. Thus far, little is known about the two other domains, the N-terminal SAM and the C-terminal START domain, and DLC1 regulation at the protein level also remains elusive. In order to get further insights into the molecular mechanisms by which DLC1 acts and possibly learn about regulatory processes, the aim of this thesis was to identify novel protein interaction partners by using a yeast-two-hybrid screen.

The yeast-two-hybrid system – firstly described in 1989 by Fields and Song – is one of the most popular technologies for high throughput screenings, searching for protein interactions. Many associations in the complex signaling network were identified by this method. A prominent example is the identification of the Raf kinase as a Ras interactor, stimulating well-characterized downstream pathways (Vojtek et al., 1993). The first protein interactors of DLC1, the tensin family members, were also found via yeast-two-hybrid screens. Their binding is essential for focal adhesion targeting of DLC1 and contributes to oncogenic inhibition, highlighting the importance for the identification of such interactions (Yam et al., 2006; Qian et al., 2007; Liao et al., 2007). However, the relevant binding site for tensins is located in the unstructured, serine-rich middle region of DLC1. For the screen performed in this thesis, the isolated SAM domain was chosen as a bait. SAM domains are known as very abundant protein-protein interaction motifs that mediate numerous versatile cellular processes (Qiao & Bowie, 2005). Therefore, this domain was predestined as a binding partner for other proteins. The choice of a human mammary gland cDNA library as a prey was made due to a particular interest of our group in understanding DLC1 tumor suppressor

function in breast cancer, where DLC1 expression is commonly downregulated or absent and even metastasis suppressive activities are reported (Goodison et al., 2005).

In the end, after sequential transformation of bait and library plasmids into yeast, the selection for colonies expressing HIS3 and β-galactosidase – the two reporter gene products under the control of Gal4 used in the screen – provided 215 putative binding partners for DLC1. However, isolation, sequencing and following database searches revealed several common false positives, such as heat shock or ribosomal proteins, unknown genes, genes out of frame and sequences that showed no similarity to any protein in the database. Finally, 16 proteins constituted potential interacting candidates. The eukaryotic elongation factor 1A1 (EEF1A1) – which was represented six times in the screen – was recently reported as a partner for the DLC1 SAM domain found by protein precipitation and mass spectrometry (Zhong et al., 2009). Even though the work of this thesis was focused on other binding partners, the identification of the same protein by a different approach demonstrates the reliability of the yeast-two-hybrid method.

Aside a diffuse cytoplasmic localization, DLC1 is also present in focal adhesions (Liao et al., 2007) and the association with caveolin-1 in caveolae, which are flask-shaped cholesterol-rich membrane microdomains, was described (Yam et al., 2006). It is possible that in these cellular compartments DLC1 interacts with additional membrane proteins. Such partners may not be identified by a classical yeast-two-hybrid screen. Here, the split-ubiquitin system, in which the interaction takes place in the cytoplasm, would have been better. However, because only very few binding partners for DLC1 are described until now, cytosolic protein interactors remain of interest and thus, for the purpose of this thesis, the classical method was sufficient. Another disadvantage of the original yeast-two-hybrid approach is the failure of posttranslational modifications in yeast such as phosphorylation, acetylation and glycosylation. Mass spectrometry analysis revealed that serine residue 80 is phosphorylated (our unpublished data) and also serine residue 86 is predicted to be phosphorylated, both of which are adjacent to the SAM domain. The absence of these modifications might have influenced the capability of the DLC1 SAM domain to associate with a subset of partners. A mammalian-two-hybrid screen could overcome this limitation, but of note, this procedure is not yet that sophisticated that large screenings could have been performed.

Taken together, in order to identify novel protein binding partners for DLC1 the classical yeast-two-hybrid approach constituted a powerful tool for a fairly simple and rapid search of several putative candidates. Every association with each of the 16 proteins identified by the screen may have an interesting and still uncharacterized impact on DLC1. Concerning the

research topics of our group, the most promising interacting proteins of this screen were assumed to be PTEN and liprin beta2.

PTEN is one of the most frequently mutated tumor suppressors in human cancer, which demonstrates the imperative of an intact protein for normal cells to prevent tumorigenesis (Yin & Shen, 2008). The association with DLC1, which itself is a tumor suppressor, prompted the exciting investigation of a relationship between these two important cellular gatekeepers and the crosstalk of their diverse signaling pathways. The relevance of interaction between distinct tumor suppressors is shown by the example of an interplay between PTEN and p53, probably the most popular tumor suppressor protein. The association of PTEN with p53 increases p53 stability by enhancing its DNA binding and transcriptional activity (Freeman et al., 2003). Therefore, aberrant interaction might be fateful for the cell. Similar consequences would be conceivable for a connection between DLC1 and PTEN. Hence, the analysis could gain deeper insights into the biological function of DLC1.

Although the main work of this thesis was focused on PTEN, liprin beta2 was also selected as a potential DLC1 interactor of special interest. The presence of a SAM domain within liprin beta2, which was part of the interacting fragment fished by the DLC1 SAM domain, is in line with the feature of SAM domains to form heterodimers (Qiao & Bowie, 2005). As a protein without own enzymatic activity it represented a potential scaffold protein for DLC1, possibly contributing to its compartmentalization. The very limited information about liprin beta2 made this investigation somehow difficult but also very exciting.

4.2 DLC1 association with PTEN

Sequencing of isolated plasmid DNAs of the HIS3/LacZ-positive yeast colonies identified a 345 bp fragment of PTEN, comprising the amino acids 288 to 403 as a putative binding partner for the DLC1 SAM domain. A pulldown assay with GST-SAM confirmed this association for endogenous wild type PTEN expressed in MCF7 cells. Furthermore, the interaction of ectopically expressed full-length DLC1 and full-length PTEN in mammalian cells was shown by coimmunoprecipitation. This verification is imperative for associations found by yeast-two-hybrid approaches. As mentioned above, by studying protein-protein interactions in a heterologous system posttranslational modifications may fail to occur. Also the use of chimeras and the randomly cloned fragments of proteins as a library represent a point of concern, because actual conformations might be altered, rendering the proteins incapable to interact with their real binding partners (Van Criekinge & Beyaert, 1999).

However, the results of pulldown and coimmunoprecipitation experiments provided evidence that the association between DLC1 and PTEN is not an artefact occurring only in yeast but an actual physical interaction in mammalian cells. A DLC1 mutant protein lacking the SAM domain failed to precipitate coexpressed PTEN, proving the specificity of the binding and the sufficiency of the SAM domain. Hence, beside EEF1A1 which was recently found as the first binding partner of DLC1-SAM (Zhong et al., 2009), PTEN represents the second.

To determine the PTEN binding site mediating DLC1 association, several PTEN mutant proteins were tested in pulldown assays for interaction with GST-SAM. Deletion of the aminoterminal catalytic (PTEN-ΔCAT) or the very C-terminal PDZ binding domain (PTEN-ΔPDZ), as well as deletion of the entire carboxyterminus (PTEN-ΔC) did not interrupt the binding and thus, all these mutants were detected by immunoblotting in GST-SAM precipitates. From these results it could be concluded that the C2 domain was involved in binding. This is in line with the fact that a sequence corresponding to part of the PTEN C2 domain was identified in the screen.

In addition to the mapping of the PTEN binding site, the pulldown experiment displayed further interesting information. The expression levels of the distinct mutant proteins were approximately the same, but binding efficiency was rather diverse. On the one hand, the very weak band observed for precipitated PTEN-ΔPDZ, and on the other hand, the strong binding of the PTEN-ΔC mutant were conspicuous. These observations – consistently seen in four individual experiments – suggested that DLC1 preferentially associates with active, membrane-bound PTEN. For the antagonistic regulation of PI3K signaling and thus, for the performance of its function as a lipid phosphatase, PTEN has to be targeted to the membrane to get into proximity of its substrates. The interaction of the carboxyterminal PDZ binding motif with PDZ domain-containing proteins contributes to this membrane recruitment, because such proteins serve as scaffolds to build membrane-localized multiprotein complexes (Vazquez et al., 2001). Phosphorylation of a cluster of serine and threonine residues at the PTEN carboxyterminal tail leads to the association of this cluster with the internal C2 domain, causing a conformational alteration. The resulting “closed” conformation somehow masks the PDZ binding motif and thus, prevents PTEN interaction with PDZ domain-containing proteins and recruitment to the plasma membrane (Vazquez et al., 2001). Furthermore, this phosphorylation also acts autoinhibitory, because phosphatase activity is diminished in the “closed” conformation ((Georgescu et al., 1999). Phosphorylation on serine 385 is thought to be the priming event for the subsequent phosphorylation of the remaining residues of the cluster. Hence, a point mutant switching this serine into an alanine residue resulted in a dephosphorylated protein, promoting membrane localization and phosphatase

activity (Odriozola et al., 2007). This mutant protein was also tested in the pulldown assay for binding to the SAM domain of DLC1 and, in fact, strong binding comparable with that of PTEN-ΔC was detected. Furthermore, the activator of PI3K/PTEN signaling, PDGF, stimulated the physical interaction of DLC1 and PTEN, which is also shown for the endogenous proteins. Together with the fact that the two proteins colocalized at the membrane, the notion that a protein complex forms upon activation of PTEN is strengthened.

The best characterized function of DLC1 is its RhoGAP activity, which primarily contributes to oncogenic inhibition (Durkin et al., 2007). Interaction with other proteins such as PTEN could impact on its enzymatic properties. However, ectopic expression of PTEN did not affect DLC1-mediated Rho inhibition in a SRF luciferase assay that reflects endogenous Rho activity. On the other hand, overexpression experiments failed to reveal synergistic effects of PTEN and DLC1 on total phospho-Akt or phospho-FAK levels upon stimulation of cells with heregulin or replating onto collagen, respectively. These results suggested that PTEN and DLC1 activity are not interdependent. However, ectopic expression might lead to artificial results, thus, small but significant differences for the cell fate were possibly not detected. Furthermore, a PTEN/DLC1 complex is likely to act locally due to our observation that the two proteins associate upon PTEN activation at the cell periphery. Thus, the impact of this interaction may only be revealed at the single cell level by imaging of complex formation and signaling events at the plasma membrane after adequate stimulation. A recent study in our group provides hints that an interdependency is conceivable. Erlmann et al. demonstrated that PIP2 binding through a polybasic region adjacent to the RhoGAP domain stimulates DLC1 GAP activity and is therefore essential for the tumor suppressive functions of the protein (Erlmann et al., in revision). Given the fact that by dephosphorylating PIP3 at the D3 position PTEN generates PIP2, one could imagine that an interaction of both is needed to make this important cofactor available for DLC1. In addition, GAP-independent mechanisms have been suggested to contribute to the tumor suppressive functions of DLC1 (Qian et al., 2007; Healy et al., 2008). Hence, it is possible that PTEN is involved in such alternative pathways, but at this stage the suitable read-out is unknown.

Different mutations to either oncogenes and/or tumor suppressor genes collaborate in the development of cancer. The finally appearing transformed phenotype of the malignant tumor cells is distinguished by uncontrolled growth, non-limited proliferation and an increase in cell motility, leading to invasion and metastasis. DLC1 expression is commonly lost or downregulated in various human tumor types including breast cancer due to genomic deletion, aberrant promoter methylation or the occurrence of mutations, leading to a reduced GAP activity, which was recently reported (Liao et al., 2008). Also the frequent loss of PTEN

expression is described in a broad range of cancers. Germline mutations lead to autosomal dominant disorders such as Cowden syndrome, causing multiple hamartomas and predisposing to breast and other cancers (Salmena et al., 2008). However, the long latency observed in different mouse models suggests that PTEN loss is not sufficient for tumor initiation and requires additional mutations for tumor progression. Several studies demonstrated a cooperation between a loss of PTEN expression and the constitutive activity of oncogenes. For example, PTEN deficiency was shown to collaborate with Wnt1, accelerating the induction of ductal carcinoma in the mammary gland (Li et al., 2001). Similarly, mammary specific deletion of PTEN alleles resulted in the accelerated formation of breast cancer induced by an activated ErbB2 and an increase in the frequency of lung metastases (Dourdin et al., 2008). The interplay of DLC1 loss with the activity of an oncogene to drive tumorigenesis was also published. This recent study by Xue et al., which provides *in vivo* evidence for DLC1 tumor suppressor activity, used a model in which DLC1 knockdown cooperated with the Myc oncogene and p53 deficiency to promote HCC in mice (Xue et al., 2008). In this thesis it was investigated if the combined loss of the two tumor suppressors DLC1 and PTEN also collaborates in the acceleration of oncogenesis. Therefore, by using RNAi both proteins were simultaneously depleted in the non-invasive MCF7 breast cancer cell line and the consequences regarding different features of transformation were examined. The utilized siRNAs specific for DLC1 and PTEN, respectively, efficiently downregulated the respective proteins. The observed increase of phosphorylated Akt upon PTEN knockdown is in line with its regulatory role of PI3K signaling and further provided evidence for PTEN functionality in MCF7 cells. These high levels of activated Akt were able to promote the proliferation of MCF7 cells depleted of PTEN, correlating with previous reported overexpression studies, in which PTEN caused a G1 cell cycle arrest in MCF7 cells due to inhibition of Akt activation (Weng et al., 1999). Interestingly, a modest but reproducible increase of phospho-Akt was observed in DLC1-depleted cells. In contrast to studies, in which ectopically expressed DLC1 caused significant growth inhibition of breast cancer cells (Yuan et al., 2003), the knockdown of DLC1 did not augment cell proliferation compared to control cells transfected with a LacZ siRNA. Thus, the loss of DLC1 might be compensated by other – regarding cell cycle control perhaps more significant – factors. Moreover, the slightly increased levels of phosphorylated Akt did not appear to be sufficient to promote cell proliferation. Accordingly, the double knockdown of DLC1 and PTEN did not favor cell proliferation compared to cells lacking PTEN alone.

Aberrant DLC1 as well as PTEN signaling is associated with metastasis and poorer prognosis in breast cancer (Goodison et al., 2005; Saal et al., 2007). The metastatic potential of cells is achieved by a migratory phenotype among other features. Accordingly, the

signaling pathways regulated by DLC1 and PTEN are known to be involved in cell motility. PI3K signaling, for example, is a key event in the control of polarization and migration during chemotactic movement. In *Dictyostelium,* the reciprocal localization of PI3K and PTEN causes a steep gradient of PIP3 from the leading edge to the back of the cell (Iijima & Devreotes, 2002). The importance of the generation of such a gradient is demonstrated in cells lacking PTEN. Instead of one large pseudopod, these cells produce multiple inappropriate pseudopodia at the sides and rear and are, thus, impaired in the speed and directionality of chemotaxis (Wessels et al., 2007). In mammalian cells the influence of PTEN on cell migration seems to differ from that in *Dictyostelium*. For example, fibroblasts ectopically expressing PTEN displayed reduced integrin-mediated cell spreading and migration in wounding assays. Accordingly, expression of antisense PTEN had the opposite effects (Tamura et al., 1998). Similarly, B cells deficient for PTEN displayed enhanced migration (Suzuki et al., 2003). In PTEN-null Jurkat T cells reintroduction of the protein reduced the speed of moving cells, but did not affect cell gradient sensing (Lacalle et al., 2004). The molecular mechanism, by which PTEN regulates cell motility, remains controversial. In PTEN deficient murine fibroblasts an increase in the migratory behavior was associated with elevated levels of active Rac1 and Cdc42. The negative control of cell motility by reintroduced PTEN was dependent on its lipid phosphatase activity (Liliental et al., 2000). In contrast, Tamura et al. demonstrated that the protein phosphatase activity of PTEN was involved in the regulation of migration, but lipid phosphatase activity was dispensable. This effect might be mediated by PTEN-induced dephosphorylation of FAK (Tamura et a., 1998). More recent studies provide evidence for the prerequisite of PTEN autophosphorylation. The C2 domain was shown to be sufficient for the robust inhibition of cell migration. However, in the full-length protein the phosphorylated carboxyterminal tail interacts with the C2 domain and precludes its inhibitory function. Through PTEN autophosphorylation inhibition of the C2 domain is relieved and cell migration can be blocked (Raftopoulou et al., 2004).

RhoGTPases also play a central role in establishing cell polarization and cellular motility. Beside its role in tail retraction via Rho-associated kinase (ROCK) it was recently shown that Rho, and not only Rac and Cdc42, localizes to the leading edge of migrating cells. Signaling through its downstream effector Dia1 is required for appropriate directionality and locomotion of cell migration (Yamana et al., 2006). Accordingly, the inhibitory effect of DLC1 on cell motility in breast cancer cells was shown to be mediated through the Rho-Dia1 signaling pathway (Holeiter et al., 2008).

The wound healing and chemotactic transwell assays with either DLC1- or PTEN- depleted MCF7 cells performed during this thesis are in line with the data discussed above. Single knockdown of both proteins resulted in an increase of the migratory behavior. Silencing of DLC1 led to an enhanced Dia1 staining at the front of cells migrating to close a wound. Migrating cells transfected with a PTEN-specific siRNA displayed increased pFAK staining although total cellular pFAK levels were not augmented. Interestingly, simultaneous knockdown of the two tumor suppressors further enhanced cell motility in an additive manner. It is possible that this applies only to cells of low invasiveness, as DLC1 knockdown enhanced migration in MCF7 and MDAMB436 cell lines (Holeiter et al., 2008), but failed to do so in the highly invasive MDAMB231 cell line (our unpublished observations).

Taken together, these data suggest that the local concerted action of a DLC1/PTEN complex, negatively regulating RhoGTPase- and PTEN-dependent signaling pathways, is required for the synchronization of signaling processes during cell migration, which is a process, relying on a complex series of events. Although the interdependence of one protein function on the other could not be detected in the overexpression experiments performed, locally restricted synergistic effects cannot be ruled out. In conclusion, the loss of both proteins is proposed to promote tumorigenesis by increasing the metastatic potential of cancer cells.

4.3 The DLC1-liprin beta2 interaction

Another putative candidate identified in the yeast-two-hybrid screen was liprin beta2. Interestingly, liprin beta2 belongs to a family of proteins characterized by a highly conserved LH domain consisting of three SAM domains (Serra-Page et al., 1998). The sequence fished as an interacting fragment partially comprised the most C-terminal SAM domain, implying the notion of a hetero-SAM interaction. GST pulldowns of endogenous liprin beta2 with the DLC1 SAM domain and coimmunoprecipitation of full-length DLC1 and full-length liprin beta2 confirmed the specificity of this association in mammalian cells.

In the yeast-two-hybrid approach time/space constraints may be detected. These interactions occur between proteins that are able to bind to each other, but are not expressed simultaneously in the same tissue or at the same point of development. DLC1 is widely expressed in human tissues (Yuan et al., 1998) and liprin beta2 was also shown to be broadly expressed (Serra-Page et al., 1998). Nonetheless, for an interaction of both proteins to be of relevance in breast carcinogenesis, which is the topic of our group, coexpression had to be investigated. Indeed, semi-quantitative RT-PCR analysis as well as immunoblotting

of cell lysates with DLC1- and liprin beta2-specific antibodies, respectively, revealed the joint expression in a subset of breast cancer cell lines.

Coimmunoprecipitation of DLC1 with liprin alpha1 and liprin beta1, respectively, showed that the interaction is not restricted to the liprin isoform beta2, but seems to be a common feature of the conserved LH domain of liprin proteins. Without any functional assay only speculations about the impact of liprins on DLC1 activity and/or regulation can be made. However, the interaction with liprins is reminiscent of that with the tensin family, which is essential for the recruitment of DLC1 to focal adhesions and its biological function (Qian et al., 2007). Similarly, liprins also serve as scaffold proteins with no internal enzymatic activity (Serra-Page et al., 1998). It is therefore conceivable that DLC1 might be targeted to a specific cell compartment via liprin binding. Liprins are multivalent proteins that form complex structures due to homo-and heterodimerization. Alpha-type liprins also interact with the LAR subfamily of RPTPs (Serra-Pages et al., 1995). In epithelial cells LAR has been shown to be involved in E-cadherin-mediated cell-cell communication. LAR localizes with the cadherin-catenin complex in adherens junctions, where it dephosphorylates β-catenin and, thus, prevents the disruption of this complex, thereby inhibiting cell migration (Muller et al., 1999). Therefore, whether DLC1 is perhaps an integral component of the LAR-liprin network during cell adhesion should be investigated.

Although liprin alpha1 as well as both beta subtypes are broadly expressed in human tissues, the main research until now has focused on their role in the nervous system. Especially liprin alpha1 is known to be essential for axon guidance, trafficking of synaptic vesicles and the formation of a functional presynaptic active zone in cooperation with LAR (Stryker & Johnson, 2007). Thus, the association with DLC1 might play a role not only in epithelial but in neuronal cells.

4.4 Conclusions and Outlook

The aim of this thesis was to identify novel protein binding partners for the tumor suppressor DLC1. Therefore, a yeast-two-hybrid screen was performed and finally 16 proteins were revealed as putative candidates. The main research was focused on the interaction of DLC1 with PTEN, a tumor suppressor itself. The association was shown to be dynamically regulated upon PTEN activation. Simultaneous depletion of both proteins enhanced the migratory behavior of MCF7 cells, implying the significance of a PTEN/DLC1 complex in the temporally and spatially restricted regulation of cell motility. Failure of the local concerted

action of DLC1, impinging on Dia1, and that of PTEN, targeting FAK, is proposed to lead to a more transformed phenotype with increased metastatic potential. In future studies it has to be investigated if there is an interdependence of one protein on the other. First experiments with ectopically expressed DLC1 and PTEN did not show any impact on downstream signaling pathways upon coexpression, but the effects might only be local and not measurable in whole cell lysates. Thus, imaging of complex formation and signaling events at the plasma membrane in single, migrating cells may possibly reveal an interplay of the two proteins.

The second protein that was characterized as a novel DLC1 binding partner was liprin beta2. The association was confirmed biochemically and was shown to extend to other members of the liprin protein family. Unfortunately, several approaches to localize liprin beta2 by immunostaining in cells did not work due to the unspecificity of the utilized antibodies (data not shown). Thus, it will be of interest to overcome these problems and define the subcellular sites of colocalization with DLC1. Since liprins are scaffold proteins the hypothesis of targeting DLC1 to a specific cell compartment has to be proven. Examination of DLC1 function in the presence or absence of liprin proteins will also be an exciting topic in order to determine the role of the identified interaction. Last but not least, it would also be interesting to investigate DLC1 function and its association with liprins in neuronal cells.

5 References

Al-Khouri AM, Ma Y, Togo SH, Williams S, Mustelin T. Cooperative phosphorylation of the tumor suppressor phosphatase and tensin homologue (PTEN) by casein kinases and glycogen synthase kinase 3beta. *J Biol Chem.* 2005 Oct 21;280(42):35195-202.

Andersen JN, Mortensen OH, Peters GH, Drake PG, Iversen LF, Olsen OH, Jansen PG, Andersen HS, Tonks NK, Møller NP. Structural and evolutionary relationships among protein tyrosine phosphatase domains. *Mol Cell Biol*. 2001 Nov;21(21):7117-36.

Bernards A, Settleman J. GAP control: regulating the regulators of small GTPases. *Trends Cell Biol.* 2004 Jul;14(7):377-85.

Bishop JM. Cancer: the rise of the genetic paradigm. *Genes Dev*. 1995 Jun 1;9(11):1309-15.

Bos JL, Rehmann H, Wittinghofer A. GEFs and GAPs: critical elements in the control of small G proteins. *Cell.* 2007 Jun 1;129(5):865-77.

Boureux A, Vignal E, Faure S, Fort P. Evolution of the Rho family of ras-like GTPases in eukaryotes. *Mol Biol Evol.* 2007 Jan;24(1):203-16.

Chagnon MJ, Uetani N, Tremblay ML. Functional significance of the LAR receptor protein tyrosine phosphatase family in development and diseases. *Biochem Cell Biol.* 2004 Dec;82(6):664-75.

Croce CM. Oncogenes and cancer. *N Engl J Med*. 2008 Jan 31;358(5):502-11.

Das S, Dixon JE, Cho W. Membrane-binding and activation mechanism of PTEN. *Proc Natl Acad Sci U S A.* 2003 Jun 24;100(13):7491-6.

Debant A, Serra-Pagès C, Seipel K, O'Brien S, Tang M, Park SH, Streuli M. The multidomain protein Trio binds the LAR transmembrane tyrosine phosphatase, contains a protein kinase domain, and has separate rac-specific and rho-specific guanine nucleotide exchange factor domains. *Proc Natl Acad Sci U S A.* 1996 May 28;93(11):5466-71.

Depowski PL, Rosenthal SI, Ross JS. Loss of expression of the PTEN gene protein product is associated with poor outcome in breast cancer. *Mod Pathol*. 2001 Jul;14(7):672-6.

Di Cristofano A, De Acetis M, Koff A, Cordon-Cardo C, Pandolfi PP. Pten and p27KIP1 cooperate in prostate cancer tumor suppression in the mouse. *Nat Genet*. 2001 Feb;27(2):222-4.

Di Cristofano A, Pesce B, Cordon-Cardo C, Pandolfi PP. Pten is essential for embryonic development and tumour suppression. *Nat Genet.* 1998 Aug;19(4):348-55.

Dourdin N, Schade B, Lesurf R, Hallett M, Munn RJ, Cardiff RD, Muller WJ. Phosphatase and tensin homologue deleted on chromosome 10 deficiency accelerates tumor induction in a mouse model of ErbB-2 mammary tumorigenesis. *Cancer Res.* 2008 Apr 1;68(7):2122-31.

Durkin ME, Avner MR, Huh CG, Yuan BZ, Thorgeirsson SS, Popescu NC. DLC-1, a Rho GTPase-activating protein with tumor suppressor function, is essential for embryonic development. *FEBS Lett.* 2005 Feb 14;579(5):1191-6.

Durkin ME, Yuan BZ, Thorgeirsson SS, Popescu NC. Gene structure, tissue expression, and linkage mapping of the mouse DLC-1 gene (Arhgap7). *Gene*. 2002 Apr 17;288(1-2):119-27.

Durkin ME, Yuan BZ, Zhou X, Zimonjic DB, Lowy DR, Thorgeirsson SS, Popescu NC. DLC-1:a Rho GTPase-activating protein and tumour suppressor. *J Cell Mol Med.* 2007 Sep-Oct;11(5):1185-207.

Dutt A, Beroukhim R. Single nucleotide polymorphism array analysis of cancer. *Curr Opin Oncol.* 2007 Jan;19(1):43-9.

Endersby R, Baker SJ. PTEN signaling in brain: neuropathology and tumorigenesis. *Oncogene*. 2008 Sep 18;27(41):5416-30.

Engelman JA, Luo J, Cantley LC. The evolution of phosphatidylinositol 3-kinases as regulators of growth and metabolism. *Nat Rev Genet*. 2006 Aug;7(8):606-19.

Esteller M. CpG island hypermethylation and tumor suppressor genes: a booming present, a brighter future. *Oncogene.* 2002 Aug 12;21(35):5427-40.

Fields S, Song O. A novel genetic system to detect protein-protein interactions. *Nature.* 1989 Jul 20;340(6230):245-6.

Freeman DJ, Li AG, Wei G, Li HH, Kertesz N, Lesche R, Whale AD, Martinez-Diaz H, Rozengurt N, Cardiff RD, Liu X, Wu H. PTEN tumor suppressor regulates p53 protein levels and activity through phosphatase-dependent and -independent mechanisms. *Cancer Cell*. 2003 Feb;3(2):117-30.

Georgescu MM, Kirsch KH, Akagi T, Shishido T, Hanafusa H. The tumor-suppressor activity of PTEN is regulated by its carboxyl-terminal region. *Proc Natl Acad Sci U S A.* 1999 Aug 31;96(18):10182-7.

Georgescu MM, Kirsch KH, Kaloudis P, Yang H, Pavletich NP, Hanafusa H. Stabilization and productive positioning roles of the C2 domain of PTEN tumor suppressor. *Cancer Res.* 2000 Dec 15;60(24):7033-8.

Ginn-Pease ME, Eng C. Increased nuclear phosphatase and tensin homologue deleted on chromosome 10 is associated with G0-G1 in MCF-7 cells. *Cancer Res*. 2003 Jan 15;63(2):282-6.

Gómez del Pulgar T, Benitah SA, Valerón PF, Espina C, Lacal JC. Rho GTPase expression in tumourigenesis: evidence for a significant link. *Bioessays*. 2005 Jun;27(6):602-13.

Goodison S, Yuan J, Sloan D, Kim R, Li C, Popescu NC, Urquidi V. The RhoGAP protein DLC-1 functions as a metastasis suppressor in breast cancer cells*. Cancer Res.* 2005 Jul 15;65(14):6042-53.

Grise F, Bidaud A, Moreau V. Rho GTPases in hepatocellular carcinoma. *Biochim Biophys Acta.* 2009 Apr;1795(2):137-51.

Guan M, Zhou X, Soulitzis N, Spandidos DA, Popescu NC. Aberrant methylation and deacetylation of deleted in liver cancer-1 gene in prostate cancer: potential clinical applications. *Clin Cancer Res.* 2006 Mar 1;12(5):1412-9.

Hanahan D, Weinberg RA. The hallmarks of cancer. *Cell.* 2000 Jan 7;100(1):57-70.

Healy KD, Hodgson L, Kim TY, Shutes A, Maddileti S, Juliano RL, Hahn KM, Harden TK, Bang YJ, Der CJ. DLC-1 suppresses non-small cell lung cancer growth and invasion by RhoGAP-dependent and independent mechanisms. *Mol Carcinog*. 2008 May;47(5):326-37.

Holeiter G, Heering J, Erlmann P, Schmid S, Jähne R, Olayioye MA. Deleted in liver cancer 1 controls cell migration through a Dia1-dependent signaling pathway. *Cancer Res.* 2008 Nov 1;68(21):8743-51.

Hope IA, Struhl K. Functional dissection of a eukaryotic transcriptional activator protein, GCN4 of yeast. *Cell.* 1986 Sep 12;46(6):885-94.

Iijima M, Devreotes P. Tumor suppressor PTEN mediates sensing of chemoattractant gradients. *Cell*. 2002 May 31;109(5):599-610.

Jackson AL, Loeb LA. On the origin of multiple mutations in human cancers. *Semin Cancer Biol.* 1998 Dec;8(6):421-9.

Jaffe AB, Hall A. Rho GTPases: biochemistry and biology. *Annu Rev Cell Dev Biol.* 2005;21:247-69.

Keniry M, Parsons R. The role of PTEN signaling perturbations in cancer and in targeted therapy. *Oncogene*. 2008 Sep 18;27(41):5477-85.

Kim RH, Mak TW. Tumours and tremors: how PTEN regulation underlies both. *Br J Cancer.* 2006 Mar 13;94(5):620-4.

Kim TY, Healy KD, Der CJ, Sciaky N, Bang YJ, Juliano RL. Effects of structure of Rho GTPase-activating protein DLC-1 on cell morphology and migration. *J Biol Chem*. 2008 Nov 21;283(47):32762-70.

Kim TY, Lee JW, Kim HP, Jong HS, Kim TY, Jung M, Bang YJ. DLC-1, a GTPase-activating protein for Rho, is associated with cell proliferation, morphology, and migration in human hepatocellular carcinoma. *Biochem Biophys Res Commun*. 2007 Mar 30;355(1):72-7.

Knudson AG Jr. Mutation and cancer: statistical study of retinoblastoma. *Proc Natl Acad Sci U S A.* 1971 Apr;68(4):820-3.

Kölsch V, Charest PG, Firtel RA. The regulation of cell motility and chemotaxis by phospholipid signaling. *J Cell Sci.* 2008 Mar 1;121(Pt 5):551-9.

Kriajevska M, Fischer-Larsen M, Moertz E, Vorm O, Tulchinsky E, Grigorian M, Ambartsumian N, Lukanidin E. Liprin beta 1, a member of the family of LAR transmembrane tyrosine phosphatase-interacting proteins, is a new target for the metastasis-associated protein S100A4 (Mts1). *J Biol Chem*. 2002 Feb 15;277(7):5229-35.

Lacalle RA, Gómez-Moutón C, Barber DF, Jiménez-Baranda S, Mira E, Martínez-A C, Carrera AC, Mañes S. PTEN regulates motility but not directionality during leukocyte chemotaxis*. J Cell Sci.* 2004 Dec 1;117(Pt 25):6207-15.

Lee JO, Yang H, Georgescu MM, Di Cristofano A, Maehama T, Shi Y, Dixon JE, Pandolfi P, Pavletich NP. Crystal structure of the PTEN tumor suppressor: implications for its phosphoinositide phosphatase activity and membrane association. *Cell.* 1999 Oct 29;99(3):323-34.

Leslie NR, Yang X, Downes CP, Weijer CJ. The regulation of cell migration by PTEN. Biochem *Soc Trans*. 2005 Dec;33(Pt 6):1507-8.

Levea CM, Mcgary CT, Symons JR, Mooney RA. PTP LAR expression compared to prognostic indices in metastatic and non-metastatic breast cancer. *Breast Cancer Res Treat*. 2000 Nov;64(2):221-8.

Li AG, Piluso LG, Cai X, Wei G, Sellers WR, Liu X. Mechanistic insights into maintenance of high p53 acetylation by PTEN. *Mol Cell*. 2006 Aug;23(4):575-87.

Li DM, Sun H. TEP1, encoded by a candidate tumor suppressor locus, is a novel protein tyrosine phosphatase regulated by transforming growth factor beta. *Cancer Res*. 1997 Jun 1;57(11):2124-9.

Li G, Robinson GW, Lesche R, Martinez-Diaz H, Jiang Z, Rozengurt N, Wagner KU, Wu DC, Lane TF, Liu X, Hennighausen L, Wu H. Conditional loss of PTEN leads to precocious development and neoplasia in the mammary gland. *Development.* 2002 Sep;129(17):4159-70.

Li Y, Podsypanina K, Liu X, Crane A, Tan LK, Parsons R, Varmus HE. Deficiency of Pten accelerates mammary oncogenesis in MMTV-Wnt-1 transgenic mice. *BMC.Mol.Biol*., 2, (2001) 2.

Liao YC, Shih YP, Lo SH. Mutations in the focal adhesion targeting region of deleted in liver cancer-1 attenuate their expression and function. *Cancer Res.* 2008 Oct 1;68(19):7718-22.

Liao YC, Si L, deVere White RW, Lo SH. The phosphotyrosine-independent interaction of DLC-1 and the SH2 domain of cten regulates focal adhesion localization and growth suppression activity of DLC-1. *J Cell Biol*. 2007 Jan 1;176(1):43-9.

Liliental J, Moon SY, Lesche R, Mamillapalli R, Li D, Zheng Y, Sun H, Wu H. Genetic deletion of the Pten tumor suppressor gene promotes cell motility by activation of Rac1 and Cdc42 GTPases. *Curr Biol.* 2000 Apr 6;10(7):401-4.

Luo Y, Batalao A, Zhou H, Zhu L. Mammalian two-hybrid system: a complementary approach to the yeast two-hybrid system. *Biotechniques.* 1997 Feb;22(2):350-2.

Maccario H, Perera NM, Davidson L, Downes CP, Leslie NR. PTEN is destabilized by phosphorylation on Thr366. *Biochem J.* 2007 Aug 1;405(3):439-44.

Maehama T, Dixon JE. The tumor suppressor, PTEN/MMAC1, dephosphorylates the lipid second messenger, phosphatidylinositol 3,4,5-trisphosphate. *J Biol Chem*. 1998 May 29;273(22):13375-8.

Mahimainathan L, Choudhury GG. Inactivation of platelet-derived growth factor receptor by the tumor suppressor PTEN provides a novel mechanism of action of the phosphatase. *J Biol Chem.* 2004 Apr 9;279(15):15258-68.

Miller JP, Lo RS, Ben-Hur A, Desmarais C, Stagljar I, Noble WS, Fields S. Large-scale identification of yeast integral membrane protein interactions. *Proc Natl Acad Sci U S A.* 2005 Aug 23;102(34):12123-8.

Müller T, Choidas A, Reichmann E, Ullrich A. Phosphorylation and free pool of beta-catenin are regulated by tyrosine kinases and tyrosine phosphatases during epithelial cell migration. *J Biol Chem.* 1999 Apr 9;274(15):10173-83.

Myers MP, Stolarov JP, Eng C, Li J, Wang SI, Wigler MH, Parsons R, Tonks NK. P-TEN, the tumor suppressor from human chromosome 10q23, is a dual-specificity phosphatase. *Proc Natl Acad Sci U S A*. 1997 Aug 19;94(17):9052-7.

Nooren IM, Thornton JM. Diversity of protein-protein interactions. *EMBO J*. 2003 Jul 15;22(14):3486-92.

Odriozola L, Singh G, Hoang T, Chan AM. Regulation of PTEN activity by its carboxyl-terminal autoinhibitory domain. *J Biol Chem.* 2007 Aug 10;282(32):23306-15.

O'Grady P, Thai TC, Saito H. The laminin-nidogen complex is a ligand for a specific splice isoform of the transmembrane protein tyrosine phosphatase LAR. *J Cell Biol.* 1998 Jun 29;141(7):1675-84.

Okumura K, Mendoza M, Bachoo RM, DePinho RA, Cavenee WK, Furnari FB. PCAF modulates PTEN activity. *J Biol Chem*. 2006 Sep 8;281(36):26562-8.

Osborne MA, Dalton S, Kochan JP. The yeast tribrid system--genetic detection of trans-phosphorylated ITAM-SH2-interactions. *Biotechnology (N Y).* 1995 Dec;13(13):1474-8.

Patel L, Pass I, Coxon P, Downes CP, Smith SA, Macphee CH. Tumor suppressor and anti-inflammatory actions of PPARgamma agonists are mediated via upregulation of PTEN. *Curr Biol*. 2001 May 15;11(10):764-8.

Perren A, Weng LP, Boag AH, Ziebold U, Thakore K, Dahia PL, Komminoth P, Lees JA, Mulligan LM, Mutter GL, Eng C. Immunohistochemical evidence of loss of PTEN expression in primary ductal adenocarcinomas of the breast. *Am J Pathol*. 1999 Oct;155(4):1253-60.

Phizicky EM, Fields S. Protein-protein interactions: methods for detection and analysis. *Microbiol Rev*. 1995 Mar;59(1):94-123.

Plaumann M, Seitz S, Frege R, Estevez-Schwarz L, Scherneck S. Analysis of DLC-1 expression in human breast cancer. *J Cancer Res Clin Oncol.* 2003 Jun;129(6):349-54.

Podsypanina K, Ellenson LH, Nemes A, Gu J, Tamura M, Yamada KM, Cordon-Cardo C, Catoretti G, Fisher PE, Parsons R. Mutation of Pten/Mmac1 in mice causes neoplasia in multiple organ systems. *Proc Natl Acad Sci U S A.* 1999 Feb 16;96(4):1563-8.

Ponting CP. SAM: a novel motif in yeast sterile and Drosophila polyhomeotic proteins. *Protein Sci.* 1995 Sep;4(9):1928-30.

Pulido R, Serra-Pagès C, Tang M, Streuli M. The LAR/PTP delta/PTP sigma subfamily of transmembrane protein-tyrosine-phosphatases: multiple human LAR, PTP delta, and PTP sigma isoforms are expressed in a tissue-specific manner and associate with the LAR-interacting protein LIP.1. *Proc Natl Acad Sci U S A.* 1995 Dec 5;92(25):11686-90.

Qian X, Li G, Asmussen HK, Asnaghi L, Vass WC, Braverman R, Yamada KM, Popescu NC, Papageorge AG, Lowy DR. Oncogenic inhibition by a deleted in liver cancer gene requires cooperation between tensin binding and Rho-specific GTPase-activating protein activities. *Proc Natl Acad Sci U S A.* 2007 May 22;104(21):9012-7.

Qiao F, Bowie JU. The many faces of SAM. *Sci STKE*. 2005 May 31;2005(286):re7.

Raftopoulou M, Etienne-Manneville S, Self A, Nicholls S, Hall A. Regulation of cell migration by the C2 domain of the tumor suppressor PTEN. *Science*. 2004 Feb 20;303(5661):1179-81.

Reichmann D, Rahat O, Cohen M, Neuvirth H, Schreiber G. The molecular architecture of protein-protein binding sites. *Curr Opin Struct Biol.* 2007 Feb;17(1):67-76.

Ross SH, Lindsay Y, Safrany ST, Lorenzo O, Villa F, Toth R, Clague MJ, Downes CP, Leslie NR. Differential redox regulation within the PTP superfamily. *Cell Signal*. 2007 Jul;19(7):1521-30.

Saal LH, Gruvberger-Saal SK, Persson C, Lövgren K, Jumppanen M, Staaf J, Jönsson G, Pires MM, Maurer M, Holm K, Koujak S, Subramaniyam S, Vallon-Christersson J, Olsson H, Su T, Memeo L, Ludwig T, Ethier SP, Krogh M, Szabolcs M, Murty VV, Isola J, Hibshoosh H, Parsons R, Borg A. Recurrent gross mutations of the PTEN tumor suppressor gene in breast cancers with deficient DSB repair. *Nat Genet*. 2008 Jan;40(1):102-7.

Salmena L, Carracedo A, Pandolfi PP. Tenets of PTEN tumor suppression. *Cell.* 2008 May 2;133(3):403-14.

Schaapveld RQ, Schepens JT, Bächner D, Attema J, Wieringa B, Jap PH, Hendriks WJ. Developmental expression of the cell adhesion molecule-like protein tyrosine phosphatases LAR, RPTPdelta and RPTPsigma in the mouse. *Mech Dev*. 1998 Sep;77(1):59-62.

Schaapveld RQ, Schepens JT, Robinson GW, Attema J, Oerlemans FT, Fransen JA, Streuli M, Wieringa B, Hennighausen L, Hendriks WJ. Impaired mammary gland development and function in mice lacking LAR receptor-like tyrosine phosphatase activity. *Dev Biol.* 1997 Aug 1;188(1):134-46.

Scholz RP, Regner J, Theil A, Erlmann P, Holeiter G, Jähne R, Schmid S, Hausser A, Olayioye MA. DLC1 interacts with 14-3-3 proteins to inhibit RhoGAP activity and block nucleocytoplasmic shuttling. *J Cell Sci.* 2009 Jan 1;122(Pt 1):92-102.

Sekimata M, Kabuyama Y, Emori Y, Homma Y. Morphological changes and detachment of adherent cells induced by p122, a GTPase-activating protein for Rho. *J Biol Chem.* 1999 Jun 18;274(25):17757-62.

Serra-Pagès C, Kedersha NL, Fazikas L, Medley Q, Debant A, Streuli M. The LAR transmembrane protein tyrosine phosphatase and a coiled-coil LAR-interacting protein co-localize at focal adhesions. *EMBO J*. 1995 Jun 15;14(12):2827-38.

Serra-Pagès C, Medley QG, Tang M, Hart A, Streuli M. Liprins, a family of LAR transmembrane protein-tyrosine phosphatase-interacting proteins. *J Biol Chem.* 1998 Jun 19;273(25):15611-20.

Shen JC, Unoki M, Ythier D, Duperray A, Varticovski L, Kumamoto K, Pedeux R, Harris CC. Inhibitor of growth 4 suppresses cell spreading and cell migration by interacting with a novel binding partner, liprin alpha1. *Cancer Res*. 2007 Mar 15;67(6):2552-8.

Shen WH, Balajee AS, Wang J, Wu H, Eng C, Pandolfi PP, Yin Y. Essential role for nuclear PTEN in maintaining chromosomal integrity. *Cell*. 2007 Jan 12;128(1):157-70.

Sherr CJ. Principles of tumor suppression. *Cell.* 2004 Jan 23;116(2):235-46.

Stambolic V, MacPherson D, Sas D, Lin Y, Snow B, Jang Y, Benchimol S, Mak TW. Regulation of PTEN transcription by p53. *Mol Cell*. 2001 Aug;8(2):317-25.

Stambolic V, Tsao MS, Macpherson D, Suzuki A, Chapman WB, Mak TW. High incidence of breast and endometrial neoplasia resembling human Cowden syndrome in pten+/- mice. *Cancer Res*. 2000 Jul 1;60(13):3605-11.

Steck PA, Pershouse MA, Jasser SA, Yung WK, Lin H, Ligon AH, Langford LA, Baumgard ML, Hattier T, Davis T, Frye C, Hu R, Swedlund B, Teng DH, Tavtigian SV. Identification of a candidate tumour suppressor gene, MMAC1, at chromosome 10q23.3 that is mutated in multiple advanced cancers. *Nat Genet*. 1997 Apr;15(4):356-62.

Streuli M, Krueger NX, Thai T, Tang M, Saito H. Distinct functional roles of the two intracellular phosphatase like domains of the receptor-linked protein tyrosine phosphatases LCA and LAR. *EMBO J.* 1990 Aug;9(8):2399-407.

Stryker E, Johnson KG. LAR, liprin alpha and the regulation of active zone morphogenesis. *J Cell Sci*. 2007 Nov 1;120(Pt 21):3723-8.

Suter B, Kittanakom S, Stagljar I. Two-hybrid technologies in proteomics research. *Curr Opin Biotechnol.* 2008 Aug;19(4):316-23.

Suzuki A, Kaisho T, Ohishi M, Tsukio-Yamaguchi M, Tsubata T, Koni PA, Sasaki T, Mak TW, Nakano T. Critical roles of Pten in B cell homeostasis and immunoglobulin class switch recombination. *J Exp Med*. 2003 Mar 3;197(5):657-67.

Syed V, Mukherjee K, Lyons-Weiler J, Lau KM, Mashima T, Tsuruo T, Ho SM. Identification of ATF-3, caveolin-1, DLC-1, and NM23-H2 as putative antitumorigenic, progesterone-regulated genes for ovarian cancer cells by gene profiling. *Oncogene.* 2005 Mar 3;24(10):1774-87.

Symons JR, LeVea CM, Mooney RA. Expression of the leucocyte common antigen-related (LAR) tyrosine phosphatase is regulated by cell density through functional E-cadherin complexes. *Biochem J.* 2002 Jul 15;365(Pt 2):513-9.

Takahashi Y, Morales FC, Kreimann EL, Georgescu MM. PTEN tumor suppressor associates with NHERF proteins to attenuate PDGF receptor signaling. *EMBO J.* 2006 Feb 22;25(4):910-20.

Tamguney T, Stokoe D. New insights into PTEN. *J Cell Sci*. 2007 Dec 1;120(Pt 23):4071-9.

Tamura M, Gu J, Matsumoto K, Aota S, Parsons R, Yamada KM. Inhibition of cell migration, spreading, and focal adhesions by tumor suppressor PTEN. *Science*. 1998 Jun 5;280(5369):1614-7.

Tcherkezian J, Lamarche-Vane N. Current knowledge of the large RhoGAP family of proteins. *Biol Cell.* 2007 Feb;99(2):67-86.

Torres J, Pulido R. The tumor suppressor PTEN is phosphorylated by the protein kinase CK2 at its C terminus. Implications for PTEN stability to proteasome-mediated degradation. *J Biol Chem.* 2001 Jan 12;276(2):993-8.

Trotman LC, Wang X, Alimonti A, Chen Z, Teruya-Feldstein J, Yang H, Pavletich NP, Carver BS, Cordon-Cardo C, Erdjument-Bromage H, Tempst P, Chi SG, Kim HJ, Misteli T, Jiang X, Pandolfi PP. Ubiquitination regulates PTEN nuclear import and tumor suppression. *Cell*. 2007 Jan 12;128(1):141-56.

Ullmannova-Benson V, Guan M, Zhou X, Tripathi V, Yang XY, Zimonjic DB, Popescu NC. DLC1 tumor suppressor gene inhibits migration and invasion of multiple myeloma cells through RhoA GTPase pathway. *Leukemia*. 2009 Feb;23(2):383-90.

Ullmannova V, Popescu NC. Expression profile of the tumor suppressor genes DLC-1 and DLC-2 in solid tumors. *Int J Oncol.* 2006 Nov;29(5):1127-32.

Van Criekinge W, Beyaert R. Yeast Two-Hybrid: State of the Art. *Biol Proced Online*. 1999 Oct 4;2:1-38.

Vazquez F, Devreotes P. Regulation of PTEN function as a PIP3 gatekeeper through membrane interaction. *Cell Cycle*. 2006 Jul;5(14):1523-7.

Vazquez F, **Grossman SR**, **Takahashi Y**, **Rokas MV**, **Nakamura N**, **Sellers WR**. Phosphorylation of the PTEN tail acts as an inhibitory switch by preventing its recruitment into a protein complex. *J Biol Chem.* 2001 Dec 28;276(52):48627-30.

Vazquez F, Matsuoka S, Sellers WR, Yanagida T, Ueda M, Devreotes PN. Tumor suppressor PTEN acts through dynamic interaction with the plasma membrane. *Proc Natl Acad Sci U S A.* 2006 Mar 7;103(10):3633-8.

Vega FM, Ridley AJ. Rho GTPases in cancer cell biology. *FEBS Lett.* 2008 Jun 18;582(14):2093-101.

Vetter IR, Wittinghofer A. The guanine nucleotide-binding switch in three dimensions. *Science.* 2001 Nov 9;294(5545):1299-304

Virolle T, Adamson ED, Baron V, Birle D, Mercola D, Mustelin T, de Belle I. The Egr-1 transcription factor directly activates PTEN during irradiation-induced signalling. *Nat Cell Biol.* 2001 Dec;3(12):1124-8.

Vivanco I, Palaskas N, Tran C, Finn SP, Getz G, Kennedy NJ, Jiao J, Rose J, Xie W, Loda M, Golub T, Mellinghoff IK, Davis RJ, Wu H, Sawyers CL. Identification of the JNK signaling pathway as a functional target of the tumor suppressor PTEN. *Cancer Cell*. 2007 Jun;11(6):555-69.

Vojtek AB, Hollenberg SM, Cooper JA. Mammalian Ras interacts directly with the serine/threonine kinase Raf. *Cell.* 1993 Jul 16;74(1):205-14.

Wang WJ, Kuo JC, Ku W, Lee YR, Lin FC, Chang YL, Lin YM, Chen CH, Huang YP, Chiang MJ, Yeh SW, Wu PR, Shen CH, Wu CT, Chen RH. The tumor suppressor DAPK is reciprocally regulated by tyrosine kinase Src and phosphatase LAR. *Mol Cell.* 2007 Sep 7;27(5):701-16.

Wang X, Trotman LC, Koppie T, Alimonti A, Chen Z, Gao Z, Wang J, Erdjument-Bromage H, Tempst P, Cordon-Cardo C, Pandolfi PP, Jiang X. NEDD4-1 is a proto-oncogenic ubiquitin ligase for PTEN. *Cell*. 2007 Jan 12;128(1):129-39.

Wells JA, McClendon CL. Reaching for high-hanging fruit in drug discovery at protein-protein interfaces. *Nature*. 2007 Dec 13;450(7172):1001-9.

Weng LP, Smith WM, Dahia PL, Ziebold U, Gil E, Lees JA, Eng C. PTEN Suppresses Breast Cancer Cell Growth by Phosphatase Activity-dependent G1 Arrest followed by Cell Death. *Cancer Res.* 1999 Nov 15;59(22):5808-14.

Wessels D, Lusche DF, Kuhl S, Heid P, Soll DR. PTEN plays a role in the suppression of lateral pseudopod formation during Dictyostelium motility and chemotaxis. *J Cell Sci*. 2007 Aug 1;120(Pt 15):2517-31.

Wiencke JK, Zheng S, Jelluma N, Tihan T, Vandenberg S, Tamgüney T, Baumber R, Parsons R, Lamborn KR, Berger MS, Wrensch MR, Haas-Kogan DA, Stokoe D. Methylation of the PTEN promoter defines low-grade gliomas and secondary glioblastoma. *Neuro Oncol*. 2007 Jul;9(3):271-9.

Wong CM, Lee JM, Ching YP, Jin DY, Ng IO. Genetic and epigenetic alterations of DLC-1 gene in hepatocellular carcinoma. *Cancer Res*. 2003 Nov 15;63(22):7646-51.

Wong CM, Yam JW, Ching YP, Yau TO, Leung TH, Jin DY, Ng IO. Rho GTPase-activating protein deleted in liver cancer suppresses cell proliferation and invasion in hepatocellular carcinoma. *Cancer Res*. 2005 Oct 1;65(19):8861-8.

Wu X, Hepner K, Castelino-Prabhu S, Do D, Kaye MB, Yuan XJ, Wood J, Ross C, Sawyers CL, Whang YE. Evidence for regulation of the PTEN tumor suppressor by a membrane-localized multi-PDZ domain containing scaffold protein MAGI-2. *Proc Natl Acad Sci U S A.* 2000 Apr 11;97(8):4233-8.

Xue W, Krasnitz A, Lucito R, Sordella R, Vanaelst L, Cordon-Cardo C, Singer S, Kuehnel F, Wigler M, Powers S, Zender L, Lowe SW. DLC1 is a chromosome 8p tumor suppressor whose loss promotes hepatocellular carcinoma. *Genes Dev*. 2008 Jun 1;22(11):1439-44.

Yamana N, Arakawa Y, Nishino T, Kurokawa K, Tanji M, Itoh RE, Monypenny J, Ishizaki T, Bito H, Nozaki K, Hashimoto N, Matsuda M, Narumiya S. The Rho-mDia1 pathway regulates cell polarity and focal adhesion turnover in migrating cells through mobilizing Apc and c-Src. *Mol Cell Biol*. 2006 Sep;26(18):6844-58.

Yam JW, Ko FC, Chan CY, Jin DY, Ng IO. Interaction of deleted in liver cancer 1 with tensin2 in caveolae and implications in tumor suppression. *Cancer Res*. 2006 Sep 1;66(17):8367-72.

Yang H, Kong W, He L, Zhao JJ, O'Donnell JD, Wang J, Wenham RM, Coppola D, Kruk PA, Nicosia SV, Cheng JQ. MicroRNA expression profiling in human ovarian cancer: miR-214 induces cell survival and cisplatin resistance by targeting PTEN. *Cancer Res*. 2008 Jan 15;68(2):425-33. Erratum in: Cancer Res. 2008 Mar 1;68(5):1609.

Yang J, Weinberg RA . Epithelial-mesenchymal transition: at the crossroads of development and tumor metastasis. *Dev Cell.* 2008 Jun;14(6):818-29.

Yang T, Zhang JS, Massa SM, Han X, Longo FM. Leukocyte common antigen-related tyrosine phosphatase receptor: increased expression and neuronal-type splicing in breast cancer cells and tissue. *Mol Carcinog.* 1999 Jun;25(2):139-49.

Yang XY, Guan M, Vigil D, Der CJ, Lowy DR, Popescu NC. p120Ras-GAP binds the DLC1 Rho-GAP tumor suppressor protein and inhibits its RhoA GTPase and growth-suppressing activities. *Oncogene.* 2009 Mar 19;28(11):1401-9.

Yin Y, Shen WH. PTEN: a new guardian of the genome. *Oncogene*. 2008 Sep 18;27(41):5443-53.

Yuan BZ, Durkin ME, Popescu NC. Promoter hypermethylation of DLC-1, a candidate tumor suppressor gene, in several common human cancers. *Cancer Genet Cytogenet*. 2003 Jan 15;140(2):113-7.

Yuan BZ, Jefferson AM, Baldwin KT, Thorgeirsson SS, Popescu NC, Reynolds SH. DLC-1 operates as a tumor suppressor gene in human non-small cell lung carcinomas. *Oncogene.* 2004 Feb 19;23(7):1405-11.

Yuan BZ, Miller MJ, Keck CL, Zimonjic DB, Thorgeirsson SS, Popescu NC. Cloning, characterization, and chromosomal localization of a gene frequently deleted in human liver cancer (DLC-1) homologous to rat RhoGAP. *Cancer Res.* 1998 May 15;58(10):2196-9.

Yuan BZ, Zhou X, Durkin ME, Zimonjic DB, Gumundsdottir K, Eyfjord JE, Thorgeirsson SS, Popescu NC. DLC-1 gene inhibits human breast cancer cell growth and in vivo tumorigenicity. *Oncogene*. 2003 Jan 23;22(3):445-50.

Zhang T, Zheng J, Jiang N, Wang G, Shi Q, Liu C, Lu Y. Overexpression of DLC-1 induces cell apoptosis and proliferation inhibition in the renal cell carcinoma. *Cancer Lett.* 2009 Apr 18.

Zhong D, Zhang J, Yang S, Soh UJ, Buschdorf JP, Zhou YT, Yang D, Low BC. The SAM domain of the RhoGAP DLC1 binds EF1A1 to regulate cell migration. *J Cell Sci*. 2009 Feb 1;122(Pt 3):414-24.

Zhou X, Thorgeirsson SS, Popescu NC. Restoration of DLC-1 gene expression induces apoptosis and inhibits both cell growth and tumorigenicity in human hepatocellular carcinoma cells. *Oncogene*. 2004 Feb 12;23(6):1308-13.

Zürner M, Schoch S. The mouse and human Liprin-alpha family of scaffolding proteins: genomic organization, expression profiling and regulation by alternative splicing. *Genomics.* 2009 Mar;93(3):243-53.

6 Appendix

6.1 Nucleotide sequences of the two investigated pACT2 clones of the yeast-two-hybrid screen

PTEN

5´-GAG TAC CCC ACC AAA CCC AAA AAA AGA GAT CTC TAT GGC TTA CCC ATA CGA TGT TCC AGA TTA CGC TAG CTT GGG TGG TCA TAT GGC CAT GGA GGC CCC GGG GAT CCG AAT TCG CGG CCG CGT CGA CGA AAA AGT AGA AAA TGG AAG TCT ATG TGA TCA AGA AAT CGA TAG CAT TTG CAG TAT AGA GCG TGC AGA TAA TGA CAA GGA ATA TCT AGT ACT TAC TTT AAC AAA AAA TGA TCT TGA CAA AGC AAA TAA AGA CAA AGC CAA CCG ATA CTT TTC TCC AAA TTT TAA GGT GAA GCT GTA CTT CAC AAA AAC AGT AGA GGA GCC GTC AAA TCC AGA GGC TAG CAG TTC AAC TTC TGT AAC ACC AGA TGT TAG TGA CAA TGA ACC TGA TCA TTA TAG ATA TTC TGA CAC CAC TGA CTC TGA TCC AGA GAA TGA ACC TTT TGA TGA AGA TCA GCA TAC ACA AAT TAC AAA AGT CTG AAT TTT TTT TTA TCA AGA GGG ATA AAA CAC CAT GAA AAT AAA CTT GAA TAA ACT GAA AAT GGA CCT TTT TTT TTT TAA TGG CAA TAG GAC ATT GTG TCA GAT TAC CAG TTA TAG GAA CAA TTC TCT TTT CCT GAC CAA TCT TGT TTT ACC CTA TAC ATC CAC AGG GTT TTG ACA CTT GTT GTC CAG TTG AAA AAA GGT TGT GTA GCT GTG TCA TGT ATA TAC CTT TTT GTG TCA AAA GGA CAT TTA AAA TTC AAT TAG GAT TAA TAA AGA TGG CAC TTT CCC GTT TTA AAA AAA AAA AAA AAA AAC TCG AGA GAT CTA TGA ATC GTA GAT ACT GAA AAA CCC CGC AAG TTC ACT TCA ACT GTG CAT CGT GCA CCA TCT CAA TTT CTT TCA TTTA TAC ATC GTT TTG CCT TCT TTT ATG TAA CTA TAC TCC TCT AAG TTT CAA TCT TGG CCA TGT AAC CTC TGA TCT ATA GAA TTT TTA ATG ACT AGA ATT AAT GC-3´

Liprin beta2

5´-ACC CCA CCA AAC CCA AAA AAA GAG ATC TCT ATG GCT TAC CCA TAC GAT GTT CCA GAT TAC GCT AGC TTG GGT GGT CAT ATG GCC ATG GAG GCC CCG GGG ATC CGA ATT CGC GGC CGC GTC GAC ATT ATC CTG GAG CCA CGC TTC ACT GGG GAC ACC CTG GCT ATG CTT CTC AAC ATC CCC CCA CAA AAG ACG CTC CTC AGG CGC CAC CTG ACC ACC AAG TTC AAT GCC TTG ATT GGT CCG GAG GCT GAA CAG GAG AAG CGA GAG AAA ATG GCC TCA CCA GCT TAC ACA CCA CTG ACC ACC ACA GCC AAA GTC CGG CCA AGG AAA CTA GGA TTT TCA CAC TTC GGA AAC ATA AGA AAA AAG AAG TTC GAT GAA TCG ACG GAC TAC ATT TGC CCA ATG GAG CCC AGT GAC GGT GTC AGT GAT AGT CAC AGG GTC TAC AGT GGC TAC CGG GGC CTC AGC CCC CTT GAT GCC CCT GAA CTG GAT GGG CTG GAC CAG GTG GGA CAG ATTA GCT GAT GCC CTT GTC ACC TGC CCT CTG TGC ACC CTG AGA GCT CAC AGT AAC ACT GTG TGT GTC ACC ATA TAA CTG CAC CTC ACC CCC GCA CGT GTG CAT GAC TCG CAG AGA ATA TTC CAG CAA TTG TGT ACC CCT GGG CCA GTC TCT TTG AAC CCT GAG GGT GGC CAG GAT CTG GAG CTG CAT CTC TAA GGG GCC AGG CTT TGG GGA CCA TTG CCA AAG GTG GAC TCA GGA GGA AAG ACA CTT AAA GAC ACT TTT ACA TGT CTA GTA ATT CTT GAT GTT CAT CTT CAG CAC CAG TGG AAA CAC ATG AAC TTC GAT GCA GGT CCA GAG ACC ATG GAC ACT CCC ACG AGG CTC AGC TCT CAG GCA CCC CCT ACA CTT CAG TTG AGG GAA AAG CTC AAG TGC CTT AGG CCC GTG GAC CAC AGT CTT GGC TGA GAT CAA AGG GAT GAG CAA CAG GGA CTT CTG CCA CAG TGA CAA TGG AA-3´

6.2 Plasmid Maps

pGBKT7 – cloning vector for generation of the bait

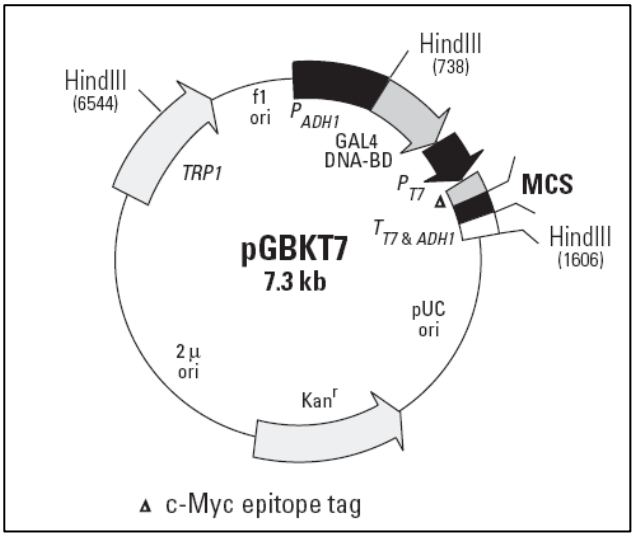

pACT2 – cloning vector for generation of the prey library

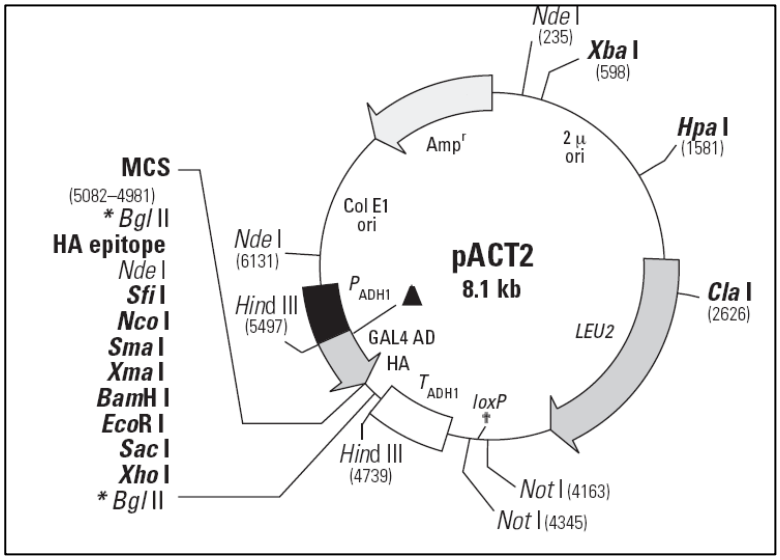

pEGFPC1 – cloning vector for generation of GFP-tagged proteins

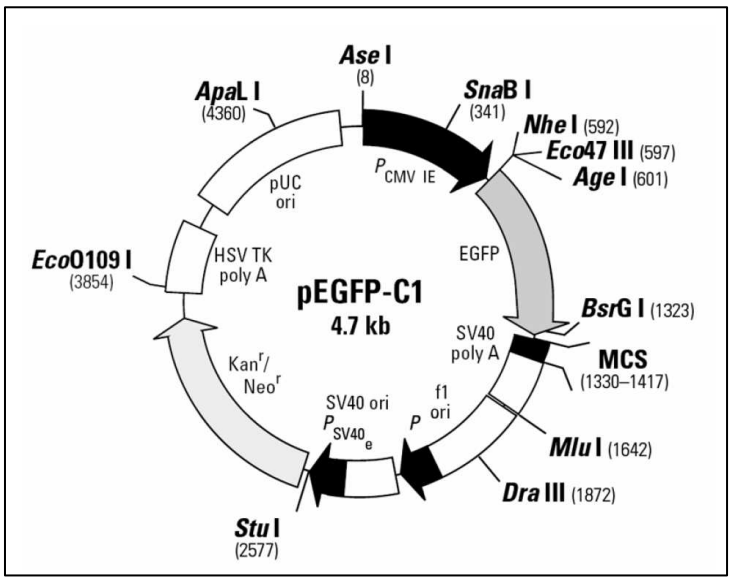

pGEX6p3 – cloning vector for generation of GST fusion proteins

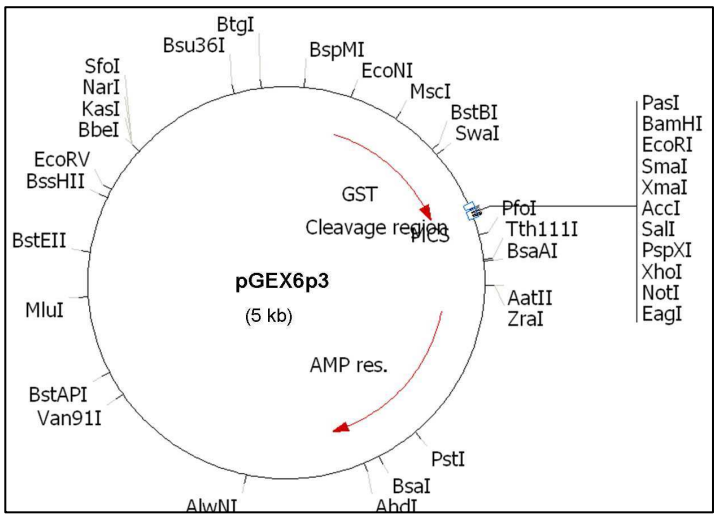

pEFrPuroFlagA – cloning vector for generation of Flag-tagged proteins/ pEFrPuroHA (consists of the backbone of pEFrPuroFlagA with the Flag-peptide replaced by a HA-peptide) – cloning vector for generation of HA-tagged proteins)

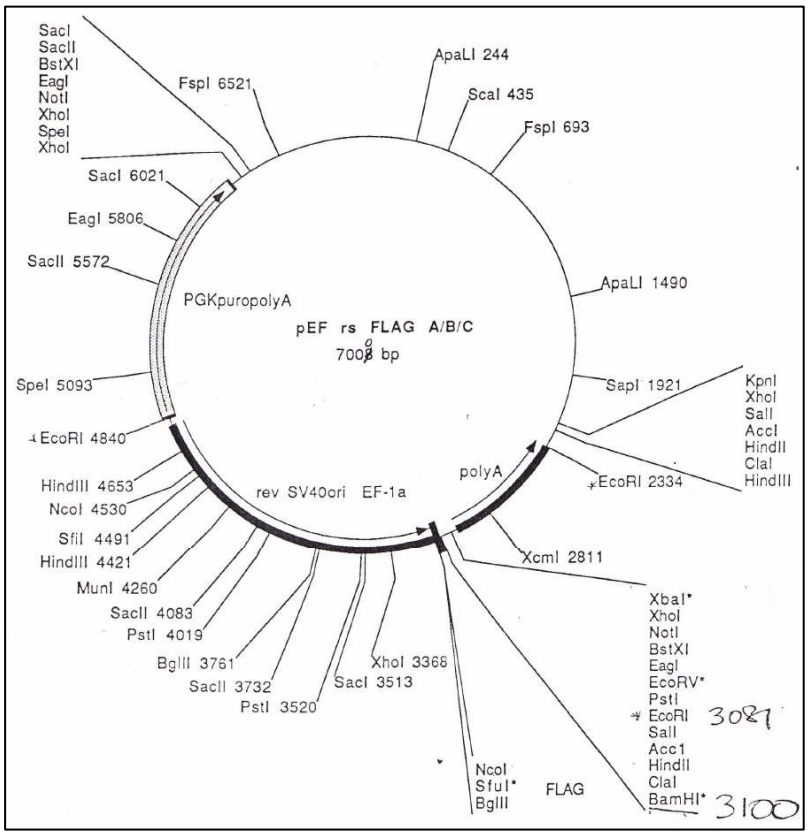

Danksagung

Mein ganz besonderer Dank gilt Frau Dr. Monilola A. Olayioye für die Bereitstellung des Themas dieser Doktorarbeit und ihre hervorragende fachliche Betreuung. Sie hatte stets ein offenes Ohr und hilfreiche Ratschläge bei Problemen, zahlreiche neue Ideen und einen mitreißenden Optimismus, der auch in schwierigen Situtationen an das Projekt glauben ließ. Zudem legte sie großen Wert auf wissenschaftlichen Austausch außerhalb des Instituts und ermöglichte daher die Teilnahme und Präsentation der Ergebnisse auf verschiedenen Kongressen. Danke für alles!

Herrn Prof. Dr. Klaus Pfizenmaier danke ich für die freundliche Aufnahme am Institut für Zellbiologie und Immunologie, die ausgezeichneten Arbeitsbedingungen, seine kritische aber konstruktive Auseinandersetzung mit der Arbeit in den Seminaren und für die Übernahme des Hauptgutachtens.
Ebenso danke ich Herrn Prof. Dr. Peter Scheurich für sein wissenschaftliches Interesse an diesem Projekt und die bereitwillige Mitberichterstattung.

Desweiteren möchte ich Monika Holeiter für die tatkräftige Mithilfe bei der Aufarbeitung der positiven Hefeklone aus dem Yeast-two-Hybrid Screen danken. Auch meinen Labor-Kollegen möchte ich ganz herzlich „Danke“ sagen für die freundliche Aufnahme und Integration in das MoLab zu Beginn meiner Arbeit und ihre Unterstützung während der gesamten Zeit.

Außerdem bedanke ich mich bei meinen neugewonnenen Stuttgarter und den „alten“ Kieler Freunden, von denen die meisten in demselben Zeitraum wie ich an ihrer Dissertation gearbeitet haben, und mit denen ich daher viele fruchtvolle Diskussionen die Arbeit betreffend geführt habe, die aber auch die Rückschläge im Labor sehr gut nachvollziehen konnten und so immer wieder aufbauend wirkten.

Abschließend möchte ich einen besonderen Dank meinen Eltern und meiner Schwester aussprechen. Ihre liebevolle Unterstützung, das Vertrauen und der Glauben an mich haben mir die Fertigstellung dieser Arbeit wesentlich erleichtert.

Lebenslauf

Johanna Heering
geboren am 14.11.1980 in Essen

Schulausbildung

1987-1991	Theodor-Heuss Grundschule, Essen
1991-2000	BMV Gymnasium, Essen
06/2000	Abschluss: Allgemeine Hochschulreife

Studium

2000	Beginn des Studiums der Biochemie/Molekluarbiologie, Christian-Albrechts Universität, Kiel
2002	Vorprüfung zur Diplomprüfung
2002-2005	Hauptstudium
Schwerpunkte	Biochemie (Hauptfach), Medizinische Mikrobiologie (1. Nebenfach), Pharmazie (2. Nebenfach), Immunologie (3. Nebenfach)
Forschungspraktika	(1) „Expression von Indikatorproteinen“ am Zentrum für Biochemie und Molekularbiologie, CAU, Kiel (2) „Molekulare Onkologie“ am Institut für Experimentelle Tumorforschung, UKSH, Kiel (3) „Rolle von PKC-Isoenzymen in der Regulation des Vesikeltransports“ am Institut für Immunologie, UKSH, Kiel
11/2004-08/2005	Diplomarbeit am biochemischen Institut, CAU, Kiel Titel: *Interaktion von Notch mit p53 in hämatopoetischen Stammzellen.*
09/2005	Abschluss: Diplom-Biochemikerin
2003-2005	Studentische Hilfskraft am biochemischen Institut, CAU, Kiel

Promotion

2005-2009	Promotion am Institut für Zellbiologie und Immunologie der Universität Stuttgart Titel: *Identification of novel protein binding partners for the tumor suppressor DLC1.*

Wissenschaftliche Veröffentlichungen

Heering J, Erlmann P, Olayioye MA. Simultaneous loss of the DLC1 and PTEN tumor suppressors enhances breast cancer cell migration. Exp Cell Res. 2009 Sep 10;315(15):2505-14.

Peterburs P, Heering J, Link G, Pfizenmaier K, Olayioye MA, Hausser A. Protein kinase D (PKD) regulates cell migration by direct phosphorylation of the cofilin phosphatase Slingshot 1 like (SSH1L). Cancer Res. 2009 Jul 15;69(14):5634-8.

Holeiter G, Heering J, Erlmann P, Schmid S, Jähne R, Olayioye MA. Deleted in liver cancer 1 controls cell migration through a Dia1-dependent signaling pathway. Cancer Res. 2008 Nov 1;68(21):8743-51.

Henning K*, Heering J*, Schwanbeck R*, Schroeder T*, Helmbold H, Schäfer H, Deppert W, Kim E, Just U. Notch1 activation reduces proliferation in the multipotent hematopoietic progenitor cell line FDCP-mix through a p53-dependent pathway but Notch1 effects on myeloid and erythroid differentiation are independent of p53. Cell Death Differ. 2008 Feb;15(2):398-407.

Erklärung

Hiermit versichere ich, dass die hier vorliegende Arbeit von mir selbstständig und unter ausschließlicher Verwendung der aufgeführten Quellen und Hilfsmittel angefertigt wurde.

Stuttgart, den 17. Juni 2009

Johanna Heering